AFFDL-TR-66-20

THEORETICAL AND EXPERIMENTAL MODEL INVESTIGATIONS OF SEMI-ANECHOIC AND SEMI-REVERBERANT ENVIRONMENTS AND THEIR APPLICATION TO THE RTD SONIC FATIGUE FACILITY

DAVID F. PERNET
GALE R. HRUSKA

IIT RESEARCH INSTITUTE

TECHNICAL REPORT AFFDL-TR-66-20

APRIL 1966

AIR FORCE FLIGHT DYNAMICS LABORATORY
RESEARCH AND TECHNOLOGY DIVISION
AIR FORCE SYSTEMS COMMAND
WRIGHT-PATTERSON AIR FORCE BASE, OHIO

NOTICES

When Government drawings, specifications, or other data are used for any purpose other than in connection with a definitely related Government procurement operation, the United States Government thereby incurs no responsibility nor any obligation whatsoever; and the fact that the Government may have formulated, furnished, or in any way supplied the said drawings, specifications, or other data, is not to be regarded by implication or otherwise as in any manner licensing the holder or any other person or corporation, or conveying any rights or permission to manufacture, use, or sell any patented invention that may in any way be related thereto.

Copies of this report should not be returned to the Research and Technology Division unless return is required by security considerations, contractual obligations, or notice on a specific document.

300 - June 1966 - 773-45-980

THEORETICAL AND EXPERIMENTAL MODEL INVESTIGATIONS OF SEMI-ANECHOIC AND SEMI-REVERBERANT ENVIRONMENTS AND THEIR APPLICATION TO THE RTD SONIC FATIGUE FACILITY

DAVID F. PERNET
GALE R. HRUSKA

FOREWORD

The research in this report was performed by IIT Research Institute, Chicago, Illinois, for the Aero-Acoustics Branch, Vehicle Dynamics Division, AF Flight Dynamics Laboratory, Wright-Patterson AFB, Ohio, under Air Force Contract No. AF 33(615)-2174, "Investigation of the Acoustic Environment of the RTD Sonic Fatigue Facility." This research is part of a continuing effort to provide reliable simulation of aero-acoustic sources for establishing design criteria in the specific area of sonic fatigue and is part of the Research and Technology Division, Air Force Systems Command's exploratory development program. This work was performed under Project 4437, "High Intensity Sound Environment Simulation," and Task 443701 "Sonic Fatigue Development."

Mr. Davey L. Smith and later Mr. Roelof C.W. van der Heyde were Project Engineers. The work was begun 15 November 1964 and ended 15 March 1966. The project leader was D. F. Pernet, responsible for the general direction of the program and was joint author of this report with G. R. Hruska. D. F. Pernet's contribution to this report consisted of Sections I, II, V, VI, VIII, IX, and XI and that of G. R. Hruska consisted of Sections III, IV, VII, and X.

The authors wish to acknowledge the significant contribution of V. J. Raelson for his assistance in gathering service field data and for his valuable advice. Acknowledgements are also extended to H. Witschonke for his valuable assistance in setting up and performing the majority of the experiments.

The manuscript was released by authors Jan. 1966 for publication as an RTD Technical Report.

This technical report has been reviewed and is approved.

Walter J. Mykytow

WALTER J. MYKYTOW
Asst. for Research & Technology
Vehicle Dynamics Division

ABSTRACT

A study of the acoustic environments that could be produced in the RTD Sonic Fatigue Facility has been made using both theoretical methods and experimental modeling techniques. An analysis is presented which enables the semi-anechoic environment to be determined at any position in the facility. This analysis is verified experimentally. An experimental program has also enabled the semi-reverberant environment to be established and has revealed the part played by the absorbing treatment in determining this environment. Experimental programs have investigated the sound fields on structures located in the facility under both modes of operation. A study of reflector devices used to modify acoustic environments was made and has enabled limited prediction of their effects. An analysis of current service noise fields on aircraft structures has enabled determination of values of the major parameters of these fields to be determined for use in simulation studies.

TABLE OF CONTENTS

TABLE OF CONTENTS (Cont'd)

LIST OF ILLUSTRATIONS

LIST OF ILLUSTRATIONS (Cont'd)

LIST OF ILLUSTRATIONS (Cont'd)

LIST OF ILLUSTRATIONS (Cont'd)

LIST OF ILLUSTRATIONS (Cont'd)

SYMBOLS

Symbol	Definition
2a	Dimensions of square test structure or reflector
A,B	Location of sound source and its image; two generalized locations in the facility
c	Velocity of sound = 1100 ft/sec (335.5 m/sec)
f	Frequency in RTD facility, cps
nf	Scaled frequency, cps
f_a, f_b	Limiting frequencies of noise band, cps
Δf	Half-band width = $(f_a - f_b)/2$, cps
g	Integer
h	Height of station Y above floor, separation between jet axis plane and a given parallel plane (m)
j	$\sqrt{-1}$
k	Wave number = $\omega/c = 2\pi/\lambda$ ft^{-1} (m^{-1})
m	Energy attenuation constant in air
n	Scaling parameter
$\underline{n}$	Number of sound sources
O	Location on floor below sound source
P	RMS pressure amplitude at unit distance from sound source (N/m^2)
$P_1(t), P_2(t)$	Sound pressures at point Y originating from source A and its image B (N/m^2)
P_i, P_j	Generalized sound pressures due to i^{th} and j^{th} sources (N/m^2)
P_r	Sound pressure at distance r from source in reverberant field (N/m^2)
Q_θ	Directivity factor of source in reverberant operating condition in direction θ
$R(\tau)$	Cross- or auto-correlation coefficient for time delay τ

SYMBOLS (Cont'd)

Symbol	Definition
$R_{A,B}$	Cross-correlation coefficient between signals at stations A and B
$R_{1,3}$	Cross-correlation coefficient between signals 1 and 3 at A and B, etc.
r	Distance from source, ft (m)
r'	Extent of direct field under reverberant operating conditions, ft (m)
S	Area of room surface, ft^2 (m^2)
T	Period of signal, sec
V	Volume of room, ft^3 (m^3)
W	Acoustic power of source, watts
X,Y	Location of point on floor of room and point located on vertical line above it
x	Separation of sound source from floor
x,y	Coordinates of point in plane of jet axis
x',y'	Coordinates of point in plane distance h from jet axis plane
Z_1,Z_2	Distances from source A to point Y and image B to point Y, ft (m)
Z	Far-field approximation for either distances Z_1 or Z_2, ft (m)
α	Angle between YO and floor of facility
α_f	Absorption coefficient of acoustic treatment at frequency f in RTD facility
α_{nf}	Absorption coefficient of acoustic treatment at frequency nf in IITRI's facility
β	Room constant, ft (m)
ϵ	Small fraction
λ	Wavelength = c/f = 1100/f (ft) = 335.5/f (m)

SYMBOLS (Cont'd)

Symbol	Definition
ρ	Density of air, slug/ft^3 (Kg/m^3)
τ	Time delay, time difference between signals $P_1(t)$ and $P_2(t)$, sec
$\psi(\tau)$	Correlation function of signal
$\omega(\tau)$	Power spectrum of signal
ω	Angular frequency, cps

LIST OF TABLES

SECTION I

INTRODUCTION AND SUMMARY

The RTD Sonic Fatigue Facility, currently under construction at Wright-Patterson Air Force Base, Ohio, will serve a dual purpose. It will provide information on the fatigue levels of structures and will also make possible the proof-testing of final design structures. The facility was designed as a tool for investigating the effects of acoustic excitation on structures of flight vehicles and on electronic and power equipment. It consists of an oddly shaped test chamber approximately 68 x 54 x 42 ft (20.7 x 16.5 x 12.8 m) in size, with a volume of approximately 155,000 ft^3 (4400 m^3). Low frequency acoustic power in the range 50 cps to 2400 cps is provided by a bank of 25 sirens located in one corner of the facility. This bank produces approximately 10^6 watts of acoustical power and an additional 90,000 watts are produced from nine high frequency sirens in the range 500 cps to 9600 cps. By means of an acoustical lining treatment with removable and collapsible elements, the facility is capable of being operated under either progressive wave or diffuse field conditions.

An initial study, using a modeling technique, was made under Contract No. AF 33(657)-10927 (Ref. 1) to investigate the acoustic environments attainable in such a facility. Under that contract analytical studies of the diffuse and progressive wave operation of the facility were made. In addition, an experimental investigation was conducted to determine the characteristics of the fields existing on structures when they are exposed to simple sound fields.

This current program has attempted to continue these studies, broadening their scope where necessary, so as to enable attainable acoustic environments to be defined in as complete detail as possible. The environments studied have been those existing under normal facility operation, with or without the presence of structures, together with those environments as modified with reflector devices. The environments have been analyzed in terms of the spatial spectral distribution and the cross-correlation properties of the field, using either or both experimental and analytical techniques where appropriate.

The study consists of:

1. a discussion of scaling techniques as applied to the problem of modeling anechoic and reverberant environments on structures;

2. an experimental and theoretical study of the semi-anechoic environment as influenced by the position in the facility and the manner in which either single or groups of sound sources are operated;

3. an experimental study of the semi-reverberant environment as influenced by the position in the facility and the location of the acoustic treatment;

4. an experimental study of the acoustic fields existing on structures which are located in either semi-anechoic or semi-reverberant environments;

5. an experimental and analytical study of the ways in which plane reflector devices can be used to modify the acoustic environment in a region in free space or at a structure's surface;

6. an analytical study of service field characteristics in which representative values of parameters defining the field were determined for use in simulation of service fields in the RTD facility.

(Note: Any absolute sound pressure level in this report is with reference to 2×10^{-5} N/m^2.)

SECTION II

MODELING CONCEPTS

The reasons for performing experimental model studies of acoustic environments rather than utilizing the RTD facility are manifold. In order that the RTD facility can be most rapidly and gainfully utilized for the purposes for which it is intended, it is desirable that guidelines for its operation be already established by the time the facility's construction and testing is complete. These guidelines, it was felt, could be more rapidly and economically established by studies performed experimentally on a suitably scaled version of the RTD facility.

The concept of modeling in acoustics is not uncommon. For example, the experimental studies performed under Contract No. AF 33(657)-10927 (Ref. 1) used modeling techniques to investigate diffraction of progressive wave sound fields by plane structures. The modeling method commonly employed in acoustics is one in which structure sizes and distances in general are geometrically scaled down and, simultaneously, frequencies of interest are scaled up by an identical factor. In this manner the ratio of either structure dimensions or distance to wavelength is preserved. Two important phenomena which control acoustic environments are interference and diffraction effects. The significant parameter for both these phenomena is the ratio of distance, or structure dimension to the wavelength of interest. If, for either of these phenomena, this parameter is maintained constant, the respective phenomena effects will be unaltered. Thus, if either interference or diffraction effects are determined for a particular situation, e.g., standing waves in an enclosure or diffraction around an object, they can be used to predict the effects in a geometrically scaled situation. The advantages of performing experiments on a small scale model include rapid acquisition and analysis of data, convenience of operation using reduced manpower, ease with which parameters of interest may be varied, and the economics involved in operating a model facility.

The phenomena of interference and diffraction affect acoustic environments through the redistribution of sound energy. An additional phenomena of importance is that of sound absorption. For this particular study, absorption produced by the acoustic treatment installed in the RTD facility is of major importance, though the effects of air absorption at high frequencies must not be ignored (especially when the acoustic treatment is removed to produce reverberant fields), because of the long path lengths associated with this large facility.

If we accept a modeling scheme in which the ratios of dimensions to wavelengths are preserved between model and full scale study, then this implies that any frequency of interest

in the full scale facility must be scaled accordingly to accomplish successful modeling. To enable sound absorption effects to maintain their correct importance in determining an acoustic environment, it is necessary that the absorption effect in the full scale operation at the particular frequency of interest should be equal to that in the model at the scaled frequency. Thus any acoustic treatment installed in a model should have an absorption coefficient at the modeled frequency equal to that of the full scale treatment at the full scale frequency of interest. This also should apply to air absorption if this contributes significantly to the total acoustic absorption. However, it is difficult to fulfill this latter condition in practice.

This discussion can best be summarized by considering the following as an illustration of the modeling approach. The problem is to determine the acoustic environment in the RTD facility in which a structure is located. The facility is assumed to have an acoustic treatment having absorption coefficient α_f at frequency f, and occupying a given region of the room. We can construct a model, geometrically similar to the RTD facility but smaller by a factor 1/n, and place in it a geometrically scaled model of the structure. An acoustic treatment can be located in a geometrically scaled location having an absorption coefficient α_{nf} ($=\alpha_f$) at a frequency nf. If we now determine in this model the spatial distribution of acoustic energy in the region of the structure, at frequency nf, this distribution will be identical to that in the full size facility at frequency f, except that it will be geometrically scaled down by a factor n.

We will refer to the scaling factor between the full size and the model facility as n. Then the ratio of dimensions, areas, and volumes in the full scale facility to those in the model facility will be n, n^2, and n^3 respectively. Similarly, the ratio of given wavelength and frequency in the full scale facility to those in the model facility will be n and 1/n respectively.

PRACTICAL CONSIDERATIONS

When the RTD facility is operated in the semi-anechoic state, the wall and ceiling will be fully acoustically treated so that only the floor will remain as a reflecting surface to influence the acoustic environment. It will be sufficient to perform model experiments in an anechoic room of arbitrary shape, as long as a reflecting surface, scaled down in linear dimensions by a factor n from the full size floor, is used as the floor of the anechoic room. The orientation and size scaling of any absorbing walls need not be preserved since these surfaces do not affect sound environments in the facility (because they represent completely absorbing boundaries).

Consequently, it is not necessary to construct an identically scaled model of the facility in this case. Therefore, we have been able to conduct model experiments in our anechoic room, which has a usable volume 16 x 12 x 8 ft (4.9 x 3.7 x 2.4 m), locating a reflecting surface on the wire mesh supporting floor. This represents an adequate scaled model of the RTD facility under semi-anechoic operation.

In the other extreme, the RTD facility may be operated as a semi-reverberant room in which all surfaces are reflecting, with the exception of a collapsed wall treatment located around the room perimeter at ceiling height and a ceiling treatment which may or may not be removed under semi-reverberant conditions. It would appear important to ensure exact scaling of the wall sizes and orientations in order to achieve successful acoustic modeling. This would be true if we were to consider the problem on a microscopic scale, because the size, shape, and orientation of each exposed surface is critical to the acoustic environment at any location in the total enclosure. However, the present state of the art only allows us to consider a macroscopic approach to the problem of reverberant sound fields (which may be currently considered sufficient for the purpose of sonic fatigue studies). For example, in a given reverberation room with a given acoustic power input, the important parameters of the environment are the sound pressure level in the diffuse field, the extent of the direct field produced in the vicinity of the source, and, possibly, phase information. Consideration of the equation $P^2 = W\rho c\ (Q_\theta/4\pi r^2 + 4/\beta)$, e.g., (Ref. 2), describing this gross nature of the acoustic environment, shows that the factor of major importance is the room constant β. Two rooms, having equal average surface absorption coefficients will have the same value for β if their surface areas are equal. However, there is no restriction as to their respective volumes, or the shape of these enclosures.

The argument that the surface area is of more importance than volume can also be expected to govern the considerations we must give to the problem of modeling a reverberation room. The model study of the reverberant (and semi-reverberant) operational mode of the RTD facility was to be performed in our reverberation chamber. The two facilities can be approximately represented by rectangular volumes having dimensions 68 x 54 x 42 ft (20.7 x 16.5 x 12.8 m) and 21 x 14 x 12 ft (6.4 x 4.3 x 3.7 m), so that they are of similar, though not identical shape. In actuality, both facilities have designed irregularities to increase diffusion (Refs. 3 and 4). In the untreated case the ratio of respective exposed surface area for the RTD and IITRI facilities are approximately 12.34:1 (see Appendix II). If we assume the typical linear dimension scaling factor is n, then the area factor will be n^2. Thus, from the surface area ratio, the value of n computes to be $\sqrt{12.34} = 3.51$. It is interesting that if we calculate n assuming that the volume ratio scaling factor is n^3 the value of n is $\sqrt[3]{43.9} = 3.53$. Thus it appears that scaling either by area or volume we

arrive at approximately equal values for n. We chose a value of 3.5 as being an average scaling factor for the following study. (It may be noted that individual linear dimensions of the respective facilities are in ratios of 3.2, 3.8, and 3.5).

The sound field distribution that is then measured in the model facility at frequency f will be equal to that measured in the RTD facility at a frequency f/3.5. An illustration of the validity of this scaling technique can be made if we consider, for example, the extent of the direct field measured in both full and model scale facilities. The extent is given by $(Q_\theta \beta/16)^{1/2}$. Thus, for any facility, it is proportional to the half-power of the room constant. From assumptions previously made on absorption, the value of $\beta^{1/2}$ for any facility, is proportional to (total area)$^{1/2}$. But the ratio of (facility area)$^{1/2}$ is proportional to $(n^2)^{1/2}$, i.e., n. So the ratio of the extent of the field will be n, i.e., it scales as typical dimension. This example illustrates the validity of the scaling method.

If we now transfer from reverberant to semi-reverberant operation, in which areas of the RTD facility are acoustically treated, our modeling approach will still be valid, so long as a geometrically scaled area of treatment is installed in the model facility in identical locations. The absorption coefficient for the treatment in the model at frequency f must be chosen equal to that of the treatment in the full scale facility at frequency f/3.5. Having decided upon this value of scaling parameter for the reverberant study, this value was also adopted for the semi-anechoic study. Table I contains a comprehensive list of parameters of a facility or its environment and the manner by which they ideally scale.

We must also consider the modeling concept as applied to the sound sources. No attempt was made to scale the acoustic power capabilities of the RTD sirens, since this serves no useful purpose. The only effect of varying the level of the sound source is to vary the overall field level accordingly, while the relative acoustic field distribution in the acoustic environment remains constant. It is this relative field distribution which requires determination from modeling experiments. The level of the field at certain selected locations may be readily computed for any situation given the power of the source. This, then, enables absolute levels to be ascribed to the field at any location in the facility.

Directivity effects of the sources affect both semi-anechoic and semi-reverberant field distributions. Loudspeaker sources were chosen whose diameter, 8 in. (.2 m), was approximately 1/3.5 the siren's exit diameter, 2-1/2 ft (.76 m), and these were mounted in a scaled baffle in an effort to scale directivity effects. It was not possible to exactly scale the size of the sources according to the chosen value, but separations of the sources of 8-5/8 in. (.22 m) were used, which did correspond to the chosen scaling factor of 3.5.

SECTION III

ACOUSTIC FACILITIES AND EQUIPMENT

The RTD facility may be used in modes of operation ranging from a semi-anechoic mode to a semi-reverberant mode. In order that a meaningful experimental study could be performed using modeling techniques, it was necessary to modify IITRI facilities so as to conform to an assumed model of the RTD facility.

ACOUSTIC FACILITIES

Consider the case of the semi-anechoic mode of operation. In this mode the absorbing treatment of the RTD facility will cover the ceiling and the four walls of the facility. The concrete floor will remain uncovered. The IITRI anechoic room is of conventional design, utilizing glass fiber wedges, and has a usable volume 16 x 12 x 8 ft (4.9 x 3.7 x 2.4 m). It was modified by introducing a floor over the entire room, consisting of two layers of 1/2 in. (.013 m) thick plywood sheets, joined randomly to prevent sound transmission by coincidence and to inhibit resonance effects (Fig. 1). This floor represents a scaled version of the RTD facility's concrete floor, whose dimensions are approximately 68 x 54 ft (20.7 x 16.5 m). However, the acoustic treatment on the walls of the RTD facility has a depth of 6-1/2 ft (1.98 m). This treatment extends down to the floor, so that the effective floor exposed to acoustic energy has dimensions approximately 55 x 41 ft (16.8 x 12.5 m). The scaled plywood treatment has dimensions 16 x 12 ft (4.9 x 3.7 m), which is approximately in accordance with the chosen scaling factor of 3.5. The reflection coefficient of the plywood floor was not determined. It was estimated to be 90 per cent, which, though not as high as that of the concrete floor (98 per cent), is sufficient to ensure that the majority of incident energy is reflected.

The siren bank source has been modeled by constructing a bank consisting of twenty-five 8 in. (.2 m) Jensen loudspeakers, which is geometrically scaled and located to model the RTD facility under semi-anechoic conditions. Details of its construction and location in the facility are shown in Fig. 1.

In the semi-reverberant mode of operation the RTD facility will have the absorbing treatment collapsed so as to approximately cover the top one-third of the four walls. The absorbing ceiling may be removed or may be allowed to remain.

The semi-reverberant mode was simulated in the IITRI reverberation room. At the commencement of the program, it was not thought that the ceiling would be removed and initial model experiments were performed with a plane 2 in. (51 mm)

thick layer of fiberglass material covering the majority of the area of the ceiling (Fig. 2). The splayed ceiling provides a variable air gap which increases the low frequency absorption. The absorption coefficient of the material, determined without an air gap backing is also shown in Fig. 2. No attempt was made to simulate the addition of a collapsed treatment covering the upper portion of the walls, since it was anticipated that the ceiling treatment would be the major factor influencing the acoustic environment because of its tendency to absorb vertically traveling sound energy.

As the work progressed, it was determined that the ceiling might be removed in the RTD facility so that the only absorbing material remaining would be confined to the upper one-third of the walls. The simulation of the collapsed wall treatment was accomplished by constructing a framework to which a fiberglass form was attached (Fig. 2). The surface area and location of this treatment conforms to the scaling factor as adopted previously in this report. Further particulars of the experimental set-up for the semi-reverberant mode are given in Fig. 3. It may be noted that the IITRI reverberation room has splayed walls and a permanent elevated platform in the center of the room. To minimize the effects of this platform, readings in the diffuse field were taken in areas remote from the track.

EQUIPMENT

Figure 4 illustrates the systems used for the generation of the acoustic fields and the analysis of the data obtained.

The sound generation system produces either a sine wave, or a noise band output, since the RTD siren operation will produce either discrete frequency or limited noise band signals. The bands of noise are obtained by filtering the output of a white noise generator.

Representative bands of noise with center frequencies 200, 500, and 1250 cps, each having a 200 cycle bandwidth, were used. This bandwidth corresponds to an approximate scaling of the 50 cycle maximum bandwidth of any given siren. The inability of the filtering system to generate 200 cycle bandwidth signals with acceptably sharp cut-offs at higher frequencies necessitated the use of a one-third octave band filter in order to obtain bands of noise centered at 3150 cps and 8000 cps. Consequently, the results of experiments performed at these two frequencies must be viewed carefully because of the excessive bandwidths used.

The speaker sources of the sound differed for the two modes of operation of interest. The semi-anechoic operation necessitated the use of the bank of 25 loudspeakers, because of the effect of speaker location on the detailed nature of the acoustic environment. In the semi-reverberant case, interest was centered in the gross nature of the acoustic environment; for this reason, only a single source was needed.

The measurement of sound pressure levels was obtained using a 1/4 in. (6 mm) condenser microphone and was recorded by passing the signal through an audio spectrometer for amplification, and recording the signal on a chart level recorder. Initially, values were obtained by manually moving the microphone from point to point in the field. This system was improved by constructing a motor and pulley system which allowed a continuous traverse along a straight line to be made.

Cross-correlation measurements were made using two 1 in. (25 mm) microphones whose outputs were correlated by the use of a random signal correlator. Due to the nature of the meter readout of the correlator, all measurements were made pointwise rather than continuously.

SECTION IV

EXPERIMENTAL INVESTIGATION OF SEMI-ANECHOIC ENVIRONMENTS

The semi-anechoic mode of operation of the RTD facility will consist of an absorbing material covering the ceiling and walls of the facility leaving only an untreated reflecting floor. This mode of operation has been simulated in the IITRI anechoic room by placing a plywood floor on the wire mesh floor. It is the purpose of this section to experimentally investigate the attainable acoustic environments under these conditions of operation.

Given this semi-anechoic environment and a bank of 25 sources, one will be able to generate a variety of sound pressure fields. One possible method of exploring these fields would be to map out the sound pressure level contours for all of the combinations of sources, operated coherently, taken one, two, three, etc., at a time. (One need not be overly concerned with combinations of non-coherent sources as the individual fields will not produce interference effects but will simply add on an energy basis.) This approach is not feasible, however; the reason being that the total number of operating conditions is excessively large for complete experimental enumeration.

The impracticality of this method of approach necessitates an alternative approach based on drawing general conclusions from a relatively small number of observations. This method has been adopted for the subsequent analysis. It should also be noted that in the following discussion sound pressure levels relative to a reference point rather than absolute sound pressure levels are the characteristics which are determined in any given acoustic environment. The absolute levels are functions only of the sound power input, but the relative field distribution is a function of several parameters, and consequently it is this relative distribution to which this study is devoted.

SOUND PRESSURE LEVELS

Figure 5 shows the sound pressure level measured along either a diagonal or a normal to the source plane at floor level with the source located in the corner of the facility. The source was operated at three discrete frequencies 200, 1250, and 3150 cps, and the plotted data, compared to inverse square law distributions, illustrates the high degree of wall absorption at the higher frequencies in this scaled model of the RTD facility. Wall effects can be observed at the lowest frequency.

Figures 6, 7, and 8 give experimentally observed sound pressure level contours for single-source excitation of bands of noise with center frequencies 200 cps, 500 cps, and 1250 cps

respectively. These measurements were taken in a plane parallel to the source plane and 7-1/2 ft (2.3 m) from the sources. This is represented by the line XY in Fig. 5.

One of the results that these contour diagrams illustrate is the effect of varying the height of a single source upon the contours. The slight ($\pm$ 1/2 db) asymmetry observed in the contours could be caused by any of several reasons:

1. the floor is not symmetrical with respect to the axis of the source system;

2. the room is not perfectly anechoic for low frequencies;

3. the floor is not constructed from perfectly homogeneous material, so that variations in reflection coefficient can occur; and

4. the inherent limits of accuracy in the measurement of noise signals.

It can be seen that as the source height is increased, the contours tend to collapse vertically. Thus an increase in source height above the floor produces a more complex spatial distribution. It is characteristic that the horizontal distribution of sound pressure levels near the floor does not vary significantly with source height while the vertical levels vary markedly. Two empirical results obtained from the contours are that the height of a given maximum or minimum is inversely proportional to the height of the source above the floor and the separation between any successive maximum and minimum is approximately constant for a given frequency.

This may be compared to the case where the source height is held constant and the center frequency of the band is varied. The observed results are quite similar to those above in that the contours become flattened, being compressed in the vertical direction and being extended in the horizontal direction, as the frequency is increased. Because of the similarity of results obtained in these two cases, it may be surmised that the contour shape is a function of the ratio of speaker height above the floor to the wavelength of the sound.

The conclusions drawn so far have concerned only the spatial distribution of the sound pressure level contours. It may be noted that, in general, the maximum sound pressure level is obtained at floor level normal to the source. Additionally, for any speaker operated at a given frequency, equal minima sound pressure levels relative to the maxima are produced, independent of the spatial distribution of these contours.

Figure 9 illustrates the effects due to a change in the separation between the measurement plane and the source plane. It is seen that the distributions become less spatially complex

as the separation increases, with the distributions at large distances tending to form parallel horizontal straight lines. An empirical rule can be observed here: The distance up from the floor to any particular extremum (maximum or minimum) is approximately directly proportional to the source-measurement plane separation.

Experimental determination of sound pressure level contours, while giving an informative picture of the acoustic environment, is generally a time-consuming operation. In order to obtain data about a larger number of source configurations, in the following experiments data was only taken along two axes: (1) a horizontal axis along the floor and parallel to the plane of the sources, and (2) a vertical axis at the center of the source axis and normal to the floor. All measurements were made at a distance of 7-1/2 ft (2.3 m) from the source plane.

Figures 10 and 11 are plots of sound pressure levels along these vertical and horizontal axes for single sources emitting bands of noise. This data, which consists of profiles along two axes of the data shown in Figs. 6 to 8, illustrates results which are not obvious in the contour diagrams. The vertical traverses more clearly show the relative maxima and minima, the spatial separation of which decreases as the height of the source from the floor is increased. The magnitudes of the maximum to minimum decibel separation can be seen to remain constant for any specific frequency and any variable source height. The horizontal traverses illustrate the gradual decrease of sound pressure level as the distance from the vertical axis to the point of measurement is increased. Furthermore, the horizontal profile shapes are seen to be geometrically identical for a given frequency, being independent of the source height. (In other words, the absolute levels vary with source height, but relative levels remain constant.)

An experiment was performed to observe the effect of using sine wave excitation rather than noise excitation. Figure 12 illustrates this comparison for a vertical traverse of the field due to a single source for both harmonic and noise excitation. It can be seen that the maxima and minima occur at the same relative positions above the floor. However, the relative differences between corresponding extrema vary considerably. The maxima and minima for the noise case are very much less in relative amplitude compared to the extrema in the harmonically excited field. Horizontal traverse distributions at floor level for harmonic cases are observed to be identical to those for noise band cases to within experimental limits and are consequently not reproduced in this report.

An experiment was performed to determine the effect of a close grouping of sources located close to, and far from the floor, upon the sound pressure level distribution along a vertical and a horizontal axis. The results are shown in Figs. 13

and 14. It is seen that as the frequency is increased, the ranges of sound pressures along a profile increase from practically zero at 200 cps noise band, to significantly large amounts (up to 15 db) at the 1250 cps noise band. This occurs for the groupings located both near and away from the floor. An important fact to note is that for vertical traverses, the results of using one source or two sources of equal height above the floor are identical. Similarly, the results of using one source or two adjacent vertical sources show identical results for horizontal traverses.

The phenomena of having two adjacent sources in a horizontal (or vertical) plane produce the same relative sound pressure level results as one source, for traverses in a vertical (or horizontal) plane respectively can be extended for several sources as shown in Fig. 15. Various combinations of sources in a horizontal line near the floor produced identical center line contours for vertical traverses and widely divergent contours for horizontal traverses. Several generalizations can be made from the previous experiments and from the results obtained from multiple-source excitation for the 1250 cps noise band as shown in Figs. 16 and 17. It can be concluded that the higher the group of sources are from the floor, the more rapid are the variations in spatial distribution of the contours in the vertical direction. Also, the closer the sources are together in horizontal directions, the less rapid are the spatial variations in contour distribution in the horizontal direction. By making use of the concept of images, a simple model can be formed to account for most of the previously discussed results of this section.

CROSS-CORRELATION

It was believed that results of the experimental investigation of the cross-correlation function in the semi-anechoic case would not justify the time and effort spent on obtaining this data. The main reason for this belief is that the nature of the cross-correlation function depends on the location of the reference point in the acoustic field. Thus, to obtain a complete picture of the cross-correlation function over the entire field, it would have to be determined for every reference point of interest. This is in contrast to the case of sound pressure levels, where a change in reference point would only alter the levels of all contours by a single constant value, leaving the shapes and relative sound pressure differences the same.

However, a single determination of cross-correlation function relative to a point at floor level was made along a vertical direction when a single source was operating under noise band conditions. This is shown in Fig. 21 and is intended only for comparison to values of the function predicted in a later section.

CONCLUSIONS

An experimental investigation of the acoustic environment under semi-anechoic operation has been made. Spatial pressure distribution has been examined for both tone and noise band signals produced by either single sources or small groups of sources. A summary of results is shown in the following.

For single sources:

1. As the source to floor separation is increased the contours compress to those approaching horizontal parallel straight lines in the limit.

2. As the frequency is increased, the contours compress to those approaching horizontal parallel straight lines in the limit.

3. As the separation between the plane of the source and the plane of measurement is increased, the contours become less complex and tend toward horizontal parallel straight lines.

4. If noise band excitation is replaced by sine wave excitation, the contours are the same geometrically. However, the magnitudes of the interference extrema are much larger.

5. The height above the floor of a given extremum is inversely proportional to the separation between the source and the floor.

6. The separation between any adjacent maximum and minimum in the plane is constant for a given frequency and source-floor separation.

7. The distance from the floor to the position of a particular extremum is directly proportional to the source-to-measurement-plane separation.

For coherent multiple sources:

1. For a close grouping of sources or for a grouping of sources in a vertical line, the horizontal distribution has a gradually decreasing value. Vertical traverses show no noticeable common characteristics.

2. For sources in a horizontal line, the positions of the extrema in a vertical direction are identical for any source combination. As the floor to source separation is increased, the distance between extrema is decreased.

SECTION V

THEORETICAL STUDY OF SEMI-ANECHOIC ENVIRONMENTS

It has been adequately demonstrated in the preceding section that the sound fields which are produced under semi-anechoic operation of the model facility cannot be considered to be simple in nature. They do not possess those characteristics that are normally associated with the field radiated from simple sound sources in free space. Large spatial variations in sound pressure level exist within the regions of the model facility. The existence of the variation can be directly attributed to the presence of the reflecting surface formed by the floor of the model facility. Any sound source within the facility will have an image source associated with the presence of the reflecting floor surface. It is the interaction between the sound fields associated with these two sources that is responsible for the complexities in the field. Acoustic interference effects are more widely associated with single frequency sound fields, but can also be associated with noise fields. Because the RTD facility is capable of operation under discrete frequency or noise band operation using single or multiple sources, we will consider the general case of interference. If we consider a point in the field produced by 'n' sources, resulting from 'n' individual pressures at the point, the mean square pressure at this point is

$$\overline{P^2} = \overline{(P_1 + P_2 \ldots + P_i + \ldots + P_n)^2}$$

$$= \sum_{j}^{n} \overline{(P_i)^2} + \sum_{i}^{n} \sum_{j}^{n} \overline{P_i P_j} \qquad i \neq j \qquad (1)$$

The term $\overline{P_i P_j}$ is the cross-correlation function between signals P_i and P_j and, consequently, knowledge of this function together with the mean square pressures resulting from the individual sources alone, enables the overall pressure field to be determined. Note that if $\overline{P_i P_j}$ is zero for all values of i and j, the signals P_i and P_j are incoherent, so that the overall mean square pressure can be determined from integrated energy considerations, i.e., from the first summation term in Eq. (1).

Now if we consider a single source located above a perfectly reflecting, infinite floor at some point Y (Fig. 18-A) the sound field is produced by the addition of a direct sound field originating from an omni-directional point source producing a pressure $P_1=P(t)$ and a reflected sound field, produca a pressure $P_2=P(t+\tau)$, where τ is the time difference associated with the difference in path lengths between the direct and reflected signals. Thus in this case Eq. (1) becomes

$$\overline{P^2} = \overline{(P_1 + P_2)^2} = \overline{(P_1^2 + P_2^2 + 2P_1P_2)} \qquad (2)$$

Because signal P_2 is the reiteration of signal P_1 delayed by a time τ, the cross-correlation function $\overline{P_1P_2}$ is equal to the auto-correlation function of signal P_1 for a given time delay τ, since

$$\overline{P_1P_2} = \overline{P(t)\ P(t + \tau)}$$

Thus the magnitude of the sound field associated with a sound source located above a reflecting plane can be established if the auto-correlation function of that original signal is known. This property of a signal can readily be obtained either by the use of electronic correlating devices of analog or digital type or by computation from spectral analysis data of the signal through use of the Fourier transforms

$$\begin{aligned} \psi(\tau) &= \int_0^\infty \omega(f) \cos 2\pi f\tau \, df \\ \omega(f) &= 4 \int_0^\infty \psi(\tau) \cos 2\pi f\tau \, d\tau \end{aligned} \qquad (3)$$

where $\omega(f)$ is the power spectrum and $\psi(\tau)$ is the correlation function of the given signal.

Because correlation functions are frequently normalized to become correlation coefficients, it is more convenient to transform Eq. (2) to the following.

$$\overline{P^2} = \overline{P_1^2} + \overline{P_2^2} + \frac{2\overline{P_1P_2}}{\sqrt{\overline{P_1^2}\ \overline{P_2^2}}} \sqrt{\overline{P_1^2}\ \overline{P_2^2}} \qquad (4)$$

where $\overline{P_1P_2}/\sqrt{\overline{P_1^2}\ \overline{P_2^2}}$ is termed cross-correlation coefficient $R(\tau)$. Thus Eq. (4) is generally expressed in the form

$$\overline{P^2} = \overline{P_1^2} + \overline{P_2^2} + 2R(\tau) \sqrt{\overline{P_1^2}\ \overline{P_2^2}} \qquad (5)$$

Because we assume $P_1 = P(t)$, $P_2 = P(t + \tau)$, it follows that $R(\tau)$ is the auto-correlation coefficient for the signal $P(t)$ for time delay τ, and has a value of unity when $\tau = 0$.

An illustration of some typical auto-correlation coefficients are shown in Fig. 19-A for cases of discrete, narrow band, and broad band signals. These may be computed for ideal

bands of noise of limiting frequencies f_a and f_b from the following expression

$$R(\tau) = \int_{f_a}^{f_b} \frac{\cos 2\pi f\tau}{2\Delta f} \cdot df = \frac{1}{2\pi\Delta f\tau} \cos 2\pi f_m\tau \cdot \sin 2\pi\Delta f\tau \quad (6)$$

where $2\Delta f = f_b - f_a$ and $f_m = (f_a + f_b)/2$. Further discussion of this subject is contained in Refs. 5, 6, and 7.

A preliminary investigation of Eq. (5) will enable a generalized picture of the sound field distribution in the facility to be determined.

Let us consider the magnitude of the sound field along a line perpendicular to the floor, where initially this location is distant from the source. Then $\overline{P_1} \backsimeq \overline{P_2}$ at all points along this perpendicular line so the value of Eq. (5) is determined almost exclusively by the value of $R(\tau)$. This has a maximum value equal to unity when $\tau = 0$, i.e., when direct and reflected signals are separated by zero time delay, i.e., for a point X located on the floor (Fig. 18-A).

Thus a maximum value of sound pressure will be experienced at the level of the floor. In the case of a discrete frequency source signal, a series of maximum sound pressure levels will occur at points along a vertical whenever the direct and reflected signal paths differ by a whole number of wavelengths, i.e., corresponding to values of $R(\tau) = +1$ and thus $\tau = gT$, where g = integer and T = period of signal. The positions of maximum sound pressure level are alternated by positions having zero sound pressure level corresponding to values of $R(\tau) = -1$. Figure 19-B shows typical distributions along a vertical line above the floor for a discrete frequency signal. In the case of noise, the auto-correlation coefficient has only a single value of 1 when $\tau = 0$; other maxima are successively decreasing (Fig. 19-A). Consequently, the interference distribution for a noise band resembles that shown in Fig. 19-C. The interference effects region is most pronounced close to the floor but at points well removed from the floor where there is a considerable path difference between direct and reflected sound paths, the cross-correlation function tends to zero and the two sound fields are incoherent and add by energy alone. It may be noted in this region the sound pressure level will be 3 db below that value at the floor.

The phase characteristics of the acoustic field can also be determined from knowledge of the correlation properties of a single signal. For example, the cross-correlation coefficient between signals received at two locations in the facility, A and B, is $R_{A,B}$, given by

$$R_{A,B} = \frac{\overline{P_A \cdot P_B}}{\sqrt{\overline{P_A^2} \cdot \overline{P_B^2}}} = \frac{\overline{(P_1 + P_2) \cdot (P_3 + P_4)}}{\sqrt{\overline{(P_1 + P_2)^2} \cdot \overline{(P_3 + P_4)^2}}} \quad (7)$$

where P_1 and P_2 are direct and floor-reflected signals received at location A, and P_3 and P_4 are those received at location B. For a simple illustration, assume that A and B lie in the far field approximately equi-distant from the source. Then

$$\overline{P_1^2} = \overline{P_2^2} = \overline{P_3^2} = \overline{P_4^2}$$

and the cross-correlation coefficient between A and B becomes

$$R_{A,B} = (R_{1,3} + R_{1,4} + R_{2,3} + R_{2,4})/4 \quad (8)$$

where $R_{1,3}$ represents the cross-correlation coefficient between the signal 1 at A and the signal 3 at B. $R_{1,3}$ may be determined, for example, by inspection of the auto-correlation coefficient of the signal originating from the source, knowing the path difference between the two signals of interest.

Figure 21 shows both the calculated and the experimentally determined cross-correlation coefficient profile along a vertical line in the interference field produced by a single noise band signal (see Appendix A). The calculated values were determined using Eq. (8) and the auto-correlation coefficient of the original signal which was obtained experimentally.

Figure 21 also shows the sound pressure level profile obtained experimentally for the same operating conditions as above as well as the profile computed using Eq. (5), again knowing the original signal's auto-correlation coefficient (see Appendix A). It is seen that the pressure profile gives excellent agreement between calculated and experimental values. The phase profile characteristics show only fair agreement. This may result from the floor's not being a perfect reflector either in its amplitude or phase characteristics.

We have now established, in general, how the presence of the reflecting surface will produce an interference field in the RTD facility.

We must now consider, more specifically, this interference field. For example, how is the spacing of the maximum and minimum values of sound pressure level related to the frequency of operation, the height of the source above the floor, and the distance of the point of observation from the source? Also, we must establish the magnitude of the maximum and minimum sound pressure level. This information will enable the overall space in the facility to be classified into smaller regions in

which the sound pressure levels are uniform, varying slowly, or contain many maximum and minimum values, for example.

If we are in the far field it is easy to calculate the spacing of the interference pattern. From the geometry of Fig. 18-A, it can be seen that the pressure at point Y due to a discrete frequency source A, and its image B, producing individual pressures $\sqrt{2}\ (P/Z_1)\ \exp[jk(ct-Z_1)]$, $\sqrt{2}\ (P/Z_2)\ \exp[jk(ct-Z_2)]$ where P is the RMS pressure amplitude at unit distance from the source, will be

$$\sqrt{2}\ \frac{P}{Z_1}\ \exp[jk(ct-Z_1)] + \sqrt{2}\ \frac{P}{Z_2}\ \exp[jk(ct-Z_2)] \qquad (9)$$

If we assume $Z_1,\ Z_2 \gg x$, so that $Z_1 \backsimeq Z_2\ (=Z)$, the pressure will be

$$\begin{aligned}
&\sqrt{2}\ \frac{P}{Z}\ \exp[jk(ct-Z_1) + \exp[jk(ct-Z_2)] \\
&\quad = \sqrt{2}\ \frac{P}{Z}\ \exp[jk(ct-Z+x\sin\alpha)] + \exp[jk(ct-Z-x\sin\alpha)] \\
&\quad = \sqrt{2}\ \frac{P}{Z}\ \exp[jk(ct-Z)]\ \left[\exp(jkx\sin\alpha) + \exp[jk(-x\sin\alpha)]\right] \\
&\quad = 2\sqrt{2}\ \frac{P}{Z}\ \exp[jk(ct-Z)]\ \cos(kx\sin\alpha) \qquad (10)
\end{aligned}$$

Thus the RMS pressure at the point Y, distance h above the floor, is

$$\frac{2P}{Z}\ \left|\cos\ [kx\ (\sin\ \alpha)]\right| \ =\ \frac{2P}{Z}\ \left|\cos\ \frac{kxh}{Z}\ \right| \qquad (11)$$

Maximum values occur when $kx \sin \alpha = g\pi (g = 0,1,2,3)$, or $h_{max} = g\lambda Z/2x$. Minimum values occur when $kx \sin \alpha = (g + 1/2)\pi$, or $h_{min} = (g + 1/2)\lambda Z/2x$.

This analysis will strictly only apply to the far field, i.e., those regions where (1) the pressure amplitudes due to each source are equal, and where (2) $DB - 2 \cdot CO < \epsilon\lambda$, where ϵ is a small fraction. This latter condition is often overlooked but derivation of Eq. (9) assumes $DB = 2 \cdot CO$ to determine the phase difference between P_1 and P_2.

Figure 18-B shows the sound field distribution plotting the maximum sound pressure levels in the field, showing how these lines appear straight in the far field, and curve approaching the source. This is plotted for the case of $x = 5\lambda$ and is typical of the distribution of these maxima. It may be shown that the locus of these maxima belong to a set of confocal hyperboloids. In Ref. 1 the distribution was calculated in a vertical

plane parallel to the source plane. Typical distributions are reproduced in Fig. 20 and show the predominance of interference in the vertical direction.

In the case of discrete frequency in the far field, successive maxima along any vertical will be approximately equal and of value twice the free field pressure existing in the region if there were no reflector present. The minimum values will be zero resulting from complete cancellation and the intermediate regions will have a cosine amplitude distribution as is seen from Eq. (11). Consequently, it is easy to calculate the sound pressure level at any point in the facility or the variation over any volume region. Equation (11) will give a good approximation in the far field, but near field determination would require allowance to be made for the error in path difference and the difference in individual signal levels due to large variation in path lengths. These near field calculations could best be performed on a digital computer.

We now consider the far field case for a noise band source having one-third octave or narrower characteristics. In the case of a discrete frequency signal the successive maximum and successive minimum have constant values respectively because the value of the auto-correlation coefficient's maxima and minima are also equal. Consequently, distributions of sound pressure levels shown in Fig. 19-B are obtained. The decreasing value of maxima and minima of the correlation function (Fig. 19-A) produce an interference pattern in which maxima and minima levels are successively less pronounced as shown also in Fig. 19-C. The auto-correlation function for narrow band noise (one-third octave) is a damped form of that for a discrete frequency equal to the center frequency of the band. That is, the positions of zero crossings and maxima and minima are identical for both discrete and narrow bands of noise.

For wider bands of noise this does not hold, especially with increasing values of τ. Thus the positions of maximum and minimum sound pressure levels in the RTD room under noise band operation will be identical with those produced with a discrete frequency equal to that of the center frequency of the noise band except at the very lowest frequencies attainable. In addition, the interference effect becomes less marked with increase in path difference. If we assume that the sirens operate with an ideal 50 cycle pass band, the following table shows the value of successive maximum and minimum values in the interference field for given frequencies of 50, 100, 250, 500, 1000, and 2500 cps.

This shows clearly how the ratio of bandwidth to frequency $2\Delta f/f$ affect the interference pattern. Decrease in this function produces a more persistent interference effect.

Freq.	$\frac{2\Delta f}{f}$	Floor Level	Relative Sound Pressure Levels of Successive Extrema of Interference Field (db)						
			Min	Max	Min	Max	Min	Max	Min
50	1	0 db	$-7\frac{1}{2}$	-3	-4	-3	$-3\frac{1}{2}$	-3	$-3\frac{1}{2}$
100	.5	0	-13	-1	$-4\frac{1}{2}$	-3	-4	-2	$-3\frac{1}{2}$
250	.2	0	*	0	$-11\frac{1}{2}$	$-\frac{1}{2}$	$-7\frac{1}{2}$	$-1\frac{1}{2}$	-5
500	.1	0	*	0	-17	0	-13	$-\frac{1}{2}$	-10
1000	.05	0	*	0	*	0	-19	0	-16
2500	.02	0	*	0	*	0	*	0	*

*Level is more than 20 db below reference level.

Again, it must be remarked that these discussions which enable the position and magnitude of the interference effect to be calculated approximately, apply only to the far field. Otherwise the services of a computer will be required.

It is important to define the far field region and the significance of this regarding calculations of pressure fields using Eq. (11). We have said that Eq. (11) is valid only when Z_1 and Z_2 are equal, so that the magnitudes of P_1 and P_2 are equal. Assume, for example, a 10 per cent difference exists between Z_1 and Z_2, resulting in an associated pressure amplitude difference between P_1 and P_2. The use of Eq. (11) produces less than 1/2 db error in calculating the pressure distribution if the correlation coefficient of the signal is always greater than -0.5. An infinite error, on the decibel scale will occur if, for example, $R(\tau) = -1.0$, because calculation yields zero pressure, but the actual pressure, though small, will be finite because of the difference in magnitudes of P_1 and P_2. Consequently, differences as large as 10 per cent between Z_1 and Z_2 should not produce significant errors in determining the acoustic field.

Thus the closer the source to the floor the more extensive will be the region in which a far field assumption is valid.

Also, $(DB-2\cdot CO)$ must be a negligible fraction of a wavelength, otherwise an error in computing the phase difference between P_1 and P_2 results in the evaluation of Eq. (11). It is obvious that higher frequencies imply that the far field extends closer to the source than for lower frequencies.

Figure 18-B shows in detail a typical near and far field distribution of maxima. The deviation of the straight line approaching the source illustrates the transition from far to near field, but it is this deviation in fractions of a wavelength rather than absolute distance which decides when a far field assumption, used to predict the interference field maxima and minima positions, breaks down. The distribution of maxima (and minima) are hyperbolic in nature.

We have now established how the interference field may be determined to a good approximation by consideration of far field criteria and how near field distributions could be calculated. These are based upon the assumption of omni-directional point sources and a perfectly reflecting floor of infinite extent. Consideration will be given to some practical aspects of the interference field in the RTD facility.

FLOOR REFLECTION

The floor of the RTD facility may be approximated to a rectangle of dimensions 68 x 54 ft (20.7 x 16.5 m). The siren sources are mounted above one corner of this rectangle and produce signals of wavelengths 1/4 ft to 20 ft (.076 to 6.10 m), corresponding to 2400 cps and 50 cps. We must consider whether, in fact, the RTD floor can be considered to represent an infinite extent reflector. This problem can be approached using results of Contract AF 33(657)-10927 reported in Ref. 1.

If a sound field is normally incident upon a plane surface whose dimensions are large compared with a wavelength, then pressure-doubling will occur, and a 6 db increase in sound pressure level will occur because the surface acts as a perfect reflector. This pressure-doubling effect will not, however, be apparent close to the surface boundaries. References 1 and 12 show that a square surface may be assumed to be a perfect reflector when $ka > 8$. Thus 2a, the side of the square, must be greater than $4/k$, i.e., $2\lambda/3$. Now the smallest RTD dimension 54 ft (16.5 m) is nearly 3λ for the lowest frequency [50 cps ≡ 20 ft (6.1 m)]. Consequently, we may consider the RTD floor to represent a perfectly reflecting floor for all frequencies of interest.

However, the interference field very close to the source may not be that which is calculated close to the edge of the floor, because of diffraction effects. This arises because the reflected wave forming the interference pattern arises near the floor edge. This edge effect is not likely to exist beyond a fraction of the wavelength from the edge (we estimated $\lambda/4$).

FINITE AMPLITUDE SIGNALS

In this analysis we have assumed linearity of the acoustic signals. No attempt has been made to consider how the interference distribution is modified when the acoustic signal amplitude is so large as to produce nonlinear effects. This would require a detailed knowledge of the characteristics of nonlinear signal propagation in free space, and the reflection characteristics at an infinite impedance reflector. In particular, the latter requirement is considered especially critical in determining whether our analysis is valid for large amplitude signals. Ref. 29 shows that the assumption of perfect reflection, resulting in pressure doubling at an infinite impedance reflector, is valid for incident signal levels up to 174 db. This offers encouragement that the interference distribution analysis will be valid at the sound pressure levels which will exist in the RTD facility.

SOURCE DIRECTIONALITY

An assumption commonly accepted in acoustic problems is that sound sources radiate omni-directionally. This is seldom true in practice and consequently consideration must always be devoted to the influence of the directionality of sources. Sound sources at low frequencies, i.e., where wavelengths are much larger than source dimensions, generally radiate sound equally in all directions. At higher frequencies, sound tends to propagate in a major beam with minor side lobes. Directionality patterns for simple sound sources such as pistons in baffles, etc., are commonly available (Refs. 8 and 9).

Less data are available for the directionality effects in sirens. However, Ref. 10 contains data for a siren similar to that to be used in the RTD facility. These were obtained for a siren with and without a horn, whose exit diameter is equal to that proposed for the RTD facility (i.e., 30 ins., .76 m). However, the siren was operated under unbaffled conditions unlike the intended RTD operation.

The effect of directionality upon the interference fields which will exist in the facility can be observed through inspection of Eq. (5), where P_1 and P_2 differ in magnitude, not because of possible slight differences in path lengths, but because of directionality effects. Only at the floor position will the values of P_1 and P_2 be always equal. The effect of their non-equal values at other locations will be to change the magnitude of the interference field, but not positions of maxima and minima. For example, in the case of discrete frequency operation true cancellation would not occur since, although the two signals at some point have opposite phase, their amplitudes are not equal.

MULTIPLE-SOURCE OPERATION

The previous discussion has concerned the field in the facility produced by a single source. Alternative operating conditions could include a group of two or more sirens operated identically, groups of sirens operating independently (incoherently) but at the same frequency, or groups of sirens operated independently at different frequencies.

We will consider some general characteristics of the acoustic fields obtained in these ways. If several sources are operated coherently at the same frequency, i.e., the pressure-time history of the signals of each siren of the group is identical, then the interference field could be computed from an extension of Eq. (1). If the signal were discrete frequency and the sources were randomly selected with separations of the order of a wavelength or more, one would expect many more locations of maxima and minima sound pressure levels then could be obtained with a single source. However, the range between maxima and minima levels would be reduced so as to produce a more uniform field over a given volume region. If their separation is small compared with a wavelength, they may be considered equivalent to a single source so that the interference pattern is equivalent to that produced by a single source. Some cases of multiple-source operation enable the sound pressure level distribution to be readily anticipated. For example, two sources may be operated coherently at a discrete frequency. Their relative separations from the floor could differ greatly. For example, a siren at the top of the bank is approximately five times as far from the floor as a siren at the bottom of the bank. Both sources will produce interference distributions which will be superimposed. However, the spatial separation of interference extrema will occur in the ratio of 1:5. Consequently, the overall distribution will resemble that shown in Fig. 19-D.

If the signal is a noise band and again the group is operated coherently, the same observation will hold.

If the sources are operated independently, either at the same or at different frequencies, then it is sufficient to compute the individual field associated with each source by means of Eq. (5) and the overall field can be derived by energy addition of individual fields by summation of the first terms in Eq. (1).

Figures 18 and 19 illustrate the interference effect of a single source and its image in a vertical direction. Interference can be obtained in horizontal directions when two or more sources are operated coherently and these sources do not lie in the same vertical line. Experimental evidence of this is shown in Fig. 17. Analysis of this problem is identical with that of a single source and its image.

SOUND PRESSURE LEVELS

The above analysis enables the relative interference characteristics of fields to be determined. The absolute sound pressure level of the field can be estimated from estimated power consideration. Each siren is capable of producing 40,000 watts of acoustic power. If we assume this to be radiated equally in all directions, the sound pressure level at any distance "x" ft (m) from the source will be

$$SPL = 10 \log_{10} \frac{W \cdot 10^{13}}{4\pi x^2} \qquad (12)$$

At full power, $W = 4 \times 10^4$ watts, so the sound pressure level at distance x in ft is given by

$$SPL = 165 - 20 \log_{10} x$$

x in m is given by

$$SPL = 155 - 20 \log_{10} x$$

The following table gives an indication of the free field sound pressure level at several distances from the source.

Distance	1 ft (.3 m)	10 ft (3 m)	100 ft (30.5 m)
SPL re 2×10^{-5} N/m^2	165 db	145 db	125 db

These sound pressure levels would be obtained if the total available power of 40,000 watts was radiated spherically in an anechoic environment. However, the output of a sound source can be influenced by its proximity to reflecting surfaces (Ref. 11).

The effect is noted both in total power output and directivity and is caused by the sound reflected from a surface reacting back on the source. The effect can be observed either to increase or decrease the power output of the source relative to the free field output. The effects are prominent only when the source is closer to the reflecting surface than a half wavelength. With the addition of further reflecting surfaces in different planes, for example, a room corner, the effects are more dramatic. In this case, a source located in the corner will radiate eight times more power than under free field conditions but located equally distant from all surfaces, one half wavelength from the corner, the power output reduces to nearly zero.

In the case of the RTD facility, the reflecting surfaces comprise the baffle in which the sirens are located and the reflecting floor. All other surfaces may be considered totally absorbing in the semi-anechoic case. Analysis of this actual situation is beyond the scope of this program. However, we may assume that the major effect will be produced by the reflecting floor, and if we further assume this floor is of infinite extent, Ref. 11 shows the following:

1. If the source is less than $\lambda/4$ from the floor, the power output is increased over the free field value, having a maximum twice the free field value when the source is located in the floor plane.

2. If the source is located between $\lambda/4$ and $\lambda/2$ away from the floor, a decrease in power output is observed. The minimum value in this region is approximately 0.8 the free field value.

3. At greater distances the effect becomes successively less pronounced.

CONCLUSION

The semi-anechoic environment has been analyzed to determine the nature of the interference field. An analysis is presented which enables the pressure and phase characteristics to be determined at any location in the RTD facility.

1. In general, using single sources, an interference field exists in the vertical direction, always with maximum levels obtained at floor level. The interference pattern decays with separation from the floor when a noise band source is used. The decay is more rapid the larger the ratio of bandwidth to frequency.

2. In general, positions of maximum and minimum sound pressure level are given by

$$h_{max} = \frac{g\lambda Z}{2x}$$

$$h_{min} = \frac{(g + 1/2)\lambda Z}{2x}$$

3. Multiple coherent sources produce fields which must be computed by extension of principles outlined for single sources.

4. Multiple incoherent sources produce an interference field which is computed by energy addition of individual fields alone.

5. Sound fields cannot be computed unless power and directivity of sources, spectral content, and floor reflectivity are known. This must be determined in situ.

SECTION VI

EXPERIMENTAL INVESTIGATION OF REVERBERANT AND SEMI-REVERBERANT ENVIRONMENTS

The characteristics of acoustic fields in rooms possessing reverberant qualities have been the subject of many acoustical studies (Refs. 13 to 17). The testing of sound-absorbing materials, the determination of sound power outputs of sources in reverberation rooms, and the successful design in architectural acoustics, all require a knowledge of acoustic environments in reverberant or semi-reverberant rooms. Analysis of sound fields has concentrated on reverberant rooms in which a diffuse field is assumed to exist, i.e., sound waves arrive at any point from any direction with equal probability and are equal in amplitude and random in phase. Statistical approaches enable the sound field to be described at any distance r from a sound source in such a room by

$$P_r^2 = W\rho c\left(\frac{Q_\theta}{4\pi r^2} + \frac{4}{\beta}\right) \tag{13}$$

This states that the sound power level decreases according to the inverse square law moving away from a sound source and at sufficiently removed distances becomes uniform. A distance r' has been defined as being the distance from the source at which the direct field is equal in magnitude to the diffuse field. Thus

$$r' = \left(\frac{\beta Q_\theta}{\pi}\right)^{1/2} 4 \tag{14}$$

The room constant β is determined by the average absorption of the room. When only room boundaries determine the absorption

$$\beta = \frac{S\bar{\alpha}}{(1 - \bar{\alpha})} \quad ft^2 \ (m^2) \tag{15}$$

and

$$\bar{\alpha} = \frac{\alpha_1 S_1 + \alpha_2 S_2 \cdots}{S_1 + S_2 \cdots} . \tag{16}$$

Air absorption effects require that this absorption coefficient be modified to the form

$$\alpha = \bar{\alpha}' + \frac{4mV}{S} \tag{17}$$

where m is an energy attenuation constant.

The reverberation time of a reverberant room has been determined to be given by

$$T = \frac{.049V}{S\bar{\alpha}} \text{ Sec (English units)}$$

$$T = \frac{.161V}{\beta\bar{\alpha}} \text{ Sec (Metric units)} \qquad (18)$$

This equation, valid only for small values of $\bar{\alpha}$ (0.2 or less), can only be used when the acoustic treatment in the RTD facility is fully collapsed.

Equations (13) through (18) are those typically used to describe the sound environment in reverberant rooms. However, their validity is questionable when diffuse field conditions do not exist in a room. For example, it has been observed that when certain room surfaces have markedly different absorbing properties from other surfaces, reverberation time determinations do not agree with predicted values (Ref. 18). It is also observed that the sound pressure level distribution as described by Eq. (13) is also found not to hold (Ref. 19).

In summary, acoustic environments in reverberation rooms can be described in general terms by Eqs. (13) through (18), but in rooms for which the diffuse field assumption is significantly erroneous these equations will be invalid. Such rooms, possessing both large reflecting and absorbing surfaces may be termed semi-reverberant.

This is, in fact, the situation that will exist in the RTD facility operated in a manner to obtain high sound pressure level diffuse fields.

There are three possible ways of operating the facility to obtain high level fields:

1. The wall treatment is collapsed and the ceiling treatment remains in location.

2. The wall treatment is collapsed but the ceiling treatment is removed from the facility.

3. Both the wall and ceiling treatment are removed from the facility, leaving it devoid of acoustic treatment.

Our study has attempted to discover the acoustic environments that will exist under all three methods of operation, with emphasis on (1) and (2). The removal of all the acoustic treatment is not practical and consequently completely reverberant operation is not anticipated.

Because current theory does not enable the acoustic environments under semi-reverberant operation to be determined, we have pursued an experimental program supported where possible by analytical studies.

Our initial experimental study was performed in IITRI's reverberation room devoid of any acoustical treatment. While this does not represent the RTD facility operation under anticipated operational conditions, it was considered desirable to explore the sound environment under completely reverberant conditions. The reason for this was that the possession of this data will enable comparison to be made with the environment obtained under semi-reverberant operating conditions. It will provide a criteria by which environments may be judged and, if attempts are made to improve semi-reverberant environments, e.g., improve diffuseness characteristics, or increase diffuse sound pressure level, it will serve as a goal. The semi-reverberant studies were conducted under two operating conditions. In one situation an absorbing treatment was applied to the ceiling of the reverberation room and in the second situation this was removed and replaced by a ceiling perimeter treatment. These treatments are described in Section III. Additional information is contained in Appendix B.

The environments were investigated by determining reverberation times, spatial distribution of sound pressure level, and cross-correlation properties. The use of reflectors and partial enclosures to improve semi-reverberant environments was investigated. The characteristics of sound fields on simple structures exposed to acoustic energy in reverberant and semi-reverberant rooms were also investigated.

REVERBERATION TIME

Reverberation time measurements were made for three conditions of operation of IITRI's reverberation room. Under fully reverberant operation these were obtained at three different stations in the center region of the room well away from reflecting wall surfaces. At each station four decay curves were obtained for each frequency of interest and their average decay rates determined. Figure 22-A shows the average of the reverberation times measured at these three locations, together with the spread of this data. Under the two semi-reverberant operating conditions, the reverberation times were determined at four stations. Two stations were 1 ft (0.3 m) above floor level, one in the center of the room and the other in a corner of the room. The other two stations were located in the upper region of the room in order that the effects caused by the proximity of the absorbing treatment could be observed. They were 7 ft (2.1 m) above the floor, one at the center of the room and the other near a wall. These four positions are shown in Fig. 3. Several decay curves were

obtained at each station and their average determined. Because of the wider variations in reverberation time between these stations, the data for each individual station is shown in Figs. 22-B and 22-C, for both methods of semi-reverberant operation. The average reverberation times for each method of semi-reverberant operation are compared to those for fully reverberant operation in Fig. 22-A.

The perimeter treatment has a surface area of 300 sq. ft. (27.9 m^2) and was scaled from the computed surface area of the collapsed curtains in the RTD facility (approximately 3721 sq. ft., 346 m^2). The ceiling treatment alone has an exposed surface area 220 sq. ft. (20.6 m^2). (Appendix B contains calculated values of the area, volume, etc., of the two facilities.)

If we assume Eq. (18) is valid under these semi-reverberant conditions, the ratio of reverberation times with perimeter and ceiling treatment should be inversely proportional to the ratio of total sound absorptions in the room under both modes of operation, assuming a constant room volume. Since the treatments are formed from identical acoustic material, the reverberation times should be in the ratio 220:300 or 1:1.36. It can be seen from Fig. 22-A that the reverberation times are approximately in this ratio.

No reverberation times were determined using both treatments simultaneously. The RTD facility contains a total exposed treatment surface area of approximately 4440 sq. ft. (413 m^2) when the ceiling is present and the wall treatment is collapsed. This would scale to an area of 360 sq. ft. (33.4 m^2). Consequently, we would anticipate reverberation times approximately 0.83 of those determined for the perimeter treatment alone. This is shown dotted in Fig. 22-A.

From the reverberation time measurements we can calculate the effective value of the room constant from Eq. (18). The following table gives calculated values as well as values calculated using Eq. (15). The reverberation times used are those obtained at 500 cps, the lowest frequency for which the absorption coefficient of the treatment is approximately unity (see Fig. 2) and for which air absorption is negligible. Values of the room parameters used in these calculations are given in Appendix B.

	Rev. Time (secs)	β, from Eq. (18)	β, from Eq. (15)	Ratio	Mean
Ceiling Treatment	0.88	198	267	.74	238 ft^2
Perimeter Treatment	0.61	314	381	.82	348 ft^2
Combined Ceiling and Perimeter	0.51	354	599	.59	477 ft^2

It can be seen that the effective room constants are much lower than their calculated values: approximately 0.59 $\rightarrow$ 0.82 times the value. This is in accordance with their location, which does not enable diffuse field theory to apply.

However, it is questionable which value of room constant should be used if it is necessary to calculate the diffuse field level for a given acoustic input power. Inspection of Eq. (13) shows that the values obtained using either value would agree to within 2 db, so the question is only of academic interest. Using the average of these two alternative values for β and scaling this up to a value for the RTD facility operation, the value for β for (a) collapsed wall and ceiling treatment, and (b) collapsed wall treatment alone are 5850 and 4260 ft^2 (.545 m^2 and 396 m^2) respectively. (This latter value may be compared to the value estimated in Ref. 1 of 5030 ft^2 (468 m^2).) Inspection of Eq. (13), shows that the diffuse sound pressure level in the facility with collapsed wall and ceiling treatment is only 1-1/2 db lower than the level with the collapsed wall treatment alone, suggesting there is little to be gained by its removal.

SPATIAL DISTRIBUTION OF SOUND PRESSURE LEVEL

No attempt was made to determine in detail the sound pressure field over the whole volume of the reverberation room operated either semi- or totally reverberant. Instead, the distribution was determined along selected axes in the room. These axes are shown in Fig. 23. They represent a floor diagonal passing through the corner of the room containing the sound source, a vertical axis originating from the floor diagonal at a point well removed from the sound source, and an axis passing through the sound source corner of the room inclined at approximately 38° to the floor. It was considered that the distribution of sound pressure levels along these axes would be sufficient to enable the extent of the direct field to be established and allow reflecting floor and wall and absorbing ceiling effects to be determined.

Figures 24, 25, and 26 show the spatial sound pressure level distribution for both the room containing the perimeter treatment and the room devoid of all treatment. Equal power inputs were used in both cases. It can be seen that the bare room exhibits normal characteristics, i.e., initially an inverse square power loss merging rapidly into a uniform diffuse field.

The room with perimeter treatment produces a less rapid transformation to uniform levels. The distribution along the inclined traverse shows a continuous decrease in sound pressure level, which indicates the absorbing effect of the treatment at the ceiling perimeter. The dashed line superimposed in Fig. 25 is an inverse square law curve and it is seen that

the experimental data fits this very well. This is substantiated by the vertical distributions whose level decreases towards the ceiling.

Similar results are obtained when the ceiling treatment is installed in the reverberation room. Figures 27 and 28 compare distributions under these conditions to those when the treatment was removed. Equal power input conditions were not maintained so the ordinate of the graph is an arbitrary decibel scale.

It is difficult to establish an average difference between sound pressure levels in the diffuse field between reverberant and semi-reverberant operation, because no truly uniform region exists under the latter conditions. However, if we confine observations to the region close to the floor, the following are average values for the case of the perimeter treatment.

Difference in Diffuse Field Level (in db)	8	6	4	2-1/2	4
Frequency (in cps)	200	500	1250	3150	8000
Calculated Difference (in db)	8-1/2	7	6-3/4	4-1/4	3

Also shown are values calculated from knowledge of room constant values determined by the reverberation time. Agreement is seen to be very good.

CROSS-CORRELATION COEFFICIENTS

Information on the phase characteristics of sound fields under reverberant and semi-reverberant conditions was obtained by determining cross-correlation coefficients in these fields.

Generally, these were determined in selected regions of the reverberation room. These regions were all chosen to be at large distances from the sound source located in a room corner. The closest region of investigation to the source was the center region of the room. This criteria was adopted to ensure that it was the diffuse field region of the room being investigated.

Under fully reverberant operation, correlation measurements were made along the floor of the facility in a vertical direction from floor level and in the center region of the facility. The actual location of these regions is shown in Fig. 3. The cross-correlation coefficients determined in these regions are shown in Fig. 29 for the five frequency bands of interest.

With the ceiling treatment installed in the facility, the correlation measurements were made horizontally 2 ft above the floor of the facility, and in the center region of the facility in both a vertical and a horizontal direction. These cross-correlation determinations are shown in Fig. 30.

With this acoustic treatment removed and replaced by the perimeter treatment, correlation determinations were made horizontally 2 ft (.61 m) above the floor and both vertically and horizontally in the center region of the room. These cross-correlation determinations are shown in Figs. 31 and 32.

It must be remarked that the data shown are only representative of typical cross-correlation coefficients for the respective operating conditions in the facility. Variations were observed in the correlation functions depending on the chosen reference position. These variations were most prominent in the case of the perimeter treatment.

The correlation measurements in the fully reverberant room illustrate that the environment is sufficiently diffuse since the form of the correlograms is adequately represented by (sin kx)/kx as suggested in Ref. 14. This curve is superimposed in Fig. 29-A only and shows excellent agreement with the experimental curve obtained at the room's center, away from reflecting surfaces.

The correlation functions determined when the ceiling treatment is installed are not unlike those produced under reverberant conditions, except in cases of the vertical determination. These correlograms are found to have a much longer spatial periodicity. This is equivalent to a greater degree of phase preservation in vertical directions. This suggests that the majority of sound energy is traveling in horizontal directions, because of the acoustic treatment on the ceiling, and so the vertical correlation measurements tend to be made parallel to wavefronts. A similar effect is noted with the perimeter treatment installed in the facility.

MODIFICATION OF ENVIRONMENT

When the facility is operated under semi-reverberant conditions, the sound pressure levels in, and the extent of, the diffuse field are reduced from the values obtained under reverberant conditions. A short experimental study was conducted to investigate the possibility of improving the acoustic environment in the facility, assuming that the absorbing treatment cannot be removed from its location. For this study we operated our facility using the ceiling treatment.

Initial experiments were conducted placing two 6 x 4 ft (1.8 x 1.2 m) reflecting panels in the central portion of the room. They were both inclined at 45° to the floor so as to

form the opposite two sides of an inverted pyramid. The objective was to reflect away from the ceiling sound that would otherwise be absorbed by the acoustic treatment. However, reverberation times were, on the average, decreased by 0.1 → 0.3 seconds over the frequency range of interest, implying that the reverse effect was achieved. The failure of the reflectors to reduce absorption was not unexpected, because a reflector which reflects vertically traveling energy into horizontal directions will likewise perform the reverse function on its rear reflecting surface. The only ultimate solution to the problem would be to locate reflectors immediately at the surface of the acoustic treatment. We were unfortunately unable to pursue this investigation.

Seeking alternative means of overcoming the disadvantages of a permanently located absorbing treatment, the following approach was taken. In many instances, high sound pressure levels may be required in volume regions much smaller than the overall size of the facility. Consequently, we have investigated the possibility of enclosing a small region close to the sound sources using movable plane reflectors, attempting to produce a relatively diffuse field of high sound pressure level in a small volume. A rhomboidal plan was adopted for this volume, having dimensions shown in Fig. 33 with a uniform height of 4 ft (1.2 m). Figure 34 shows the spatial pressure distribution measured along a line inclined at 38° to the floor. The effects of a standing wave system can be observed at the two lowest frequencies but the extent of the direct field at all frequencies, shown below, is less than that experienced when this enclosure is removed.

Frequency (cps)	Extent of Direct Field (ft)	Extent of Direct Field (m)
200	1-1/2	.45
500	1 to 1-1/2	.30 to .45
1250	1/2	.15
3150	1	.30
8000	1/2	.15

This suggests that the diffuse field levels in this enclosure will be higher than those in the room when the enclosure is removed. At a representative station X, in the enclosure, shown in Fig. 33, it was established that sound pressure levels were obtained which were greater than those measured at that point in the absence of the enclosure. The differences, shown below, range from 3-1/2 to 9-1/2 db.

	Sound Pressure Levels Using Enclosure (db)		Sound Pressure Levels Enclosure Removed (db)	
Frequency (cps)	Station X	Station Y	Station X	Station Y
200	109.0	93.5	102.5	95.5
500	106.5	87.5	98.5	91.5
1250	113.5	95.5	104.0	96.5
3150	92.5	73.0	89.0	77.5
8000	80.5	57.0	76.5	63.5

These are significant increases in level in spite of the considerable amount of energy which was transmitted through the 1/2 in. (13 mm) plywood enclosure walls into the outer reverberation room. At a typical station Y, in the outer room, the sound pressure level decreased by only 1 $\longrightarrow$ 6-1/2 db when the plywood enclosure surrounded the sound source, implying that there was a considerable leakage of energy into the outer room.

In the RTD facility such a proposed structure could not be completely contained, because the gas exhaust from the sirens must be removed from the enclosure. Consequently, the effect of displacing one wall so as to produce a slit opening between two adjacent walls through which sound (and air flow) could leak was investigated. An opening 0.25 x 4 ft (.076 x 1.2 m) produced less than 1-1/2 db drop in sound pressure level at a representative point X, in the interior of the enclosure over the frequency range 200 cps to 8000 cps and an opening of 1 x 4 ft (.3 x 1.2 m) produced less than a 3 db drop in level.

These experiments suggest that it would be feasible to enclose a small volume close to the siren system, using movable plane reflectors, to produce higher sound pressure levels than would otherwise exist in the facility if the collapsed acoustic treatment were exposed.

CONCLUSIONS

Experimental studies have revealed the spatial sound pressure level and phase distribution in the model facility of the RTD facility operated under semi-reverberant conditions.

1. It is found that there is a gradual merging of the direct field into the diffuse field, which does not enable the extent of these fields to be determined with certainty. This is caused by the large degree of absorption provided by the ceiling treatment.

2. This treatment is shown to produce pronounced phase preservation in vertical directions but not in horizontal directions. Phase characteristics in horizontal direction are approximately equal to those obtained under fully reverberant conditions.

3. The room constants determined experimentally are shown to be approximately 0.6 $\rightarrow$ 0.8 the calculated values. This will not, however, produce significant error in the determination of sound pressure levels in the facility.

4. A small enclosure located near the source system was shown to produce more intense levels in this region (up to 10 db).

SECTION VII

SOUND FIELDS ON STRUCTURES IN A SEMI-ANECHOIC ENVIRONMENT

A mode of operation (called semi-anechoic case) of the RTD sonic fatigue facility will occur when the absorbing treatment in the facility covers the ceiling and the walls while leaving the floor reflecting. In Sections IV and V the results of the experimental model studies and a theoretical prediction and discussion of these results for the prediction of the incident sound pressure field in the semi-anechoic mode, were examined. The purpose of this section is to attempt to determine the sound field on a simple structure when the interference field into which the structure will be placed is known.

One may attempt to look at the problem theoretically. Reduced to its simplest elements, the problem is: "Knowing the solution to a problem for a certain set of boundary conditions, what is the relation of this solution to the solution obtained if one or more conditions are additionally imposed?" For the case of the RTD facility, this is equivalent to the question: "Knowing the incident acoustic interference field, what relation does this have to the field on a structure subsequently introduced into this field?" At the present time this is a complex, unsolved problem except in a relatively small number of specialized cases, for example, the case of diffraction of a progressive plane wave field at a plate (Refs. 1 and 12).

For this reason, the attack on the problem of sound fields on structures in a semi-anechoic environment was undertaken from a primarily experimental approach. Because of the large number of attainable interference fields and the infinite number of simple structures and possible positions in these interference fields, it was practical only to attempt a limited number of experiments on the simplest of structures, the flat panel. The results of these experiments were used to draw very general conclusions about the characteristics of sound fields on structures, relative to the characteristics of the incident field. To further reduce the complexity of the situation, only single source excitation was used.

First, one may consider the case of a small panel in an interference field, the plane of the panel being parallel to the plane of the source. The panel may be in an interference maximum or minimum, or somewhere in between. Figure 35 shows the sound pressure level contours on a 2 ft (.6 m) square panel with its center (a) in an interference maximum and (b) in an interference minimum. Those contours for surfaces in an interference minimum are relatively more complex in shape than those in a maximum and there is usually a greater range of levels for the contours in the minimum. (It will be seen that the statements in the last sentence are true in general for

all orientations of the plate.) Figure 35 also shows the general fact that the contours on the back of the plate bear little resemblance, in regard to shape, to those on the front of the plate, even though the range of pressure levels are the same.

The form of the sound pressure level contours is due to a combination of sound pressure levels of the incident interference field and the diffraction field on the panel. For the case in Fig. 35, with a ka value of 3, the diffracted field for a plane wave on the panel would have the form of a broad single peak hump of maximum level 9 db above the incident level. When the panel is in an interference maximum, the portion of interference field the panel sees is almost uniform in level. Thus the combined field on the panel would be expected to be a single peaked hump. When the center of the panel is in a minimum, the interference field is one producing high levels on the outer portion of the panel and low levels at the center. This combination of the incident and diffracted fields might be expected to produce a distribution similar to the combined individual distributions (added algebraically on a db scale). These predictions are verified, as illustrated in Fig. 35.

Figures 36 and 37 show the results of rotating a vertical (to the floor) panel about its vertical axis. The panel being perpendicular to the plane of the sources, shows a more or less random geometrical distribution over a relatively small range of sound pressure levels. As the plate is rotated so that it faces toward the source, the contours become well defined, changing from parabolic shapes finally to concentric circles when the plate is parallel to the source plane. Also, as the plate is rotated, the gradients and range of sound pressure levels increase. It should be noted that the contours for the intermediate angles of rotation are similar to those obtained on wings in actual service fields.

Figures 38 and 39 illustrate sound pressure level contours on larger flat panels (4 x 8 ft, 1.2 x 2.4 m) in the vertical position. The resemblance to contours observed on wings in actual service fields is to be again noted. When the panels are in the position of being perpendicular to the plane of the sources (that is, when there is grazing incidence), these contours are seen to be very similar to those obtained when no structure is present. This is a reasonable result since at grazing incidence diffraction effects are minimized.

In order to obtain less complex distributions of a structure, the structure was placed in a simpler orientation to the incident field, parallel to the floor and near the floor.

The results of placing such a horizontal panel in the semi-anechoic interference field is illustrated in Fig. 40. It is seen that the geometry of the contour shapes becomes

more complex (going from parallel straight lines to concentric oval shapes) as the panel is raised from a point on an interference maximum to a point on a minimum. The gradients and range of decibel levels also increase as the plate goes into a region of interference cancellation. This is identical to what occurs in the case of the vertical panel. Another reason for the increasing complexity is the fact that as the diffraction angle increases the diffraction effects become increasingly more noticeable.

In order to further minimize the effect of the incident interference field variation, consideration was next given to the problem of the sound pressure levels on a flat panel inclined at an angle such as to intersect at the point where the floor and source bank meet. This alignment would result in a symmetry of the source and its image with respect to the panel and would have the effect of putting the entire panel in a plane of constant value interference effect. Figures 41 and 42 illustrate typical contour patterns observed when the panel is in interference minima and maxima respectively. Again, it may be generalized that relative to the contours obtained on the panel in interference maximum, the contours obtained with the panel in a relative minimum are more complex and have greater ranges of both pressure levels and gradients.

A comparison of the distributions in Figs. 41 and 42 invites a further generalization. When the panel is in an interference maximum, the highest pressure levels occur on the portion of the panel nearest to the source; when the panel is in an interference minimum, the highest levels occur on the portion of the panel away from the source. Furthermore, it can be seen that the sound pressure contours tend to oscillate in the area of the back one-third of the panel away from the source. The reason for these phenomena is not entirely known at the present time.

It is also noted that for a panel in a position vertical with the floor and at an angle to the sources in a relative minimum of the interference field (Fig. 37), the highest levels are also away from the source. Unfortunately, results for the case where the vertical panel was in an interference maximum were not obtained. However, the data in Fig. 35 for the side of the panel away from the source indicates that the asymmetry holds for the vertical case also. Thus the generalization made in the previous paragraph would seem to be true for any panel orientation.

Figure 43 illustrates the fact that the orientation of a panel is much less critical in determining the contour distribution when the panel is in an interference maximum than when it is in a minimum. This is reasonable when it is noted that the spatial rate of change of pressure levels, measured on a decibel scale, is much smaller near the interference maximum regions than near the minimum regions.

CONCLUSIONS

Due to the complexity of the problem of structures exposed to interference fields, only sound fields on flat panels were investigated in this study. In addition, the study was limited to small ranges of panel size and frequency. The general conclusions obtained are:

1. Contours on panels in incident interference field maxima are usually less complex geometrically, have a smaller range of pressure levels, and have smaller gradients relative to contours on panels in interference minima. The position of the incident interference field maximum or minimum occurs at the same point on the panel at which the combined field maximum or minimum occur respectively.

2. Contour shapes on the two sides of a panel bear little relation to each other.

3. As a vertical (with respect to the floor) panel is rotated so as to face the sources, the contours change from random to parabolic to circular in shape. The gradients and range of pressure levels also increase. When the plane of the panel is perpendicular to the plane of the sources, the sound pressure level distribution is the same as that of the incident interference field.

4. When a panel is in an incident interference maximum, the highest levels occur on the portion of the panel nearest the source; when it is in an interference minimum, the highest levels occur on the portion of the panel farthest from the source.

5. The contour distribution is more sensitive to variation in panel orientation when this panel is located in an interference minimum rather than in an interference maximum.

6. The field on a structure can be determined, to a first approximation, by considering it as a direct algebraic sum on a db scale of the field due to diffraction on the structure and the incident interference field.

7. As the angle of incidence approaches grazing, so the contour distribution approaches that of the incident sound field, i.e., diffraction effects are minimized.

SECTION VIII

SOUND FIELDS ON STRUCTURES IN REVERBERANT OR SEMI-REVERBERANT ENVIRONMENTS

Section VI describes experiments to determine the characteristics of the acoustic environment existing in the reverberation room operated under reverberant or the two semi-reverberant conditions. When a test structure is located in a diffuse field the sound pressure level at its surface will be affected by: (1) its shape and size compared to the wavelength of the frequency of interest, (2) its distance from, and orientation to, the room boundaries, and (3) its surface impedance. If the structure is located in the direct field, i.e., in immediate proximity to the speaker, it is chiefly subject to a uni-directional progressive wave field. The sound field on the structure under these conditions can be determined in the manner reported in Section VII. In this section we consider only structures exposed to diffuse fields. If the test structure is very small compared to the wavelength of interest, the sound pressure level at its surface will be that existing at that point in the absence of the structure. A structure with dimensions large compared to a wavelength will have a sound pressure level at its surface 3 db higher than the level in that region in its absence. This will be true only if the structure's surface impedance is large compared to that of the air medium and if the field is truly diffuse. In general, the surface impedance criteria for structures will be met. The diffuse field condition will not be met if the facility is operated under semi-reverberant conditions when energy flow is absent in certain directions. At intermediate conditions of structure size, diffraction effects comparable to those experienced under progressive sound wave conditions are anticipated.

Consequently, an experimental study was conducted to determine the diffraction effects on structures located in diffuse and semi-diffuse fields. Both pressure amplitude and phase characteristics of the field were investigated for several ka values ranging from $0 \longrightarrow 80$ with major emphasis on semi-diffuse field conditions. The semi-diffuse field condition chosen was that obtained using the full ceiling treatment.

SPATIAL DISTRIBUTION OF PRESSURE ON STRUCTURES

A 2 ft (.6 m) square plane structure was initially located in a vertical plane in the diffuse region of the reverberation room with ceiling treatment, with its center 4-1/2 ft (1.37 m) above floor level. It can, therefore, be considered distant ($> \lambda$) from surface boundaries of the room and consequently lies in the diffuse field rather than the room boundary field.

The sound field distribution, measured along a vertical and horizontal axis through the panel's center, was determined at several frequencies. The sound field was redetermined at the same location with the panel removed. The difference between these sound pressure levels, shown in Fig. 44, is an indication of the diffraction effect under diffuse field conditions. At all frequencies investigated, except 8000 cps, a positive diffraction effect was experienced, i.e., an increase in level was obtained when the structure was inserted in the sound field. The negative effect at the high frequency case was suspect but was repeatable. In addition, when the investigation was repeated for the reverse side of the panel, again a negative effect was observed. The panel was moved to an alternative location in the diffuse field and again the effects of diffraction were investigated on both sides of the panel at the frequency of 8000 cps. Figure 44 shows that a positive effect is observed on one side of the board while a negative effect is observed on the reverse side.

It is seen, in the semi-reverberant facility, that when a plane structure is mounted in a vertical plane, the sound pressure level on its surface is greater than the incident value, because of diffraction effects. This increase reaches a maximum value of approximately 3-4 db for a ka value of 3, being only 1 db for ka = 1. An average value for large values of ka ($>$ 20) is 2 db. It is anticipated, though it was not experimentally verified, that these effects would closely approximate those found under completely reverberant conditions.

The 2 ft (.61 m) square plane structure was then located in a horizontal plane 4-1/2 ft (1.37 m) above the reflecting floor in the diffuse region of the room. The sound pressure level was determined in the plane of the panel in the absence of the panel and again with the panel in position. In this latter case the pressure distribution was measured on both the upper and the lower surfaces of the panel. Again the measurements were made along the two major axes of the panel. Figure 44 shows the diffraction effect averaged for both axes, determined on the upper and lower surfaces of the panel. It may be noted that a positive diffraction effect is experienced on the lower surface of the panel, but on the upper surface diffraction effects are negligible ($\ll$ 1 db) but negative.

The maximum effect on the lower surface is approximately 4 db for a ka value of 7, being only 1 db for ka = 1. An average value for large ka ($>$ 20) values is 2 db. The negligible, but negative, effects on the upper surface of this horizontal panel at all frequencies occurs because little or no sound energy is incident on this surface, since such energy would have to propagate downwards and this direction of propagation is inhibited by the ceiling treatment.

To verify this the panel was left in this location with the ceiling treatment removed and the experiments repeated at

3150 and 8000 cps. The increase on both top and lower surfaces was found equal and for these ka values, 18 and 45, were found to be approximately 2-1/2 db.

CROSS-CORRELATION COEFFICIENT ON STRUCTURES

The 2 ft (.61 m) square panel was replaced in the vertical location, described previously, under the semi-reverberant conditions produced with ceiling treatment. A reference microphone was located on a horizontal major axis of the panel 2 ins. (51 mm) from its edge. This location was chosen to ensure a minimal edge effect. The other microphone was traversed across the same axis to determine correlation function across the panel. This was repeated on the vertical axis of the panel. The distributions obtained are shown in Fig. 46. They may be compared to the correlation coefficient in the undisturbed field shown in Fig. 30. (Note: Figs. 30 and 45 are not drawn to identical scale.)

The panel was then located in the horizontal position described in the previous section on pressure level determination and the correlation function determined on its upper and lower surfaces. The distributions obtained are shown in Fig. 45.

It can be seen in general that the correlograms obtained over the structure's surfaces is very similar to that determined in the same location but with the structure removed. An exception occurs at the lower two frequencies, ka = 1.14 and 2.85, where it is observed that the correlation coefficient over the structure decays less rapidly than in the field alone.

CONCLUSIONS

1. When a plane structure is mounted vertically in the semi-reverberant environment, the diffraction effect produces an increase in the sound pressure level experienced on the structure. This increase has a maximum value of 3 $\rightarrow$ 4 db for a ka value of 3, being only 1 db for ka = 1. For larger ka values, the increase is approximately 2 db.

2. When a plane structure is mounted parallel to the floor of the facility, there is a negligible diffraction effect on its upper surface due to the presence of the absorbing ceiling. On the lower surface a pressure increase is noted, whose values are identical with those described in (1) above.

3. The phase characteristics of the field on the vertically or horizontally mounted panel are generally similar to those at the same location in the absence of the structure. But, for a ka value of 3 or less, phase is preserved over a larger region than when the panel is removed from the environment.

SECTION IX

SOUND FIELD MODIFICATION USING REFLECTORS

A certain versatility has been built into the RTD facility which enables acoustic environmental parameters to be varied to a limited degree. This is achieved through the use of either a single siren or combinations of sirens, the degree of acoustic treatment exposed, the location of the test structure in the large available volume, etc. However, because the versatility of the RTD facility is not unlimited, at some stage in the development of service field simulation techniques, it will be necessary to use some device to modify the acoustic environment in a prescribed region of the facility. The device offering most potential would appear to be a reflector. It has the advantages that (1) it is responsive to a broad range of frequencies, (2) it is not a 'lossy' device and consequently modifies fields with minimal energy loss, and (3) it can be of simple and inexpensive construction.

Surprisingly little information concerning reflectors exists in the literature, especially where the wavelengths of interest are comparable to reflector dimensions. However, the close connection between the scattering (and consequently reflecting) properties of objects exposed to sound fields and the radiating properties of these same objects when they are caused to vibrate enables radiation properties, which have received considerable attention, to be applied to the problem of reflection (Refs. 20 and 21). This formed the basis of our initial approach to the problem of establishing the capabilities of reflector devices. However, experimental approaches were later found necessary to provide the required information on reflector potential.

In order to establish a given reflector's potential to modify the acoustic environment in its vicinity, the following three questions need to be answered.

1. What percentage of the energy incident on the reflector is reflected?

2. What are the directional properties of this reflected energy?

3. What phase relationships exist between the reflected and the incident sound field?

We can anticipate that the answers to these questions will be functions of chiefly structure size and shape, frequency, and angle of incidence of the sound field. We will consider the reflector of interest to be a flat rigid circular disc of diameter 2a, since the radiation problems for pistons have

received most attention. The experimental study, described later, uses a square plate of dimensions 2a x 2a. The analysis for circular discs will be applicable to square plates for identical values of 'a' to first approximation. Figure 47 attempts to predict the percentage of the energy incident on the plate's surface which is reflected from this circular plate when it is exposed to normally incident sound of wave number k. This has been obtained from consideration of the allied radiation problem. It can be seen that for high ka values (> 2.2) 100 per cent of the incident energy is reflected. There are ranges of ka for which over 100 per cent reflection is predicted, the range ka = $2.2 \rightarrow 3.5$ producing the most significant effects (up to 114 per cent at ka = 2.7). It is in this range of ka values for which the most significant diffraction effect is reported in Ref. 1. In that study, sound pressure levels, as much as 10 db above incident value, were observed at the surface of a square structure of dimensions 2a x 2a exposed to a normally incident sound wave for a ka value of 3.5. This suggests that this assumption of reflected energy in excess of incident energy is justifiable, if we assume in these instances that the scattering cross-section of the plate exceeds unity.

The most significant feature of Fig. 47 is that the reflected energy decreases rapidly as the ka values fall below 2 (75 per cent energy reflection). This gives a critical value for 'a' of approximately $\lambda/3$. As 'a' is reduced below this value, so the efficienty of the reflector decreases rapidly. For example, when ka = 1, i.e., "a' is approximately $\lambda/6$, the reflected energy is only 3 per cent of the incident value.

This analysis, which is applicable only to normally incident sound, serves to indicate the lower limiting ka value beyond which a reflector ceases to be efficient.

The directional properties of this reflected energy is of major importance in determining the modifying effect of reflectors on acoustic environments.

The majority of existing data on the directivity of radiating devices is limited to the far field. Under these circumstances the directional properties of a small reflector ($ka < 2$) for normally incident sound are very similar to a doublet source. A large reflector ($ka \gg 2$) produces a highly directional beam, behaving as a specular reflector. Intermediate cases are contained in the literature, e.g., Ref. 8. However, for any anticipated operational reflector, it is the near field directivity which is important since it will be in these regions containing the most intense reflected field that the most efficient sound field modification will occur. Detailed near field radiation patterns are contained in Ref. 22 for limited selection of ka values. In addition, conditions other than normal incidence are anticipated. Consequently,

we adopted an experimental approach to determine the near field of reflectors exposed to an incident sound field.

REFLECTOR CHARACTERISTICS

We chose a square reflector for simplicity and exposed this to an incident sound field under completely anechoic conditions, which required the removal of the reflecting floor from our anechoic room. The anechoic environment was necessary so that we could evaluate the reflector's performance to a uni-directional field obtained from a single-sound source. Using a pure-tone source the region into which the reflector was to be placed was explored to determine the incident sound pressure level distribution. This was achieved by traversing a microphone along a tracking system. The reflector was then located in position and the sound pressure level distribution was re-determined at locations identical to those previously measured. Figure 48 illustrates how the region in front of the reflector was explored in radial directions from the plate's center for the case of normal sound incidence. Exploration along these radial directions revealed a standing wave system formed from combination of the incident sound field in the region of interest and the field formed by reflection from the square plate. Also shown in Fig. 48 is a typical standing wave system measured along a radial direction. Measurement of the successive maximum and minimum levels in the standing wave system enabled the sound pressure level of the reflected wave to be determined relative to the known level of the incident sound field. In this manner it was possible to map out the near field of the reflector at selected locations, which are determined by the positions of the maxima and minima in the standing wave system.

Figures 48, 49, and 50 illustrate the near field distribution determined for normal and 45° incidence for a range of ka values between 1.14 and 32. The contours of equal sound pressure level are relative to the incident sound pressure level at the plate's center. They are observed to become very complex in nature for high ka values and under such conditions must be considered to be only approximate in their position and magnitude. The reason for this is that the method of data analysis produces data at certain discrete locations which are insufficient to construct accurate contour systems. However, the contours serve to indicate the potential of reflector devices in that they can be used to predict approximately the modification to sound fields using a reflector. It may be noted there is a similarity between the magnitude and distribution of the sound pressure level contours for both normal and 45° incidence cases having identical ka values. Their difference is associated with the orientation of the contour distributions. In both cases, the distributions emphasize that the majority of reflected energy is radiated in the direction for which the angle of reflection is equal to the

angle of incidence. Consequently, we believe this data obtained for normal and 45° incidence cases will be representative of a reflector using any anticipated angle of incidence, i.e., approximate range of incidence $0 \rightarrow 45°$. It would not be practical to use reflectors under conditions approaching grazing (i.e., 90°) incidence because the reflected energy would be considerably reduced. In the extreme, at grazing incidence, no acoustic energy would be reflected at all. The experimental method we adopted for discrete frequency signals is not suitable for noise band signals. However, it is anticipated that, if reflectors are used in conjunction with a noise band signal, the complexity of the distribution in the reflected field would be reduced. However, the reflected field sound pressure levels could be expected to resemble some average of the levels obtained for discrete frequency operation.

Phase information on the reflected field for discrete frequency operation was not determined. However, as following studies indicate, phase properties of the reflected field may be satisfactorily assumed to be those based upon a simple ray tracing procedure. This is justified experimentally for reflectors having a ka value greater than 5 (see also Ref. 23).

SOUND FIELD MODIFICATION WITH REFLECTORS

The data obtained on reflector field properties was used to predict sound field modification under the following two conditions: (1) modification to a region in free space, i.e., fully anechoic condition, and (2) modification to a region in free space containing a structure. A discrete frequency source was used for these experiments. Figure 51 shows the orientation of a reflector and sound source to a region of interest. This region was on a radius through the sound source. The region was explored both with the reflector present and with it absent to determine the sound field modification obtained using this reflector. Figure 51 shows a typical measured distribution along line AB. Values for successive maximum and minimum levels in the modified field are listed. These values are relative to the incident sound field level. Also shown are the computed levels of the modification to the sound field, using the reflector amplitude data obtained experimentally. Phase characteristics were obtained using simple ray tracing assumptions.

It can be seen that the agreement between calculated and experimentally determined values of the magnitude of the field in the region of interest is excellent. The positions of maxima and minima were also predicted with accuracy assuming a simple ray tracing technique. This good agreement between computed and experimentally determined fields was found using reflectors with ka values of 5 or greater. Fields calculated for reflectors with lower ka values did not agree with

experimental data either in terms of the magnitude or the position of the interference extrema. This results from the fact that the phase characteristics of the reflected field cannot be determined using ray tracing. Thus for reflectors with low ka values it will be necessary to evaluate the phase in their reflected fields before their modification effects can be computed.

This experimental investigation of an actual sound field modification was repeated with a structure located in the plane of interest. Again, Fig. 51 shows a typical modified sound field along the structure's surface, and shows experimental values for the maximum and minimum sound field modification. Theoretical determination must take into account the effects of diffraction. We assumed that the reflected pressure level, incident almost normally to the surface of the structure, was increased by a factor of two.

Since the ka value for the test panel used in this experiment is 7, this is a justifiable assumption because this pressure doubling as observed in Ref. 1 (p. 60) occurs for ka values of approximately 8 and greater. It can be seen in Fig. 51 that good agreement between calculated and experimental sound pressure levels is obtained. Analysis at other ka values for panel or reflector has not been made, but it can be assumed that good agreement between calculated and experimental sound pressure levels will be obtained if the following conditions are met.

1. ka value for reflector must be greater than 5 so that phase of reflector field is readily determined using ray tracing.

2. ka value for the test structure is greater than 8, so that the pressure doubling of the reflected field incident on the test panel can be assumed.

Using noise signals it is anticipated that this prediction method would also apply. However, the degree of coherence between direct and reflected signals in the region of interest will determine whether the signals must be combined on a pressure amplitude and phase or on an energy basis. Limited experimental studies using noise band signals indicate that the field distributions are spatially identical to those using tone signals but that the interference extrema are less pronounced.

SPECIALIZED REFLECTOR STUDIES

We have considered in earlier parts of this section the generalized problem of sound field modification with reflector devices. We now consider specific cases of sound field modification with reflectors, but now under semi-anechoic operating conditions.

One feature of semi-anechoic operation is that the major variation in sound pressure level exists in a vertical direction because of the interference effect caused by the presence of the reflecting floor. In regions close to the floor the only variations are caused by spherical spreading producing a gradually decreasing level. If major variations in level are required along the floor, a modification to the existing field must be made. One method of achieving this is by the use of reflectors. The following experiments use noise band rather than discrete frequency signals.

Figure 52 shows a simple manner in which this was achieved experimentally. A vertical 4 ft (1.2 m) square reflector was located parallel to and directly in front of the source plane. The sound pressure level distribution both in the presence and in the absence of the reflector was determined: (1) along a vertical line occupied by the vertical axis of the reflector; and (2) along a horizontal line immediately in front of the position of the base of the reflector. This was performed for three noise bands: 200, 500, and 1250 cps. Figure 52 shows both the vertical distribution at the reflector's surface and the horizontal distribution along the floor. It can be seen that the interference distribution in the vertical direction is preserved, except that the overall levels are increased when the reflector is present. This increase is approximately 6 to 7 db, suggesting the structure is acting as a perfect reflector.

The horizontal distribution along the floor which initially is approximately uniform over the region of interest, exhibits interference effects with the introduction of the reflector. It is coincidental that the spatial separation between successive extrema for both vertical and horizontal interference patterns are identical. This occurs because it is the distance of source from reflecting surface which determines the separation and in this particular case the height of the source above the floor is equal to the separation of the vertical reflector from the source. Figure 53 illustrates how a horizontally located reflector can be used to modify the vertical interference pattern in the room. In this particular experimental study the source was located midway between the floor and a horizontal reflector above the floor. Figure 53 shows the sound pressure distribution along a vertical before and after introduction of the reflector. Calculation of the pressure amplitude (before and after introduction of the reflector) along the vertical is also shown. This was computed from knowledge of the signal's auto-correlation function in the manner described in Section V, with the assumption that only a single-source image is produced by the floor and the reflector. In actuality, an infinity of images is produced but successive images have decreasing amplitude and become increasingly incoherent with the original direct and reflected signals.

The experiments described on field modification with reflectors under semi-anechoic conditions have been simple

in that (1) only simple reflector locations and orientation were used, and (2) no structure was present in the region of interest.

The following section describes more experiments for which these conditions were not maintained.

GENERALIZED REFLECTOR STUDIES

Chronologically, this study of sound field modification under semi-anechoic conditions was performed before that performed under anechoic conditions. It was anticipated that generalized reflector information could be obtained as a subsidiary result of experiments on modifying sound fields on structures under semi-anechoic conditions using reflectors. While this task was not accomplished successfully, the experiments are reported here because, besides illustrating the complexity of the problem of modifying sound fields, they do provide indications of reflector potential.

Figure 54 shows views of the experimental set-up. XY represents a plane inclined at 13° to the floor and passing through the base of the speaker bank. This region was selected for the study because of the initial simple distribution existing in any such plane passing through the base of the speaker bank, either in the presence or in the absence of a structure. A square structure of sides 2 ft (.61 m) could be located in this plane at XY for the experiment in which modifications on a structure rather than in a free region were required. A square reflector of sides 3-1/2 ft (1.1 m) was located with rotational or vertical orientations as shown in Fig. 54.

The study was conducted using bands of noise only at the three lowest frequencies: 200, 500, and 1250 cps. In the first study the effect of reflector inclination was investigated. The test structure was located at XY and the sound field determined along the major axis in the direction XY. Several reflector inclinations were investigated and Fig. 55 shows the sound field redetermined on the test structure in the presence of the reflector device. It may be noted that the maximum notification to the sound field at all three frequencies investigated is obtained for reflector positions C, D, and E, i.e., when the reflector is inclined at angles for which an assumption of specular reflection would give maximum effect over a region of the test structure. The change in the sound pressure level on these structures when using reflectors is observed generally to be positive but its magnitude and distribution over the region of interest (XY) varies considerably with inclination or frequency. In our experiments, at each frequency, the reflector inclination was chosen to be that giving the major modification in the previous experiments. Then the sound field modification was re-determined in the

region XY with and without the test structure located in this region. The results of this experiment are shown in Fig. 56. It can be seen that the modification to the region of interest, XY, is greatest when the test structure is present. This is because the additional energy supplied by the reflector to the region of interest is subject to a further diffraction modification caused by the presence of a structure in the region.

A final study was chosen for which the reflector inclination remains constant but its separation from the region of interest XY is varied. In this study the test structure was permanently located in position XY. Figure 57 shows how the sound field modification on the test structure is affected by the distance of the reflector from this region. In general it can be seen that the closer the reflector is to the test structure, the larger is the field modification. At the highest frequency investigated, it is seen that large modifications are obtained using the reflector. The reason for this is not that the reflector is sending considerable energy into the region of interest, but that because the test panel is located in an interference minimum at this frequency, any additional energy will nullify this acoustic cancellation effect.

CONCLUSIONS

This study has shown that reflectors can be used successfully to modify acoustic environments. The near field of reflectors has been explored for a ka range 1.1 to 32 for normal and 45° incidence conditions. The following conclusions on sound field modification using reflector devices can be made.

1. Under fully anechoic conditions the sound field modification, to a region in free space, can be predicted using the near field data acquired in this study using reflectors with ka values greater than 5.

2. Under fully anechoic conditions the sound field modification at a structure's surface can also be predicted if the structure has a ka value greater than 8 so that a pressure-doubling assumption is valid for the reflected energy incident upon it. In addition, the reflector must have a ka value greater than 5.

3. Under semi-anechoic conditions, reflectors were found to produce significant modifications to sound fields on structures. However, because both the structure and the reflector were located in the interference field, no attempt was made to analytically justify the experimental results.

SECTION X

ANALYSIS OF SERVICE FIELD ENVIRONMENTS

One of the main purposes of the RTD Sonic Fatigue Facility is to simulate sound fields encountered on structures in actual service fields. The question arises as to what parameters of the service field are of importance and should be simulated. As an indication of the answer to this question, one may ask what parameters of the field are typically measured as reported in the literature?

First, characteristics of the noise fields of jet engines have been determined while mounted on test stands. Frequency analyses (wide, octave, one-third octave, or narrow band) are made at near and far field locations (Refs. 24 to 26), and attempts have been made to correct for ground reflection effects (Refs. 6 and 24). Consequently, the power spectral content of jet engine noise fields is known at selected stations from which spatial contour distributions can be obtained. Measurement of other parameters, such as correlation properties of the field, is less available. In general, for a given particular operating condition of a specific engine, the noise field is not completely defined in all its parameters or over its whole extent.

One way the RTD facility could be operated is by simulation of the sound field of an engine in the region in which a structure is to be located under service conditions. When this is done the structure could be located in this region and then the field it is subject to should be a simulation of the service field it experiences. Unless the service field is defined in all its parameters and simulation is achieved in all of them, this assumption is not necessarily valid. For example, supposing that the field were defined in the region of interest only in terms of the power spectral content of the noise field; and supposing simulation were achieved in the RTD facility of this power spectral content using several sirens to cover the frequency band desired; then there exist several propagation directions of the incident signal in the region of interest because of the finite siren spacings. If these propagation directions bear no resemblance to those of the service field signal there, although simulation has been achieved, the desired field will not be produced on the structure when it is located in this field. This is because the field on the structure will be diffraction controlled, which is dependent on the angle of incidence.

Consequently, a more reliable approach would be to attempt simulation of the service field as measured on the structure of interest. Even if the service field is defined in terms of only a single parameter, power spectral content for example,

one can attempt to simulate the actual field the structure is subject to. This reasoning has governed our approach to the problem, resulting in a survey of service field data on aircraft structures, rather than the service field alone.

A measurement typically found in the literature is the RMS sound pressure level contours on a structure. Most typical are overall and band sound pressure level contours on wings of aircraft operating under various engine conditions. This is probably the major parameter that it would be desirable to simulate. Pointwise simulation is a very difficult and inefficient way to simulate a distribution which may be quite complex in practice. A less complex method would be to simulate simple areas of distribution having definable characteristics and to "patch" these areas together to obtain the total distribution. A sound pressure level area may be classified in a relatively simple manner by first classifying the general geometric shape of the sound pressure level contours and then statistically classifying the range of pressures, gradients, and radii of curvature. This has been done for measured sound pressure level contours on the B-58A jet airplane (Ref. 28) and the KC-135 jet transport (Ref. 26). Figures 58 to 60 show measured band pressure levels on half wings of the above two aircraft as well as the division of the wing area into regions where simple contours are obtained. Tables II-A to II-E give the statistical range distributions of sound pressure levels, gradients, and radii of curvature along with a general characterization of each region. This statistical data was obtained by first dividing the wing area into a rectangular grid and determining the value of the desired parameter at the intersection of the grid lines.

No mention has been given so far of correlation on structures. The reason for this is that little work has been published on correlation on flight vehicles, so that it is impossible to determine an actual correlation field to be simulated.

The preceding discussion defines the acoustic data which has been reported in the literature and presents a dissection of a representative sampling of the available data into categories of parameters to be simulated. It is expected that this sampling will give a range of the acoustic parameter variation which we would expect to have to be simulated in the facility for present sonic fatigue studies.

PREDICTION OF SERVICE FIELD ENVIRONMENTS

Since there is only a relatively small amount of sufficiently measured data on aircraft structures, an attempt was made to calculate the sound pressure level at a wing's surface knowing only the distribution of pressure levels in a plane passing through the axis of the engine, when the engine

is in a free field. The effect of being able to do this would be to increase inexpensively and conveniently the amount of service field data on structures by simple calculations from previously measured free field engine data.

Let the distribution of sound pressure levels (due to an engine in a free field) in any plane passing through the axis of the engine be known. Making the assumption that these levels are the same for any plane through the jet axis (in other words, cylindrical symmetry) consider a plane parallel to the plane of the wing's surface. The question becomes: "Given a sound pressure level in the engine plane, what will the pressure distribution be in a plane parallel to the original plane?"

Since the distance from the axis through the engine is the determining factor, a simple construction will determine the point on the second plane which has the identical pressure of a given point on the jet axis plane. This is given by the equations

$$y' = \sqrt{y^2 - h^2} \tag{19}$$

$$x' = x \tag{20}$$

where (x', y') are the coordinates of the point in the plane parallel to the jet-axis plane corresponding to the point with coordinates x and y, and where h is the distance between planes (Fig. 61). It is to be noted that this calculation does not take into account effects such as pressure doubling at the surface and diffraction effects which occur on real surfaces. A simple generalization of this procedure, equating sound pressure levels of points the same distance from the engine axis on a plane perpendicular to the axis, will allow the sound pressure levels along any surface to be determined.

A calculation of sound levels on the wing of the KC-135 was attempted from known data on the near field overall sound pressure levels of the J-57 jet engine (Ref. 26) at military power (Fig. 61). These results were compared with results measured on the KC-135 wing at full wet power (Ref. 27). A comparison of levels measured on the B-58 wing (Ref. 28) at maximum preheat and those calculated from engine data (Ref. 25) with afterburner was also made for overall and band levels (Figs. 58 and 62). (Other comparisons could not be made because of the lack of sufficient coordinated data.) Since the C-135 has two engines on each half wing, the sum of the contributions due to each engine was added under the assumption that they were incoherent relative to each other.

A comparison of the calculated results and the actual measured results shows a high degree of geometrical congruence between contours on the wings. However, the absolute sound

pressure levels of the contours as calculated are as much as 15 db lower than those measured on the wings. This discrepancy could be due to a combination of several causes. First, the operating conditions for the engine alone and the engine on the plane were different. Second, the effects of pressure diffraction were not considered in the calculations. Nevertheless, this method is of value since it predicts the shape of the sound pressure level contours to a close degree.

CONCLUSIONS

Sound pressure level contours as obtained on structures in actual service fields were obtained. These distributions were subdivided into areas with simple characteristics that could be simulated more easily than the distribution on an entire surface. The significant characteristics themselves were delineated. A method was devised for permitting the calculation of sound pressure levels on a surface, when the spatial distribution of levels for the engine alone was known. This method allowed the shape of contours on a wing to be accurately predicted, but it was unable to predict their absolute levels.

SECTION XI

CONCLUSIONS AND RECOMMENDATIONS

As a result of the research concerning utilization of the RTD Sonic Fatigue Facility for the production of acoustic environments, the following conclusions and recommendations are made.

CONCLUSIONS

1. An analysis has been presented which will enable the sound environment existing under semi-anechoic operating conditions to be determined at any point in the facility for any method of siren operation. Experimental verification of this analysis has been demonstrated.

2. An experimental program has enabled the nature of the semi-reverberant environment to be established and has revealed the part played by the absorbing treatment in determining the characteristics of this environment.

3. An experimental program to determine the acoustic field on structures subjected to a semi-anechoic environment has demonstrated the complexity of combined interference and diffraction effects.

4. An experimental program to determine the acoustic field on structures subjected to a semi-reverberant environment has enabled the diffuse field diffraction effects to be determined. The role of the absorbing treatment in determining these effects has been established.

5. A study of reflector performance has enabled sound field modification effects to be predicted under anechoic operating conditions and has enabled limited prediction under semi-anechoic operation.

6. An analysis of current service noise fields on aircraft structures has enabled ranges for the values of the major service field parameters to be determined. This data provides an indication of the fields which must be produced in the facility for service field simulation purposes.

RECOMMENDATIONS

1. In order that the environment under semi-anechoic operating conditions can be predicted with high accuracy, the characteristics of the sirens' performance, in situ, must be determined. We therefore recommend an experimental study, conducted in the RTD facility, to evaluate the sirens' performance as well as that of the acoustic treatment, and the reflection characteristics of the floor, etc.

2. Effort should be devoted to evaluating the performance of the facility both under semi-anechoic and semi-reverberant operating conditions to verify conclusions we have established in this model study.

3. A major area requiring further research effort is that in which combined interference and diffraction effects take place. This occurs when structures are located in the semi-anechoic environment.

4. Finally, it is recommended that further consideration be given to sound field modification using devices such as reflectors.

REFERENCES

1. Tyzzer, F.G. and Pernet, D.F., "Analytical and Experimental Investigation of the Acoustic Environment of the RTD Sonic Fatigue Main Test Chamber," FDL TDR 64-26, April 1964.

2. Hopkins, H.F. and Stryker, N.R., "A Proposed Loudness Efficiency Rating for Loudspeakers and the Determination of System Power Requirements for Loudspeakers," Proc. Inst. Radio Engrs., Vol. 36, March 1948, pp. 315-335.

3. McAuliffe, D., "Design and Performance of a New Reverberation Room at Armour Research Foundation, Chicago, Illinois," J. Acoust. Soc. Am., Vol. 29, No. 12, December 1957, pp. 1270-1273.

4. Kolb, A.W. and Rogers, O.R., "The ASD Sonic Fatigue Facility," 30th Symposium on Shock and Vibration, Detroit, Michigan, 10-12 December 1961.

5. Franken, P.A., "A Theoretical Analysis of the Field of a Random Noise Source Above an Infinite Plane," NACA TN 3557, November 1955.

6. Howes, W.L., "Ground Reflection of Jet Noise," NASA TR R-35, 1959.

7. Pernet, D.F., "Interference and Correlation," 5th International Congress on Acoustics, Liege, Belgium, September 1965.

8. Olson, H.F., Acoustical Engineering, Van Nostrand Co., Inc., New Jersey, 1957.

9. Beranek, L.L., Acoustics, McGraw-Hill Book Co., Inc., New York, 1954.

10. Cole, J.N., Powell, R.G., Oestreicher, H.L., and Von Gierke, H.E., "Acoustic Siren for Generating Wide-Band Noise," J. Acoust. Soc. Am., Vol. 35, No. 2, p. 173, 1963.

11. Waterhouse, R.V., "Output of a Sound Source in a Reverberation Chamber and Other Reflecting Environments," J. Acoust. Soc. Am., Vol. 30, No. 4, p. 4, 1958.

12. Wiener, F.M., "The Diffraction of Sound by Rigid Discs and Rigid Square Plates," J. Acoust. Soc. Am., Vol. 21, No. 4, p. 334, 1949.

13. Morse, P.M. and Bolt, R.H., "Sound Waves in Rooms," Rev. Mod. Phys., Vol. 16, April 1944, p. 69-150.

14. Cook, R.K., Waterhouse, R.D., Berendt, R.D., Edelman,S., and Thompson, M.C., Jr., "Measurement of Correlation Coefficients in Reverberant Sound Fields," J. Acoust. Soc. Am., Vol. 27, November 1955, p. 1072.

15. Knudsen, V.O., Architectural Acoustics, Chapter V, John Wiley and Sons, Inc., New York, 1932.

16. Balachandran, C.G., "Random Sound Fields in Reverberation Chambers," J. Acoust. Soc. Am., Vol. 31, October 1959, p. 1319.

17. Waterhouse, R.V. and Cook, R.K., "Interference Patterns in Reverberant Sound Fields," J. Acoust. Soc. Am., Vol. 37, No. 3, March 1965, p. 424.

18. Fitzroy, D., "Reverberation Formula Which Seems to be More Accurate with Nonuniform Distribution of Absorption," J. Acoust. Soc. Am., Vol. 31, No. 7, July 1959, p. 893.

19. Beranek, L.L., Noise Reduction, McGraw-Hill Book Co., Inc., New York, 1960, p. 242.

20. Wiener, F.M., "On the Relation Between the Sound Fields Radiated and Diffracted by Plane Obstacles," J. Acoust. Soc. Am., Vol. 23, No. 6, November 1951, p. 697.

21. Morse, P.M., Vibrations and Sound, McGraw-Hill Book Co., Inc., New York, 1948, p. 348.

22. Stenzel, H., Leitfaden zur Berechnung der Schallvorgange, Berlin, J. Stringer, 1939.

23. Rschevkin, S.N., A Course of Lectures on the Theory of Sound, MacMillan Book Co., New York, 1963, pp. 442-444.

24. Eldred, K.M., White, R.W., Mann, M.A., and Cotis, M.G., "Suppression of Jet Noise with Emphasis on the Near Field," ASD TDR 62-578.

25. Cox, R., Parry, H., and Clough, J., "A Study of the Characteristics of Modern Engine Noise and the Response Characteristics of Structures," WADD TR 60-220, 1961, p. 24-27.

26. "Acoustic Data--Moses Lake Sonic Environment and Vibration Test," Report No. ESD 906S, Boeing Airplane Co.

27. Morgan, J., "B-526 Half-wing Sonic Test," Final Report, Boeing Airplane Company.

28. Anderson, J.D., "Ten Hour Maximum Afterburner Power Ground Sonic Fatigue Test of B-58A S/N-1021," Convair Division, General Dynamics Corp. Report No. FZS-4-212, 1960.

29. Blackstock, D.T., "Propagation and Reflection of Plane Sound Waves of Finite Amplitude in Gases," NR-384-903, Tech. Mem. No. 43, Office of Naval Research, June 1960, p. 177.

TABLE I

SCALING PARAMETERS FOR ACOUSTICAL ENVIRONMENTAL STUDIES IN ANECHOIC AND REVERBERATION ROOMS

	IITRI's Anechoic and Reverberation Rooms	RTD Sonic Fatigue Facility
	Anechoic Operation	
Signal Frequency, cps	nf	f
Signal Bandwidth, cps	$n.\delta f$	δf
Structure Dimensions, ft (m)	d/n	d
$\frac{\text{Structure Dimensions}}{\text{Frequency}}$, ft sec (m sec)	$\frac{d}{f}$	$\frac{d}{f}$
Facility Dimensions, ft (m)	Independent	$L_i (i = 1,2,3)$
	Reverberant Operation	
Frequency, cps	nf	f
Structure Dimensions, ft (m)	d/n	d
$\frac{\text{Structure Dimensions}}{\text{Frequency}}$, ft sec (m sec)	$\frac{d}{f}$	$\frac{d}{f}$
Facility Dimensions, ft (m)	L_i/n	$L_i (i = 1,2,3)$
Facility Volume, ft^3 (m^3)	V/n^3	V
Facility Surface Area, ft^2 (m^2)	S/n^2	S
Acoustic Treatment Area, ft^2 (m^2)	A/n^2	A
Absorption Coefficient at Frequency nf in Model f in Full Scale Facility	α_{nf}	$\alpha_f (=\alpha_{nf})$
Room Constant, ft (m)	β/n^2	β
Reverberation Time, sec	T/n	T
Mean Free Path, ft (m)	M/n	M
Extent of Direct Field, ft (m)	r'/n	r'

TABLE II-A

CHARACTERISTICS OF SERVICE FIELDS ON WINGS

Aircraft: B-58-A with Engines at Maximum Pre-heat

Area (1): Rear Half of Wing, Truncated Right Triangle (see Fig. 60)

Parameter	Value of Parameter in Band			
	Overall	20-74 cps	150-300 cps	600-1200 cps
Range of Sound Pressure Levels (db)	150-168	128-148	142-162	146-154
Range of Gradients (db/ft)	.30-1.40	.10-2.0	.17-1.95	0.0-.87
Range of Radii of Curvature (ft)	.9 -47.5	1.4-37.4	1.3-53.0	5.5-43.8

Comments

1. Sound Pressure Level Contours

The contours are concentric and generally parabolic in Region (A) and changed to hyperbolic in Regions (B) and (C). The highest levels occur in Region (A). The highest band levels are in the 150-300 cps band.

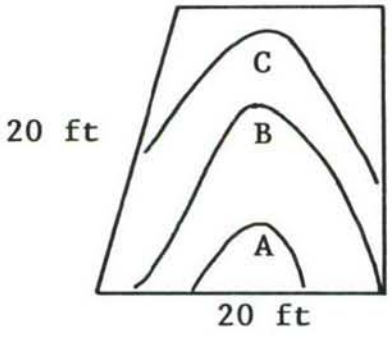

2. Gradients

The gradients vary relatively little with frequency with the highest values in Region (B).

3. Radii of Curvature

The radii of curvature appear to be independent of frequency, and are generally larger towards the inner and outer regions of the wing.

TABLE II-B

CHARACTERISTICS OF SERVICE FIELDS ON WINGS

Aircraft: B-58-A with Engines at Maximum Pre-heat

Area (2): Front Half of Wing, Right Angle Triangle (see Fig. 60)

Parameter	Value of Parameter in Band			
	Overall	20-74 cps	150-300 cps	600-1200 cps
Range of Sound Pressure Levels (db)	140-150	120-130	130-140	134-142
Range of Gradients (db/ft)	.21-.80	.03-.31	.16-.44	.27-.61
Range of Radii of Curvature (ft)	9.1-34.7	20.1-40.2	9.1-21.9	14.6-36.5

Comments

1. Sound Pressure Level Contours

The contours are slightly curved and parallel, with the levels decreasing as one proceeds from Region (A) to Region (B). The highest band levels are in the 600-1200 cps band.

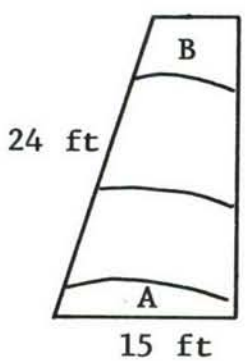

2. Gradients

The gradients are nearly constant with regard to both frequency and position.

3. Radii of Curvature

The radii of curvature appear to be independent of frequency and tend to increase from Region (A) to Region (B).

TABLE II-C

CHARACTERISTICS OF SERVICE FIELDS ON WINGS

Aircraft: KC-135 with Engines at Full Wet Power

Area (1): Wing Section Behind and Out from Outboard Engine, Rectangular Area (see Fig. 60)

Parameter	Value of Parameter in Band			
	Overall	37.5-75 cps	150-300 cps	600-1200 cps
Range of Sound Pressure Levels (db)	152-165	130-155	140-160	148-160
Range of Gradients (db/ft)	1.0-2.2	.80-2.6	.75-5.0	.7-2.0
Range of Radii of Curvature (ft)	6-25	4-22	9-44	2-10

Comments

1. Sound Pressure Level Contours

The general shape of the contours are concentric hyperbolas, with the levels decreasing from (A) to (C). The highest band levels occur in the 600-1200 cps band.

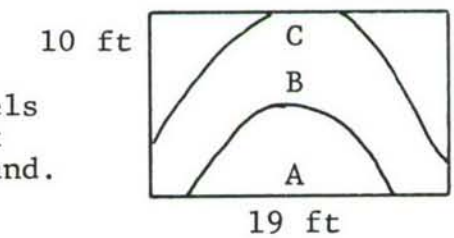

2. Gradients

The largest gradients occur in the central portion of the (B) region. The largest gradients occur in the 150-300 cps band.

3. Radii of Curvature

The radii of curvature increase almost linearly from Region (A) to Region (C).

TABLE II-D

CHARACTERISTICS OF SERVICE FIELDS ON WINGS

Aircraft: KC-135 with Engines at Full Wet Power

Area (2): Wing Section Behind and Out from Inboard Engine, Rectangular Region (see Fig. 60)

Parameter	Value of Parameter in Band			
	Overall	37.5-75 cps	150-300 cps	600-1200 cps
Range of Sound Pressure Levels (db)	157-164	130-150	145-160	150-155
Range of Gradients (db/ft)	.35-1.0	0-6.0	.6-5.0	.2-1.4
Range of Radii of Curvature (ft)	1.8-25.6	1.8-44	4.6-65	2.7-18.3

Comments

1. Sound Pressure Level Contours

The contours are concentric and generally parabolic (compared to those in Area (1)). They exhibit a less regular pattern than those in Area (1). The highest levels occur in the 150-300 cps and 600-1200 cps bands.

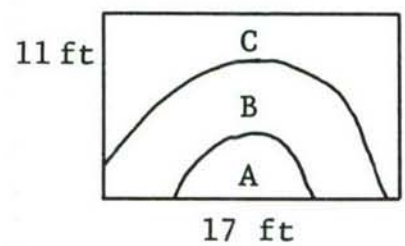

2. Gradients

There is no specific pattern but the highest levels are usually in the center of Region (C). The largest gradients are found in the 37.5-75 cps band.

3. Radii of Curvature

The radii of curvature tend to increase from Region (A) to Region (C). The largest radii occur in the 150-300 cps band.

TABLE II-E

CHARACTERISTICS OF SERVICE FIELDS ON WINGS

Aircraft: KC-135 with Engines at Full Wet Power

Area (3): Outer Section of Wing to Wing Tip, Approximate Rectangle (see Fig. 60)

Parameter	Value of Parameter in Band			
	Overall	37.5-75 cps	150-300 cps	600-1200 cps
Range of Sound Pressure Levels (db)	145-158	125-135	140-150	143-153
Range of Gradients (db/ft)	1.1-1.3	.9-1.6	.6-1.25	.5-.9
Range of Radii of Curvature (ft)	35-73	25-51	6-91	16-40

Comments

1. Sound Pressure Level Contours

The contours tend to be slightly curved, parallel arcs which tend to straighten out in Region (D) levels decrease from Region (A) to Region (C). Highest levels occur in 600-1200 cps band.

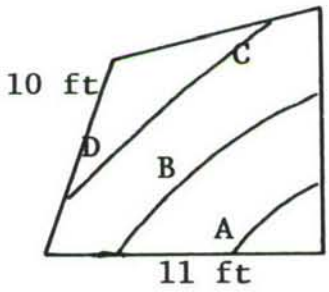

2. Gradients

The range of gradients vary relatively little in any frequency band, compared to other areas; (1), (2), and (5). The highest gradients occur in the 37.5-75 cps band.

3. Radii of Curvature

The radii tend to be large relative to other areas of the wing. The radii increase from Area (A) to Area (B).

TABLE II-F

CHARACTERISTICS OF SERVICE FIELDS ON WINGS

Aircraft: KC-135 with Engines at Full Wet Power

Area (4): From Inboard Engine to Fuselage (see Fig. 60)

There was insufficient data to make an analysis.

TABLE II-G

CHARACTERISTICS OF SERVICE FIELDS ON WINGS

Aircraft: KC-135 with Engines at Full Wet Power

Area (5): Behind and Between Engines, Square Area (see Fig. 60)

Parameter	Value of Parameter in Band			
	Overall	37.5-75 cps	150-300 cps	600-1200 cps
Range of Sound Pressure Levels (db)	152-162	132-142	142-155	147-159
Range of Gradients (db/ft)	.6-1.1	0.0-3.0	.75-1.7	.5-1.25
Range of Radii of Curvature (ft)	6-66	1.8-45	7-46	4-15

Comments

1. Sound Pressure Level Contours

The contours are generally concentric hyperbolas, with the highest levels occurring in Region (A). The highest band levels occur in the 600-1200 cps band.

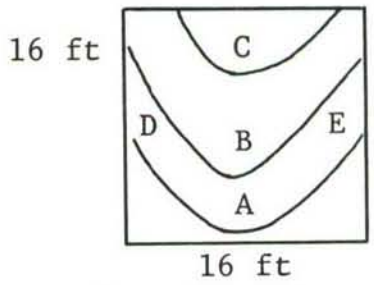

2. Gradients

There are no significant characteristics other than that the gradients tend to be highest in Regions (D) and (E). The highest gradients occur in the 37.5-75 cps band.

3. Radii of Curvature

There is a wide range of radii for the two lower bands. The 600-1200 cps band has a much smaller range. Area (C) tends to have the largest radii.

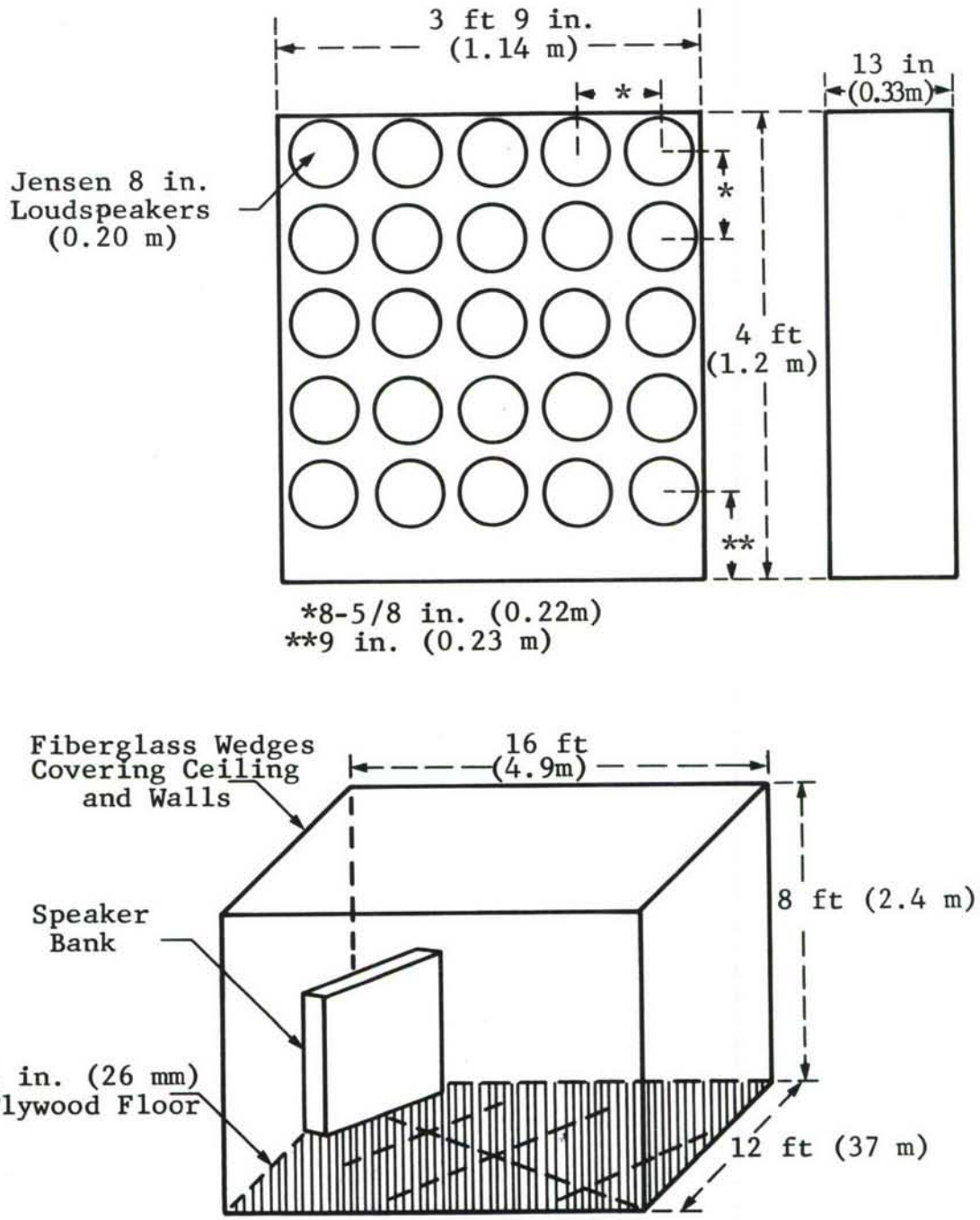

Figure 1. Speaker Bank and its Location in Model Semi-Anechoic Facility.

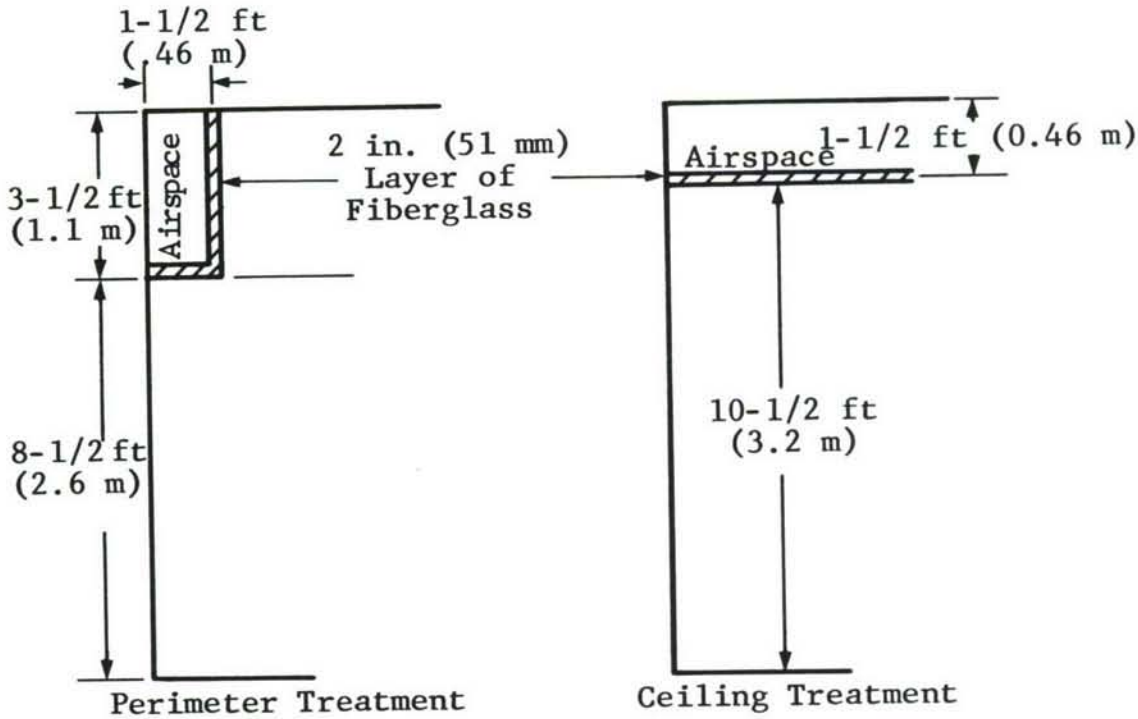

Note: 1. Wall and Ceiling Splaying Not Shown.
2. Numerical Dimensions Represent Average Values (see Appendix B).

Frequency cps	125	250	500	1000	2000	4000
Absorption Coefficients	0.44	0.72	0.99	0.99	0.95	0.93

Figure 2. Details of Absorbing Treatments for Semi-reverberant Model Facility Operation.

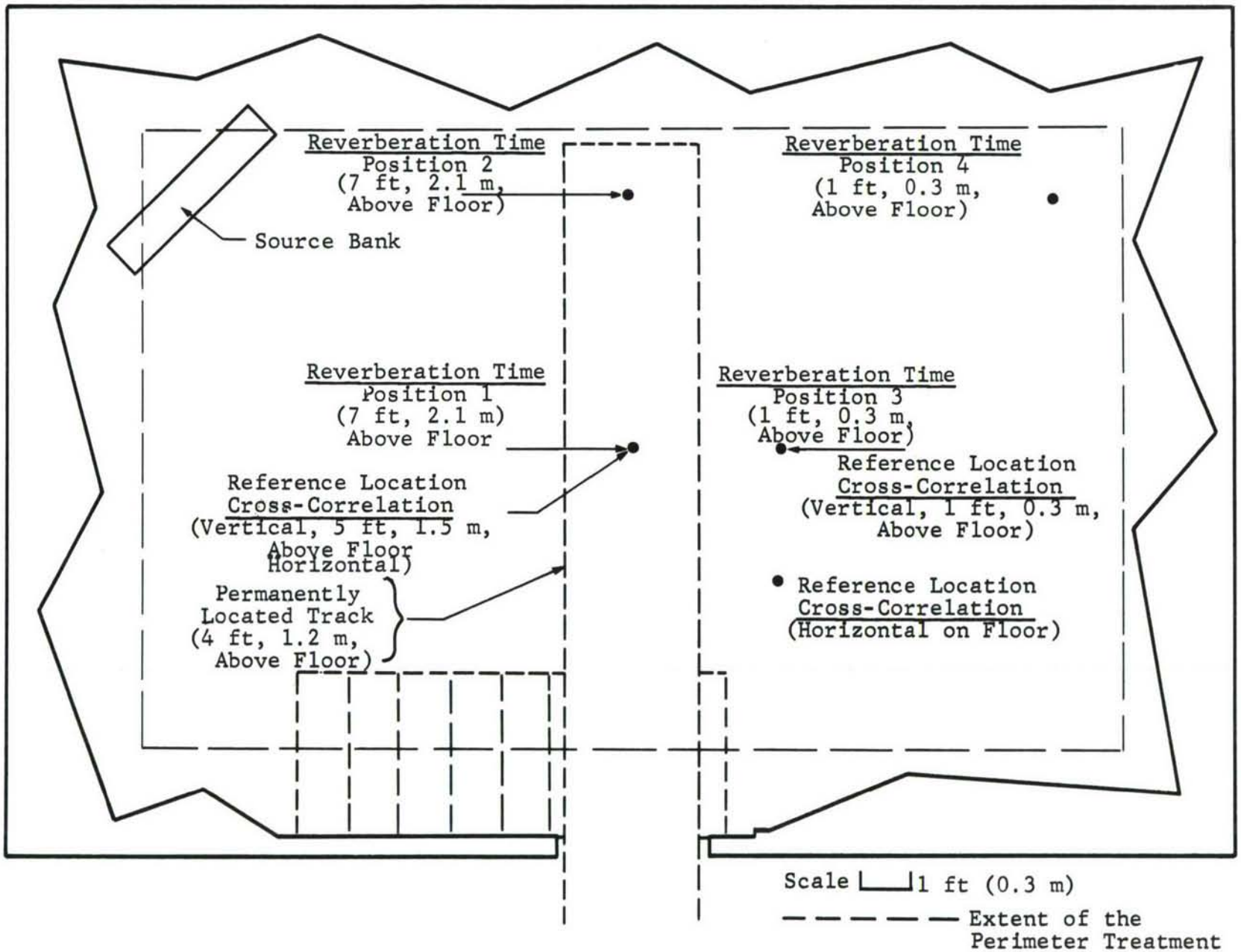

Figure 3. Plan of Reverberation Room, Showing Source and Measuring Stations Positions.

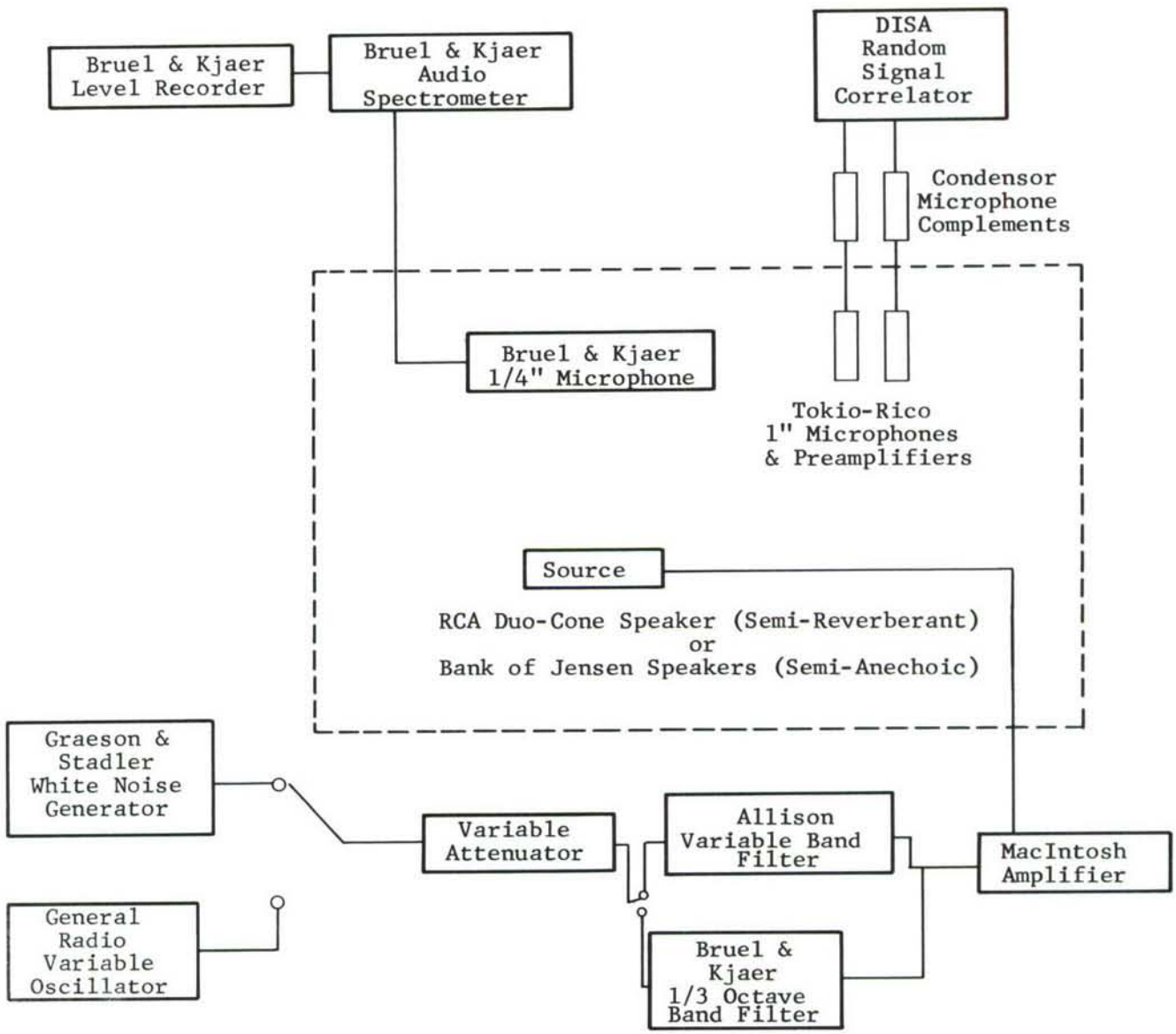

Figure 4. Experimental Setup.

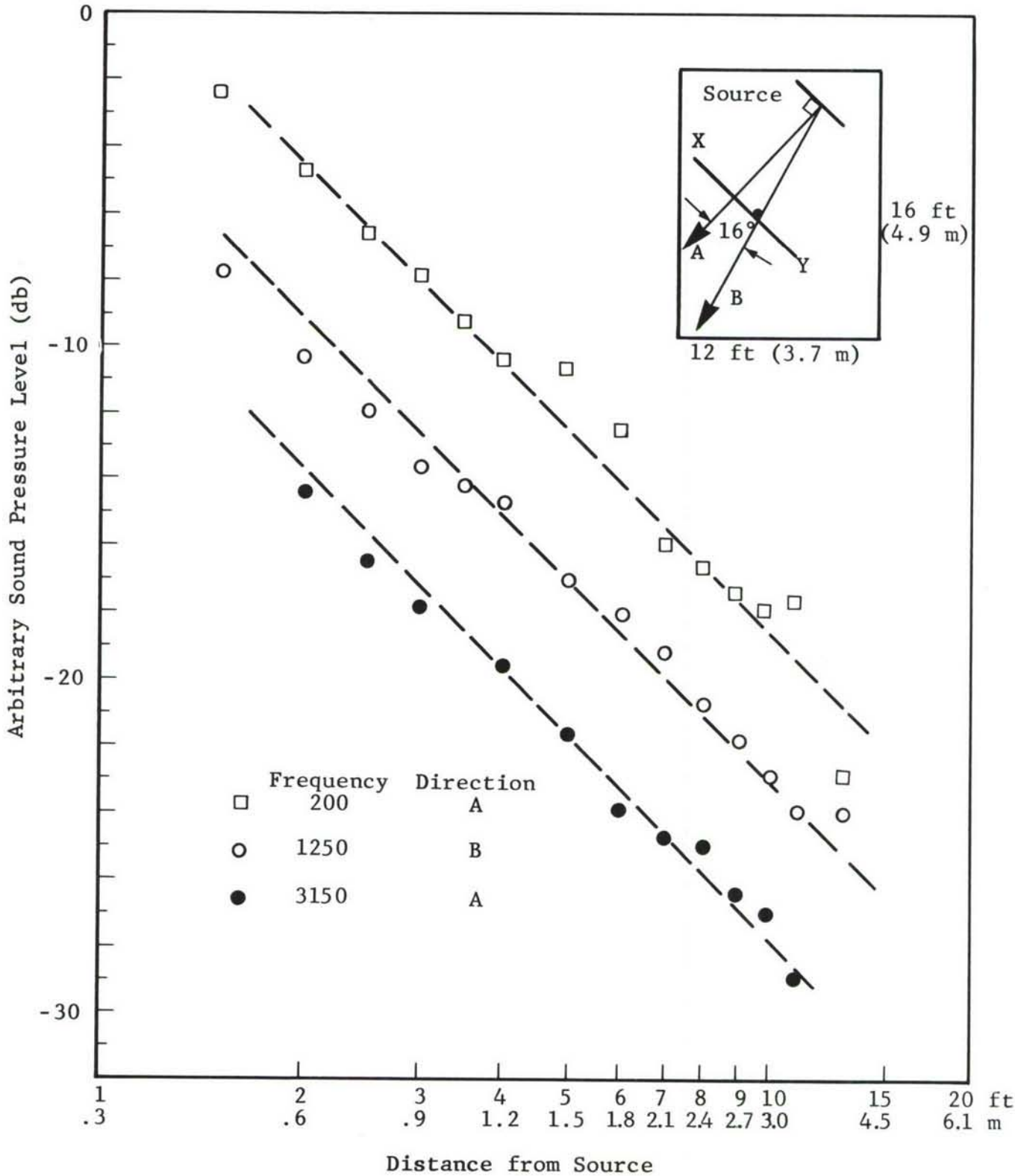

Figure 5. Inverse Square Law Effects

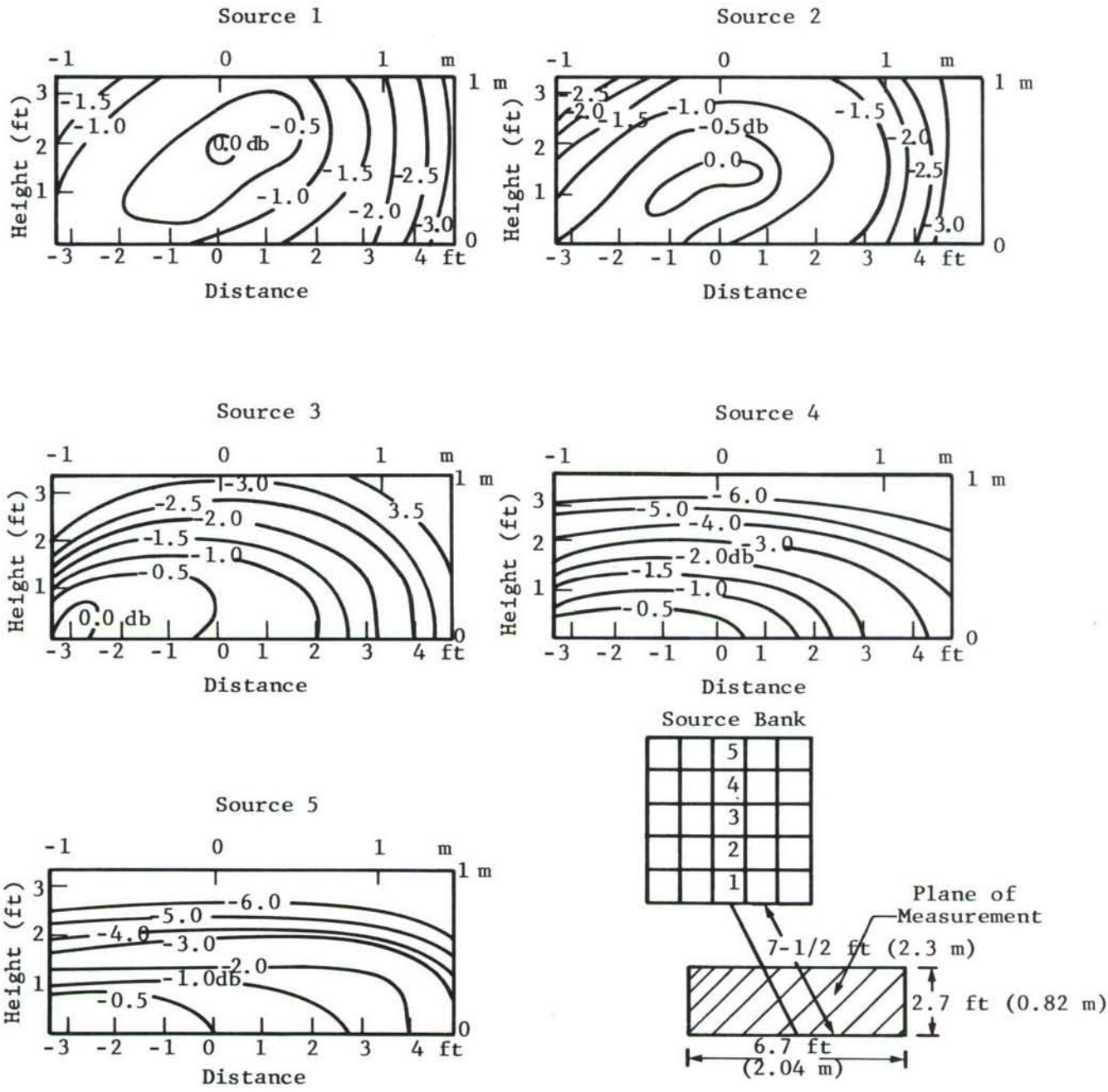

Figure 6. Sound Pressure Level Contours in a Plane, Semi-anechoic Environment, Single Source Excitation: White Noise Band 200 $\pm$ 100 cps.

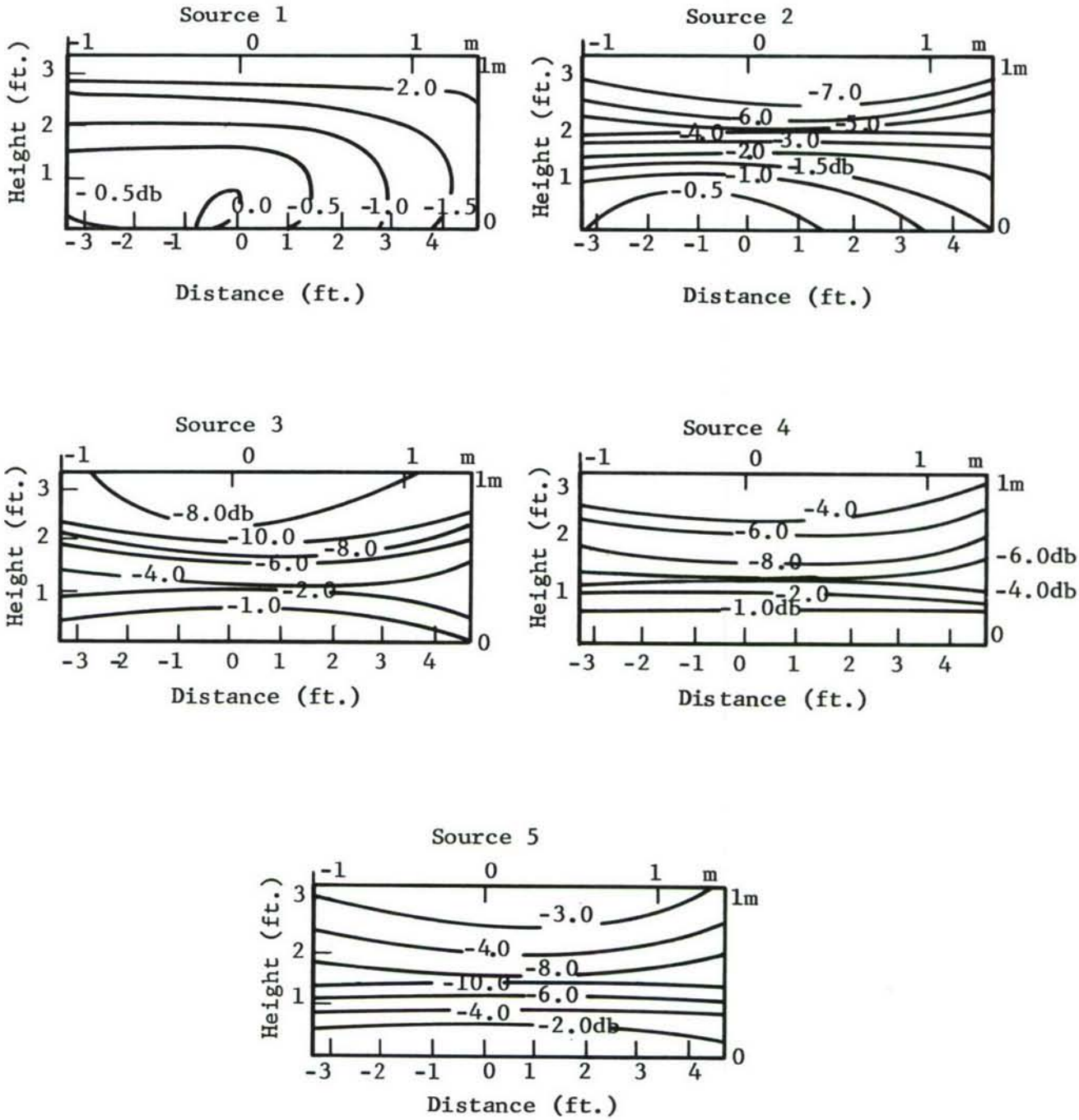

Figure 7. Sound Pressure Level Contours in a Plane Semi-Anechoic Environment. Single Source Excitation White Noise Band: 500 ± 100 cps

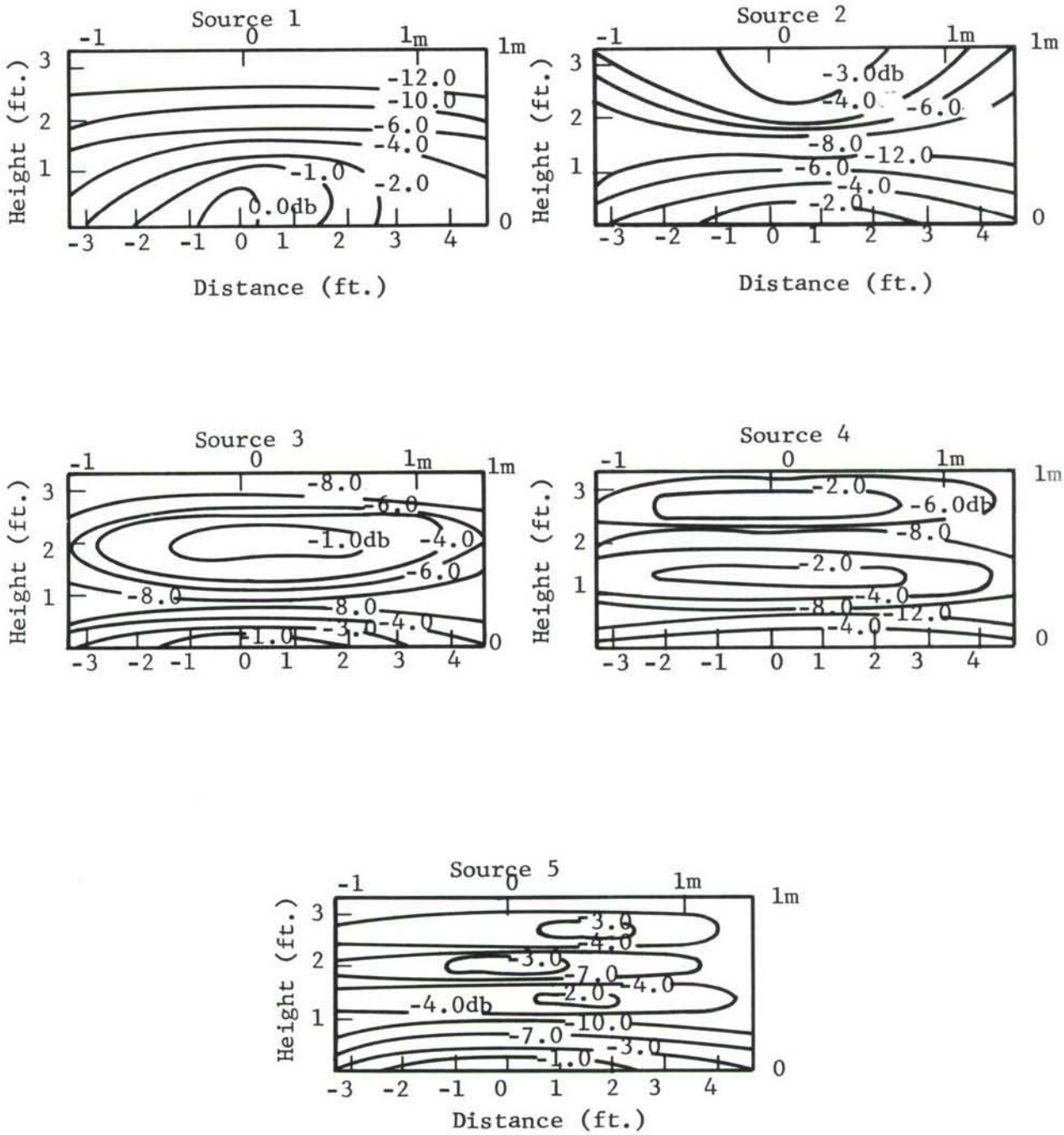

Figure 8. Sound Pressure Level Contours in a Plane, Semi-Anechoic Environment. Single Source Excitation. White Noise Band 1250 $\pm$ 100 cps.

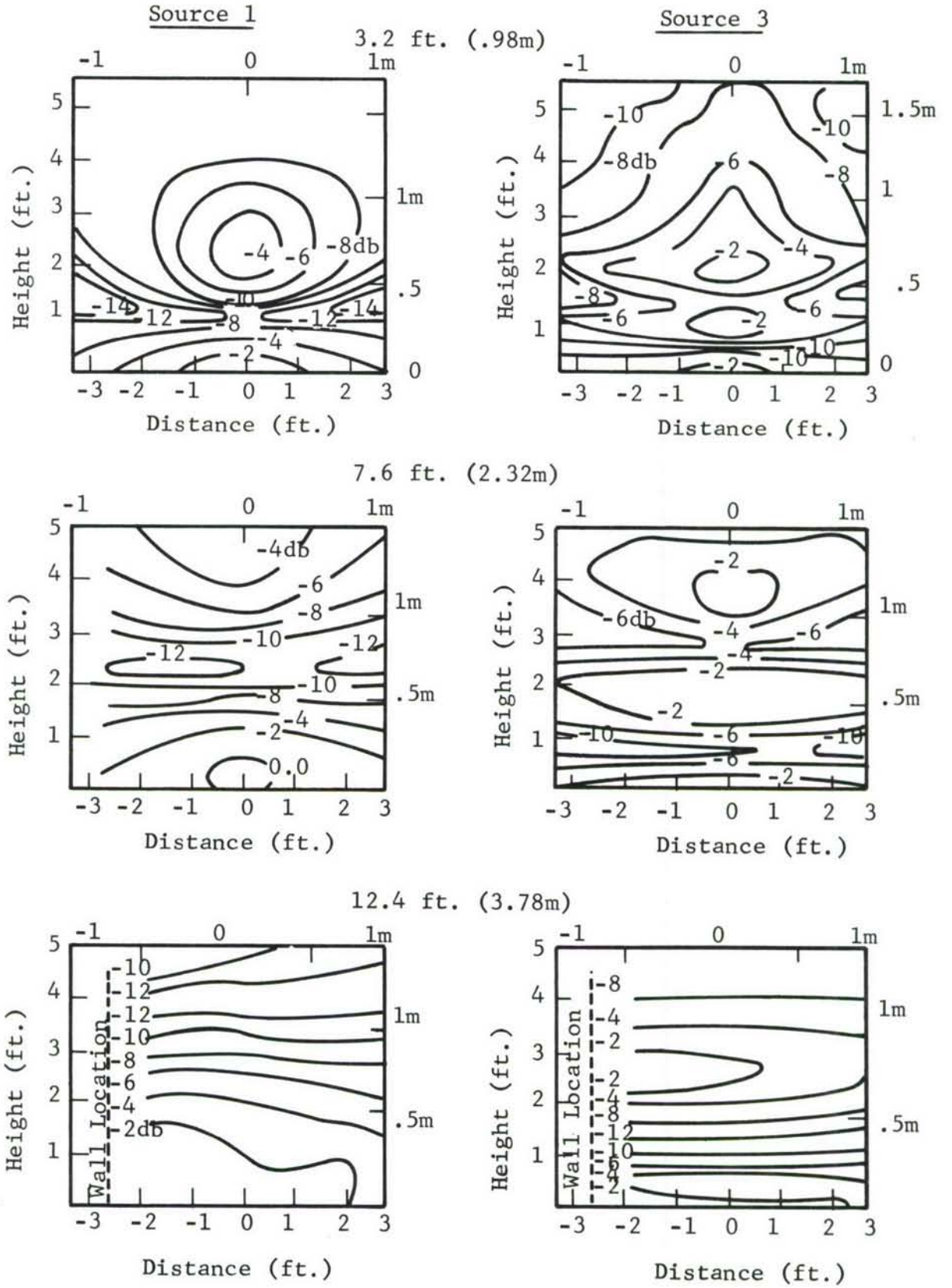

Figure 9. Sound Pressure Level Contour Distributions as A Function of Source Separation, Single Source Excitation Semi-Anechoic Environment, White Noise Band 1250 ± 100 cps.

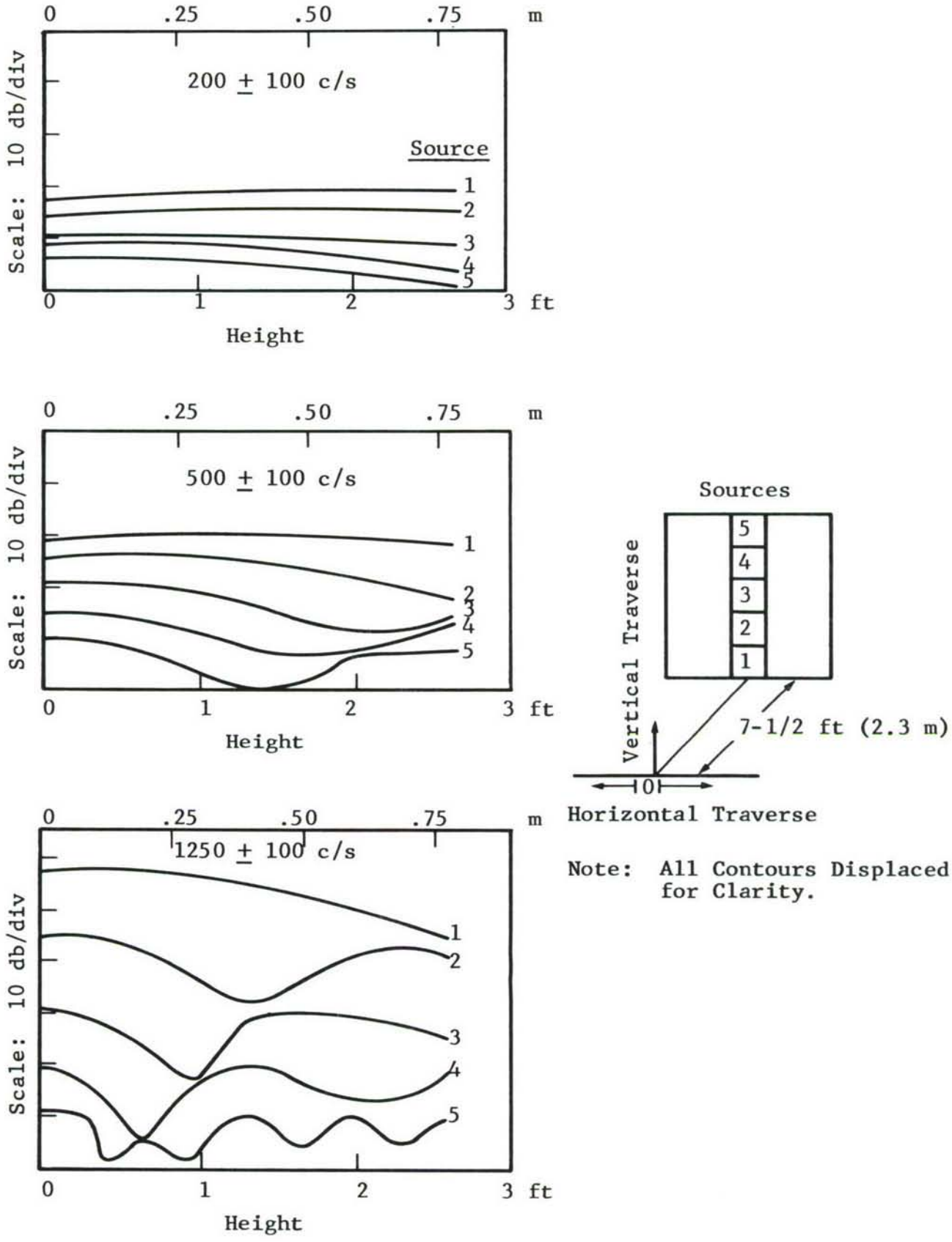

Figure 10. Sound Pressure Level Profiles in a Vertical Line, Semi-anechoic Case, Bands of White Noise, Single Source Excitation.

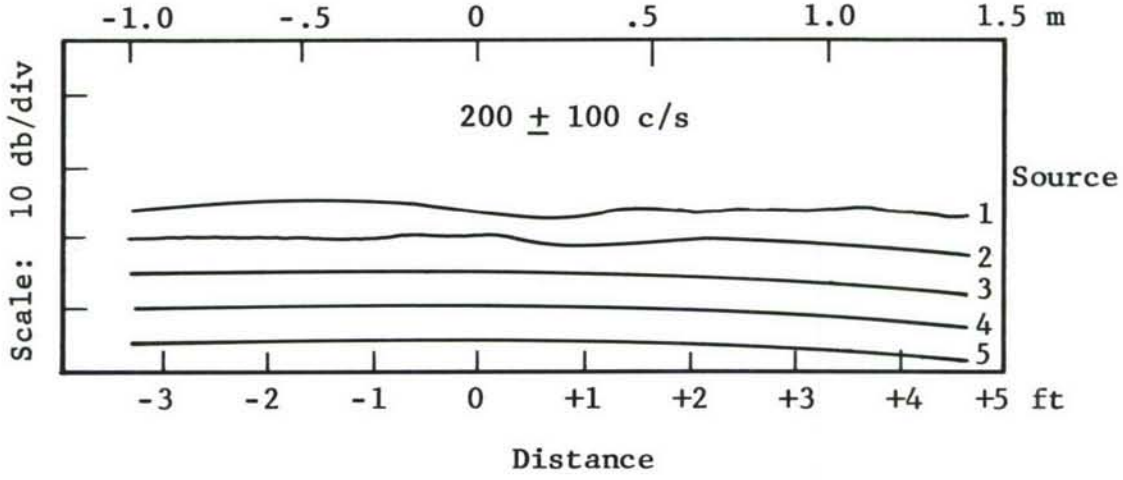

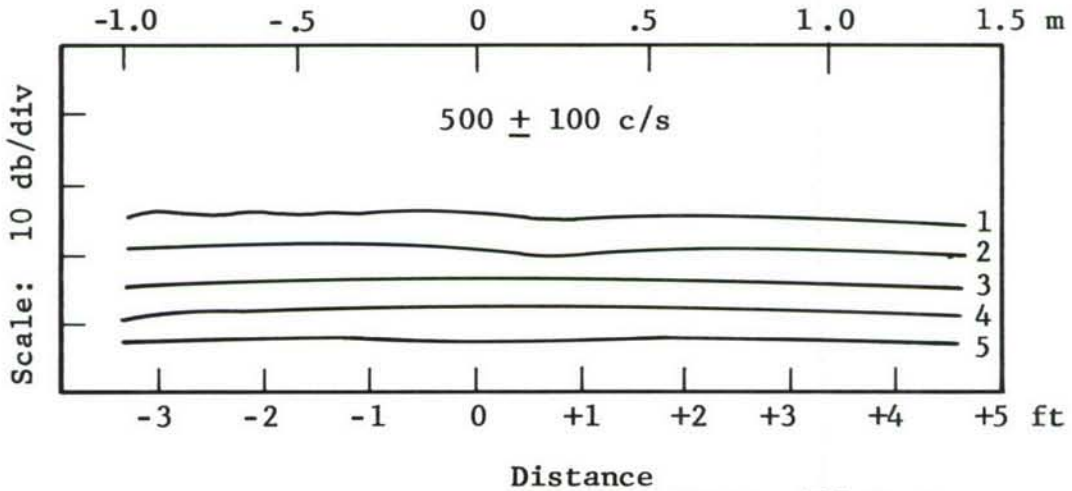

Note: All Contours Displaced for Clarity.

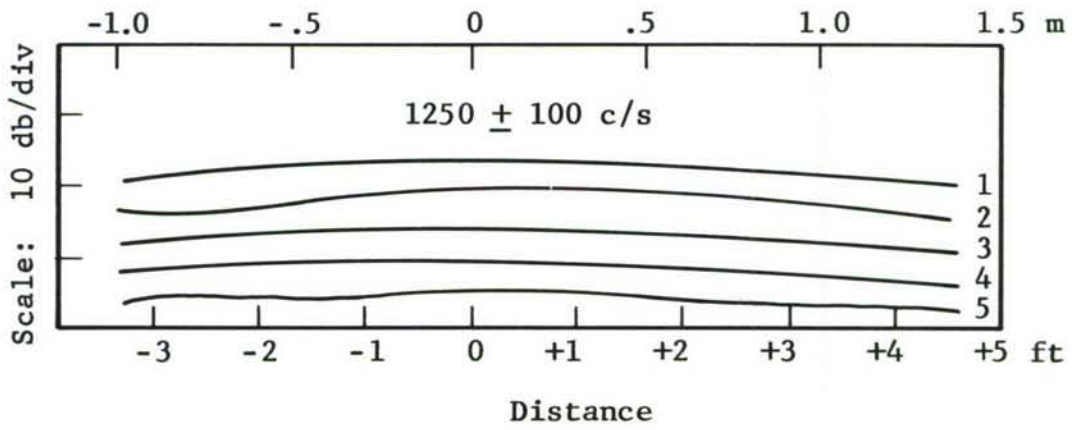

Figure 11. Sound Pressure Level Profiles in a Horizontal Line Along the Floor. Semi-anechoic Case, Bands of White Noise, Single Source Excitation.

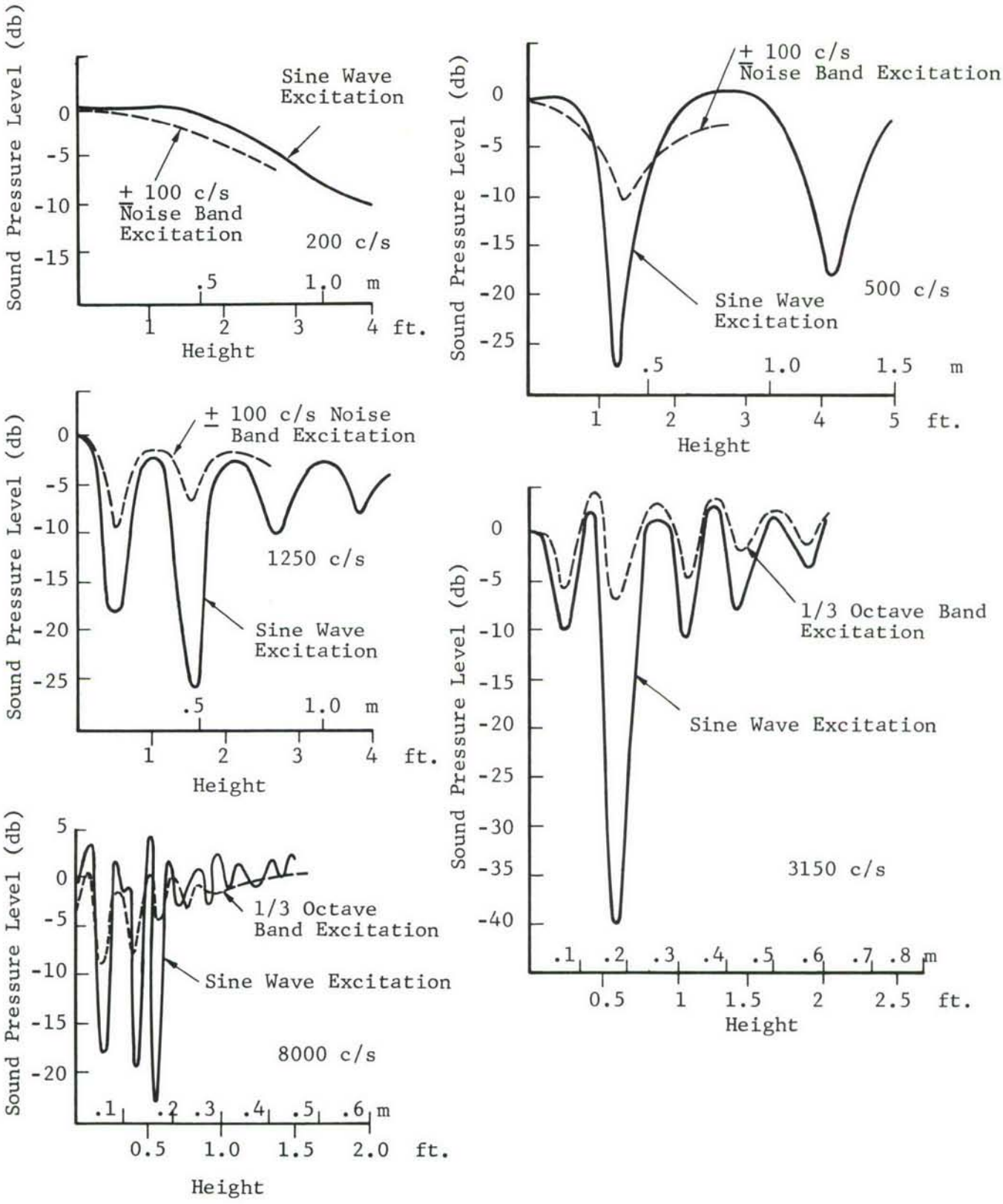

Figure 12. Vertical Sound Pressure Level Profiles for Sine Wave Excitation and Noise Band Excitation, Semi-Anechoic Case, Single Source Excitation. (Source 5 - see Figure 10).

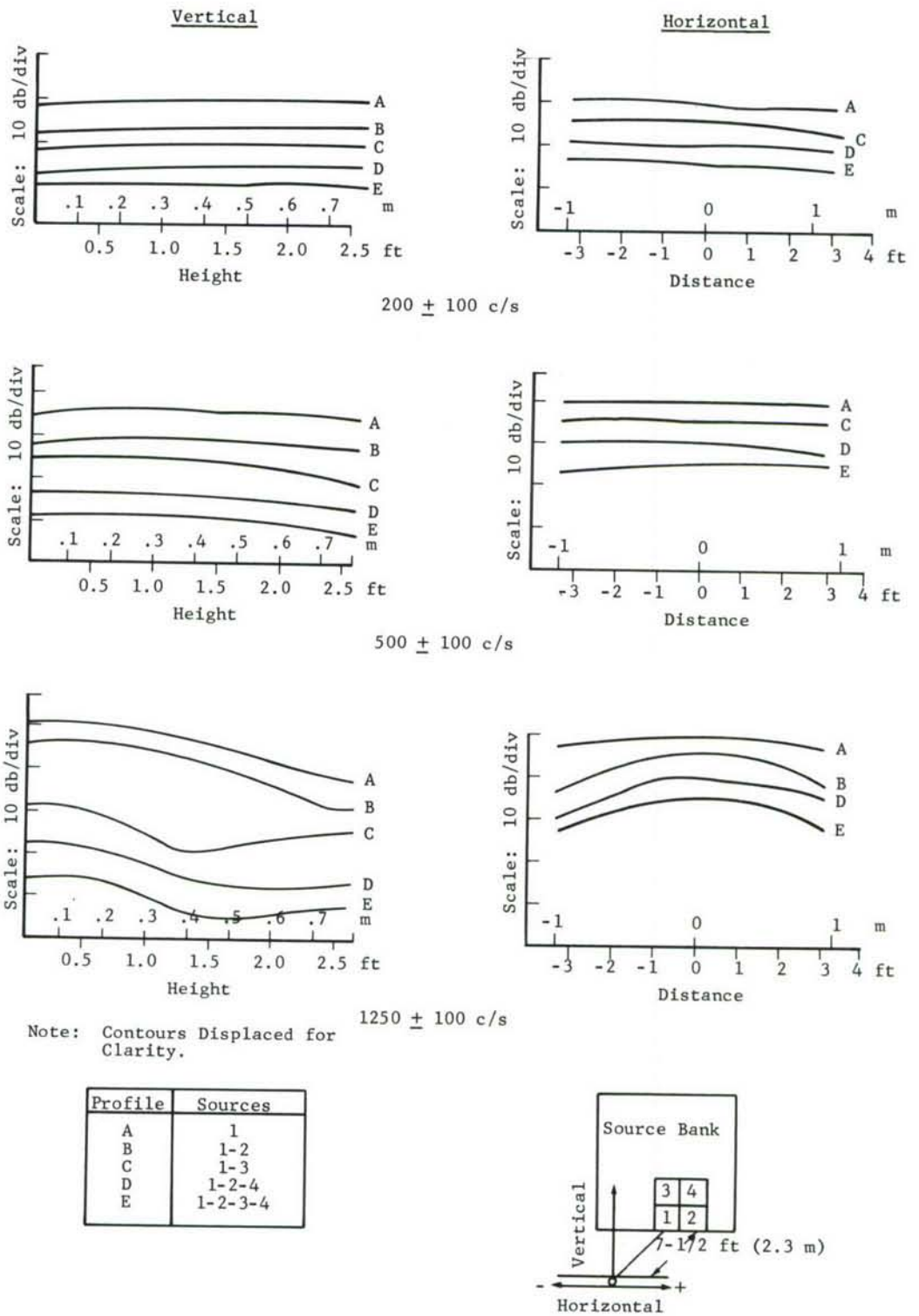

Note: Contours Displaced for Clarity.

Profile	Sources
A	1
B	1-2
C	1-3
D	1-2-4
E	1-2-3-4

Figure 13. Sound Pressure Level Profiles for Closely Spaced Groups of Sources Near the Floor, White Noise Band Excitation, Coherent Sources, Semi-anechoic Case.

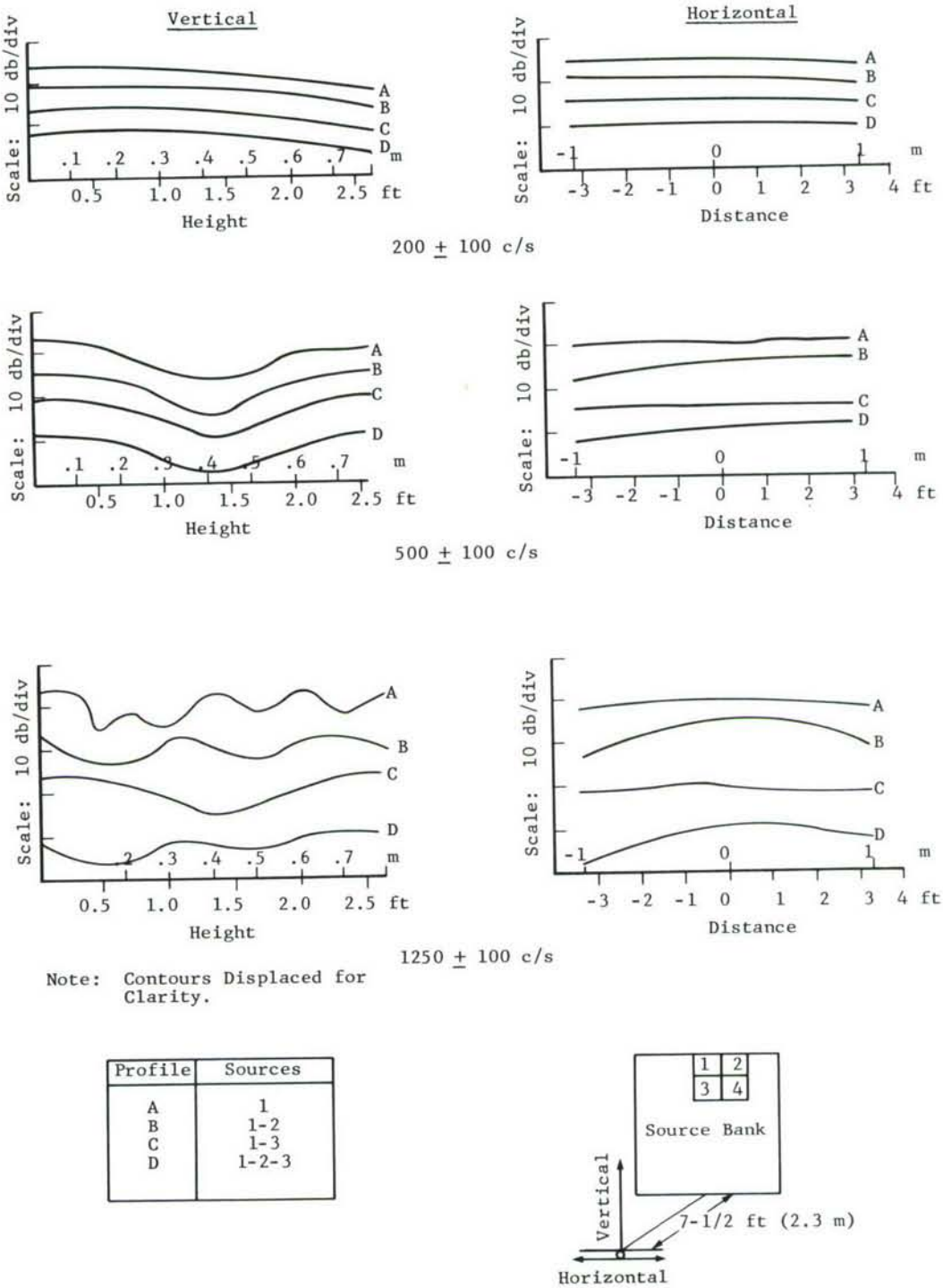

Note: Contours Displaced for Clarity.

Profile	Sources
A	1
B	1-2
C	1-3
D	1-2-3

Figure 14. Sound Pressure Level Profiles for Closely Spaced Groups of Coherent Sources Away from the Floor, White Noise Band Excitation, Semi-anechoic Case.

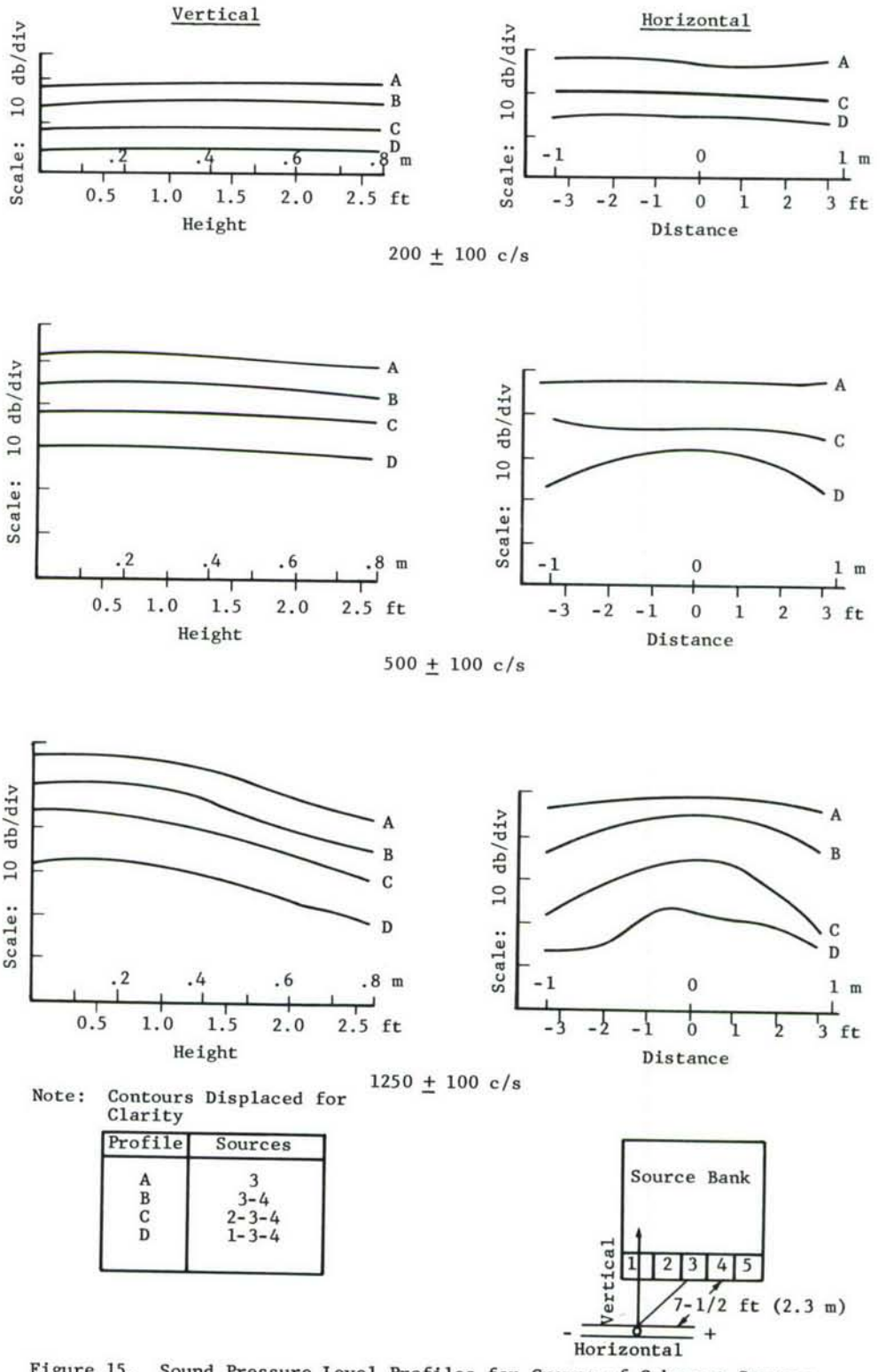

Figure 15. Sound Pressure Level Profiles for Groups of Coherent Sources in a Horizontal Row Near the Floor, White Noise Band Excitation, Semi-anechoic Case.

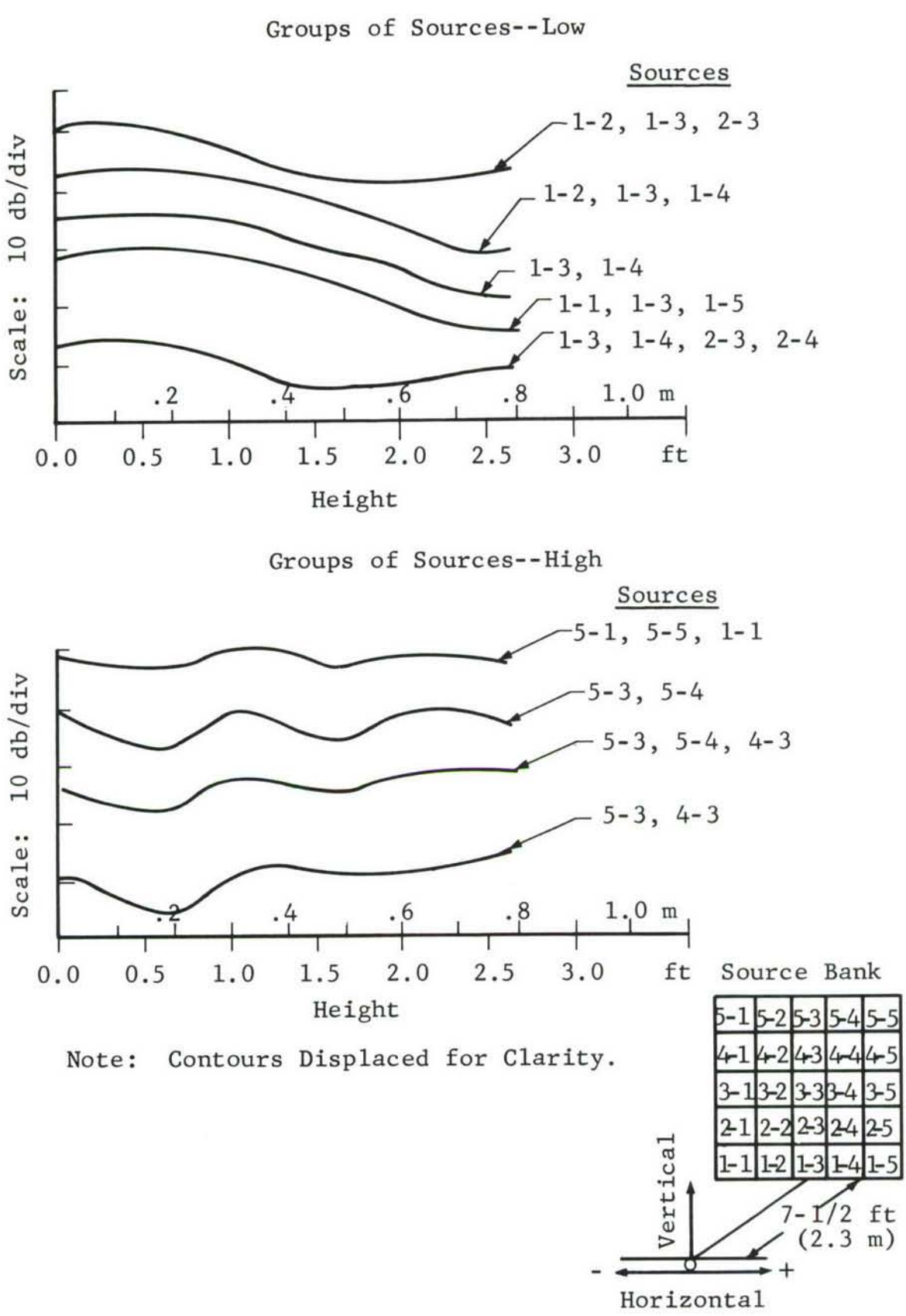

Note: Contours Displaced for Clarity.

Figure 16. Effects of Heights of Groups of Coherent Sources Upon Sound Pressure Level Profiles in a Vertical Direction, Semi-anechoic Case, White Noise Band: 1250 $\pm$ 100 cps.

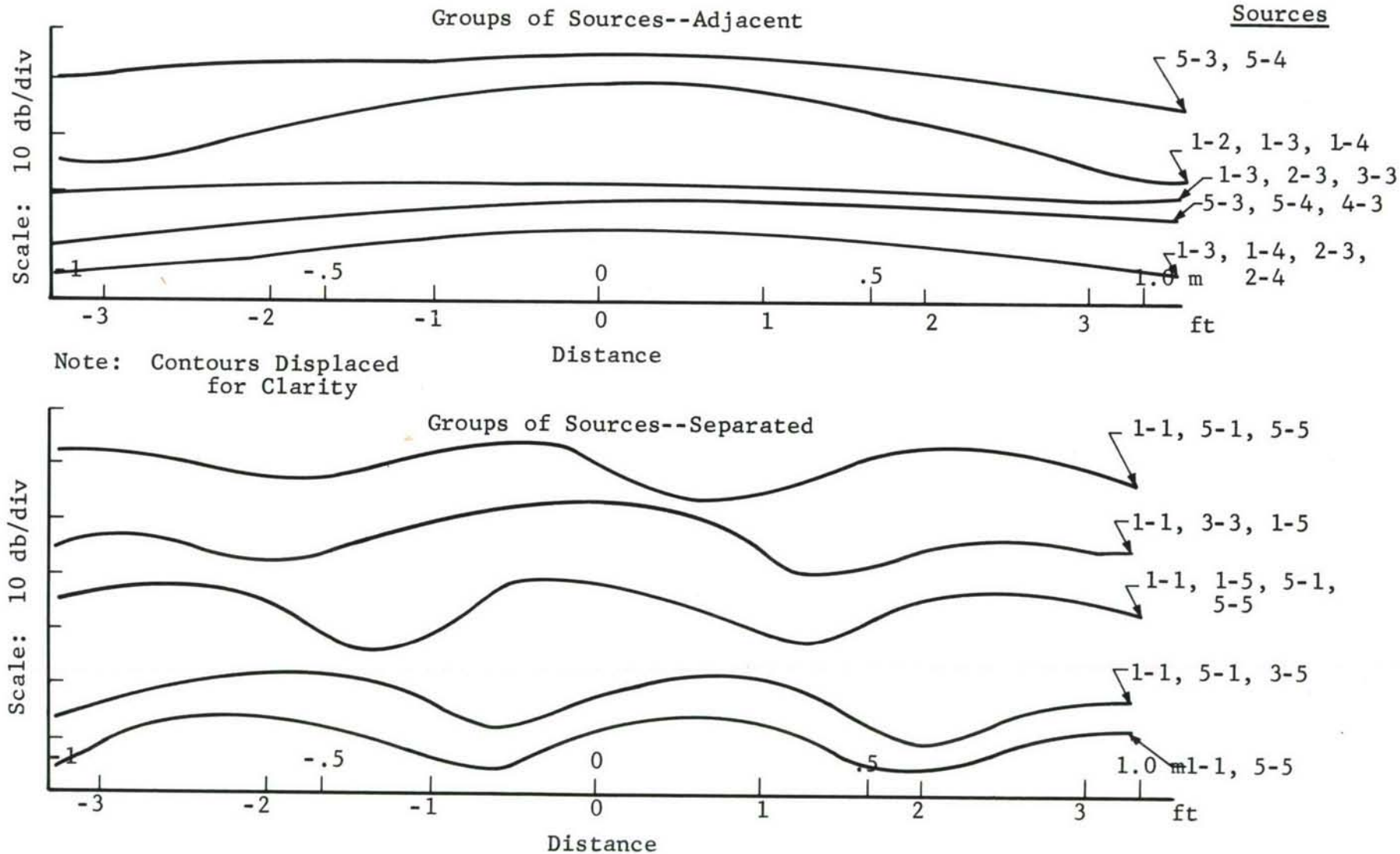

Figure 17. Effects of Separation of Sources upon Sound Pressure Level Profiles for Groups of Coherent Sources, Profiles Along Floor, Semi-anechoic Case, White Noise Band: 1250 $\pm$ 100 cps.

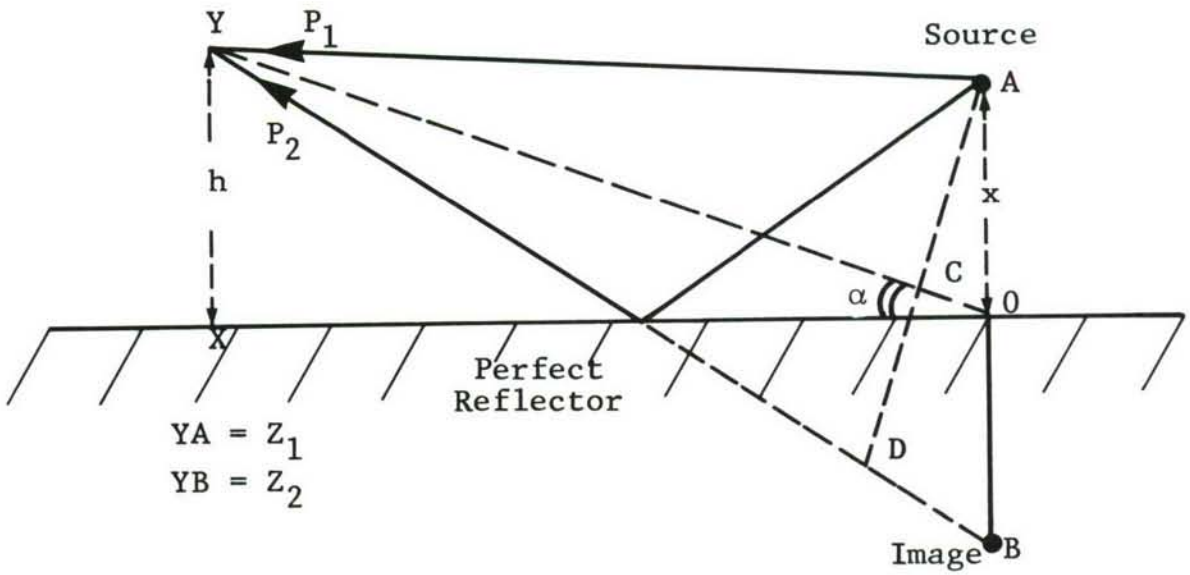

(a) Geometry

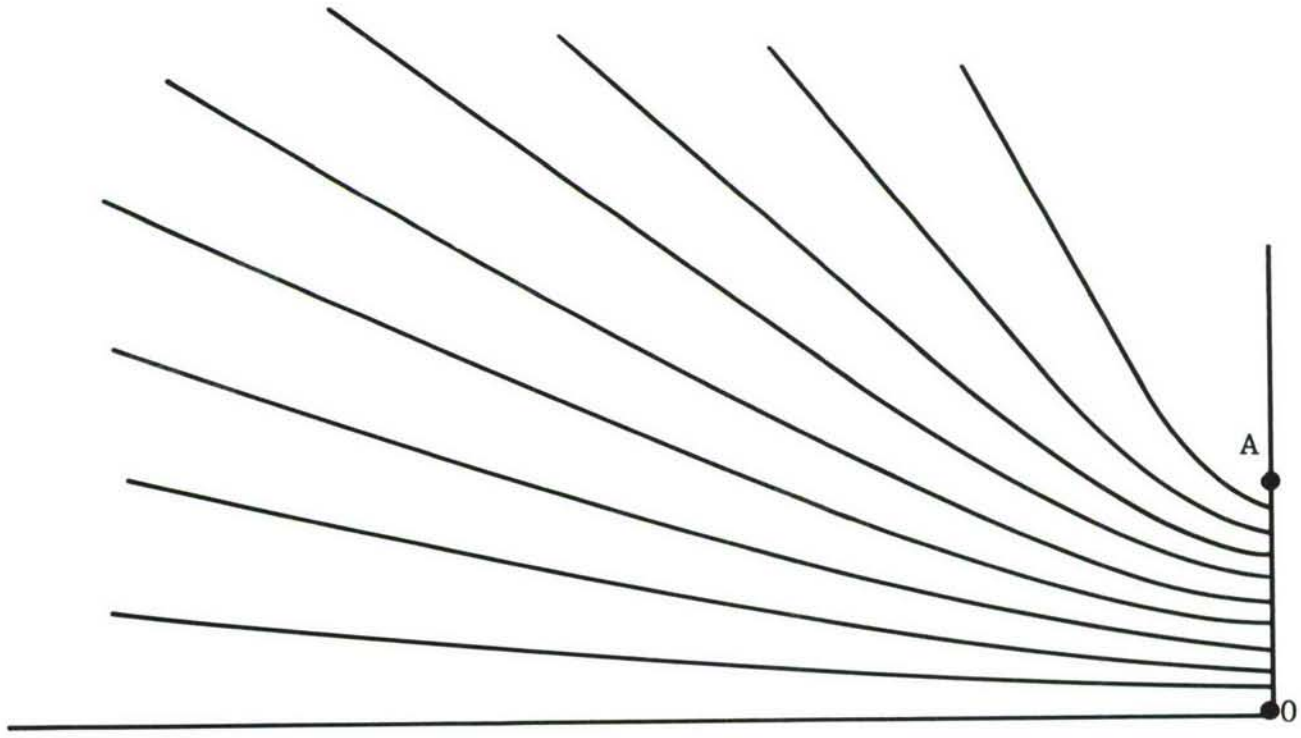

(b) Loci of Interference Maxima for A0 (=x) = 5λ

Figure 18. Interference Field of a Source A, Located Above a Reflecting Surface.

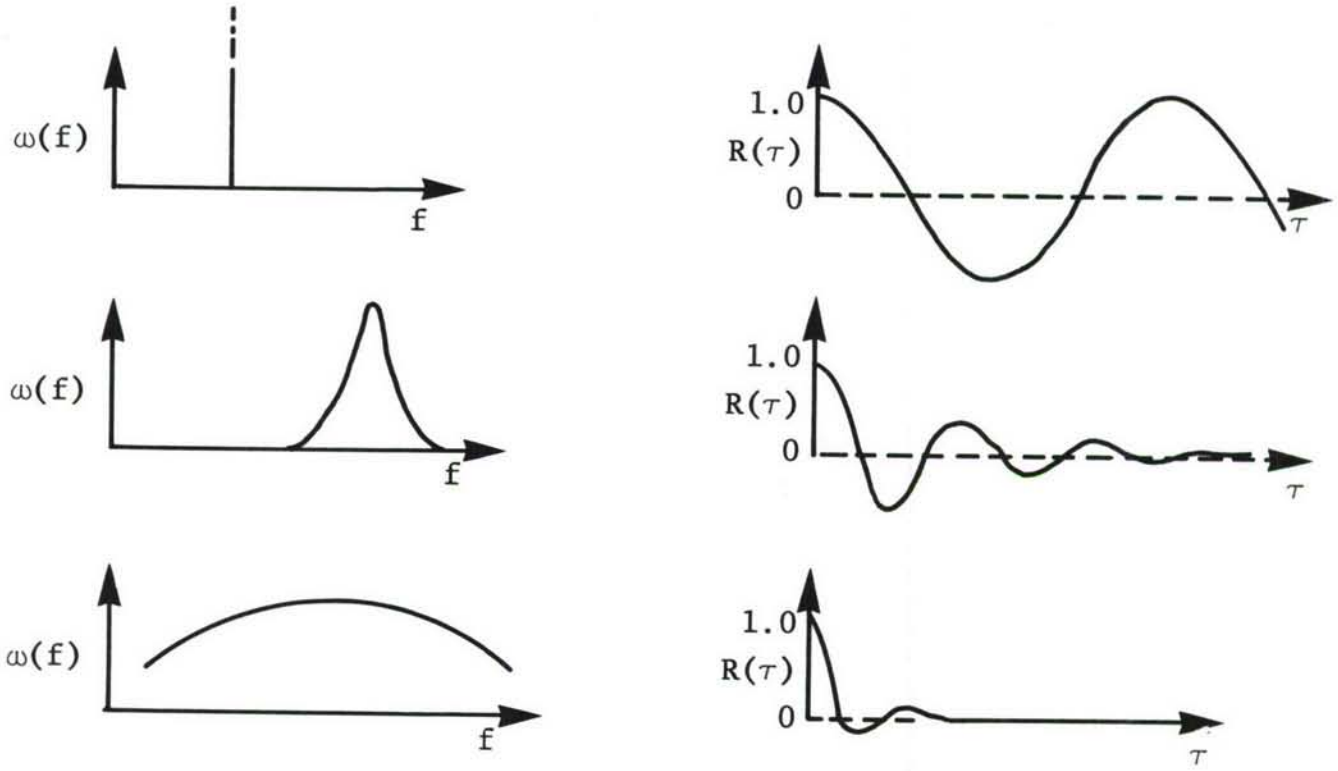

(a) Signals and Auto-Correlation Coefficients for Discrete, Narrow-, and Broad-Band Signals.

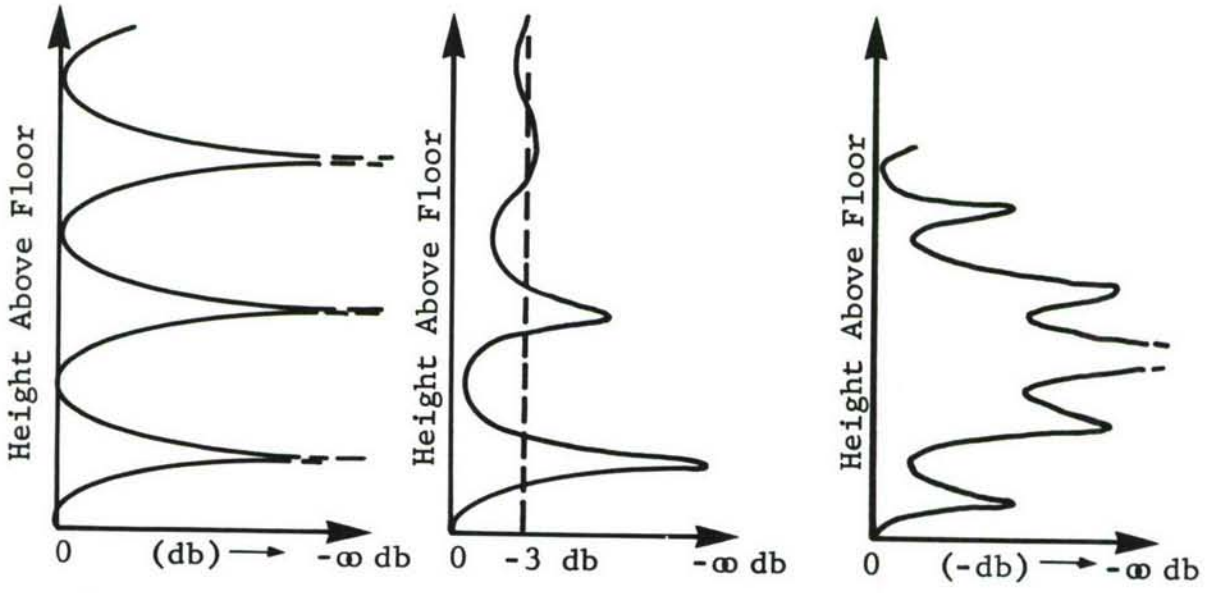

(b) Tone Source (c) Noise Source (d) Two Tone Source

Figure 19. Correlation Coefficients and Interference Fields.

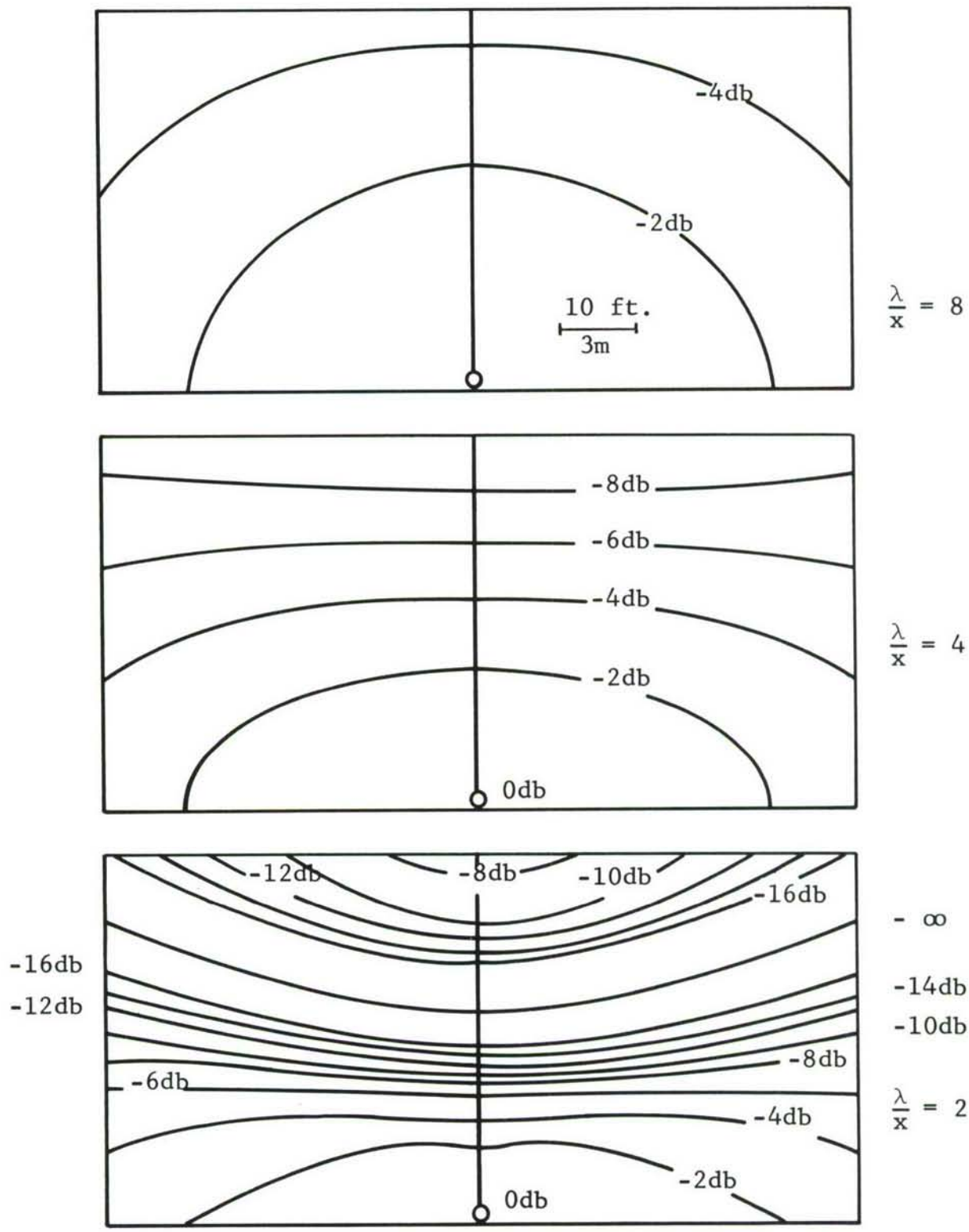

Figure 20. Distribution in Vertical Plane 50 ft. (15.25m) from Siren Bank in RTD Facility for $\lambda/x = 8$, 4 and 2.

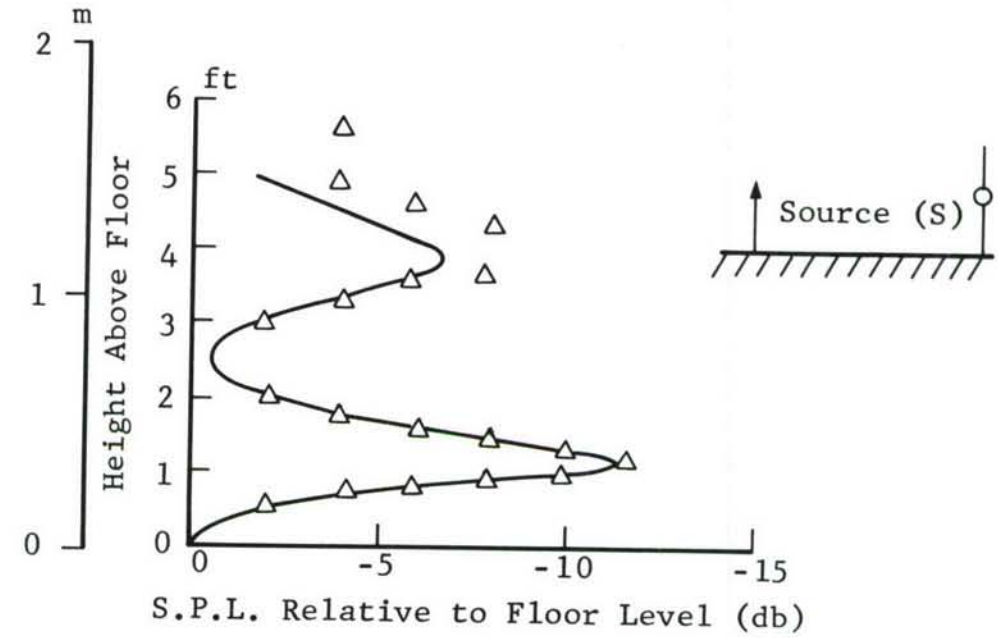

(a)

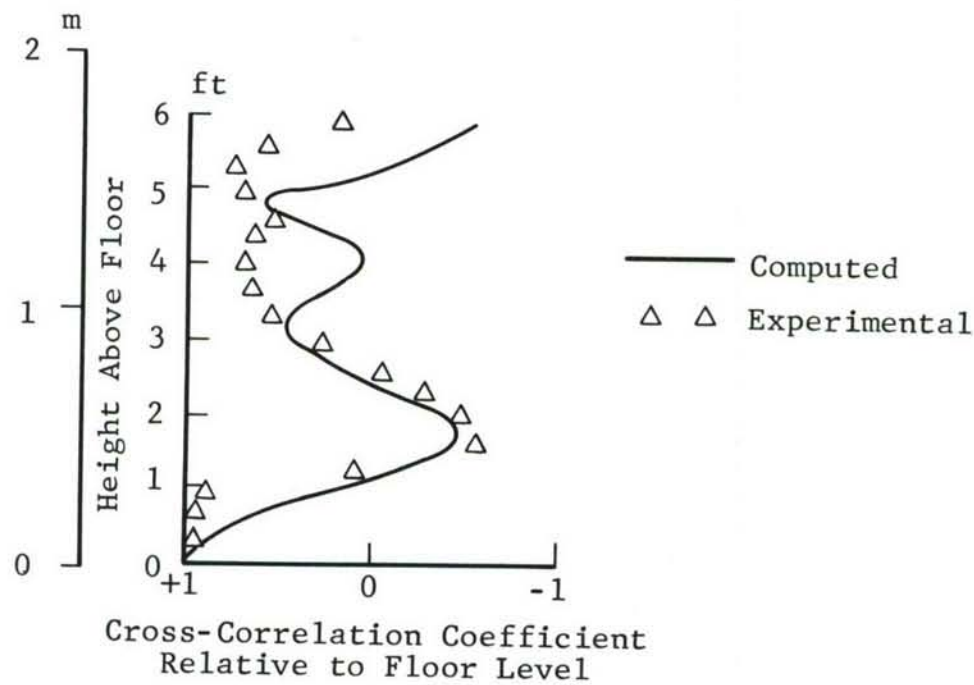

(b)

Figure 21. Interference Sound Pressure Level and Phase Distribution Along Vertical Line Above Floor.

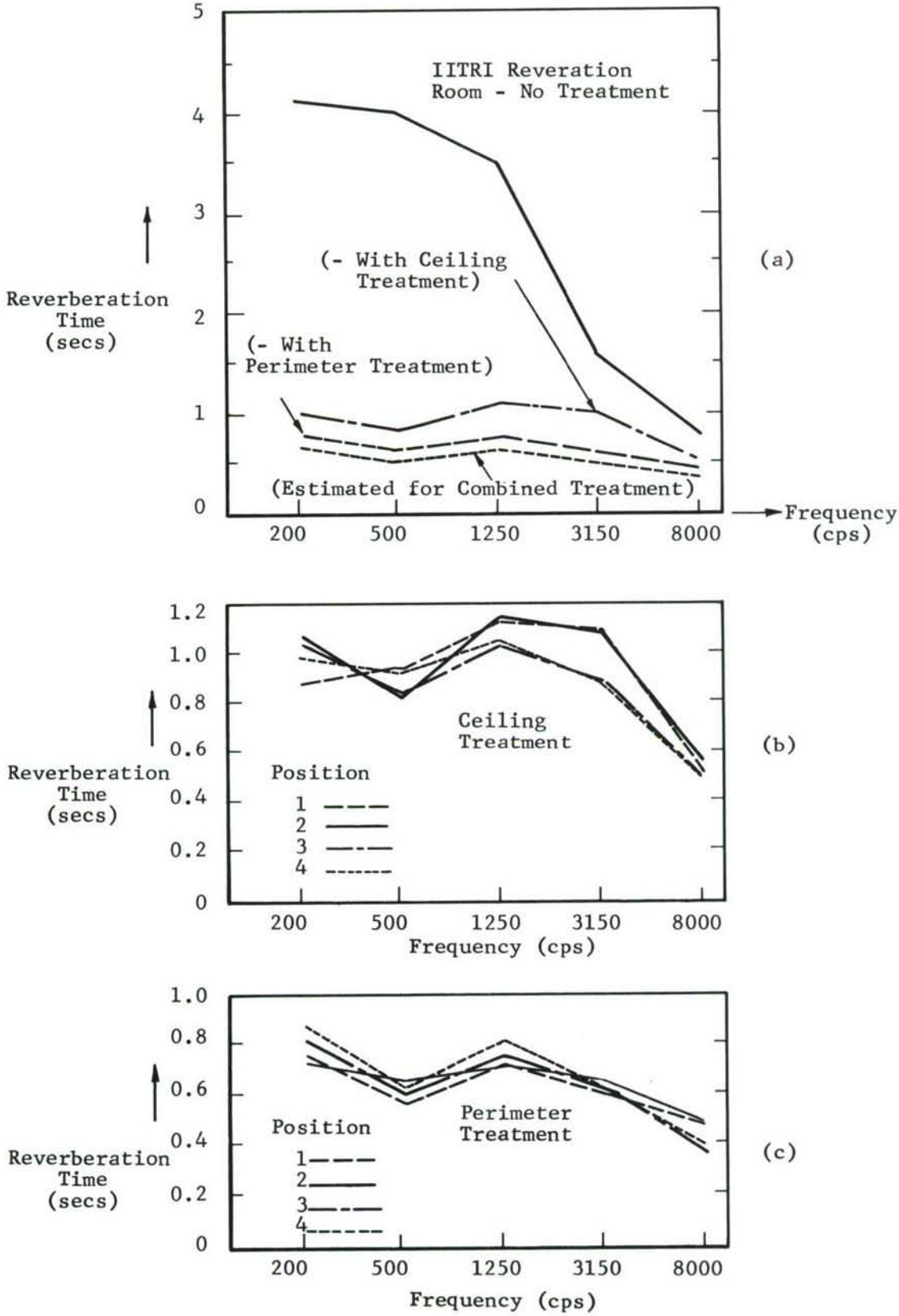

Figure 22. Reverberation Times in Modified and Unmodified Reverberation Room.

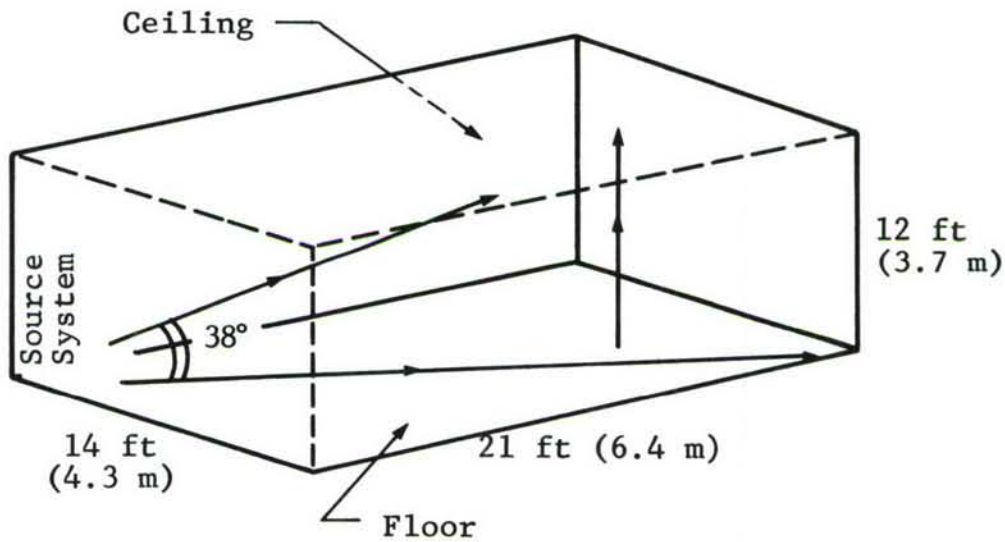

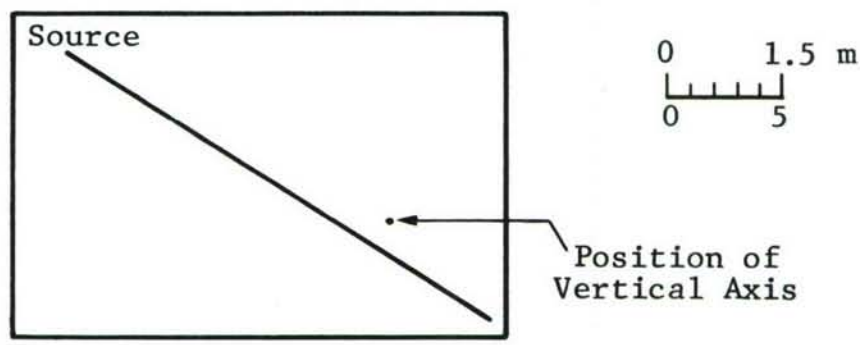

Figure 23. Axes in Reverberation Room for Spatial Sound Pressure Level Distribution Determination.

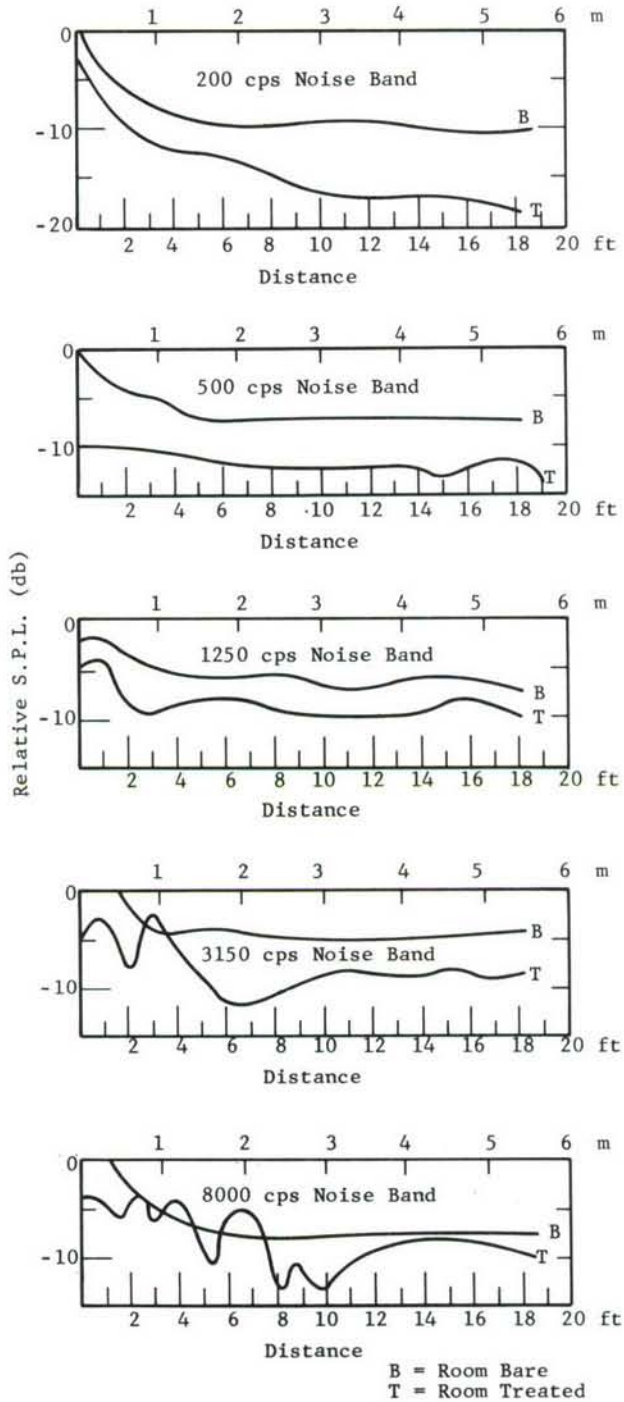

Figure 24. Spatial Sound Pressure Level Distribution Along Floor Diagonal in Reverberation Room with Perimeter Treatment.

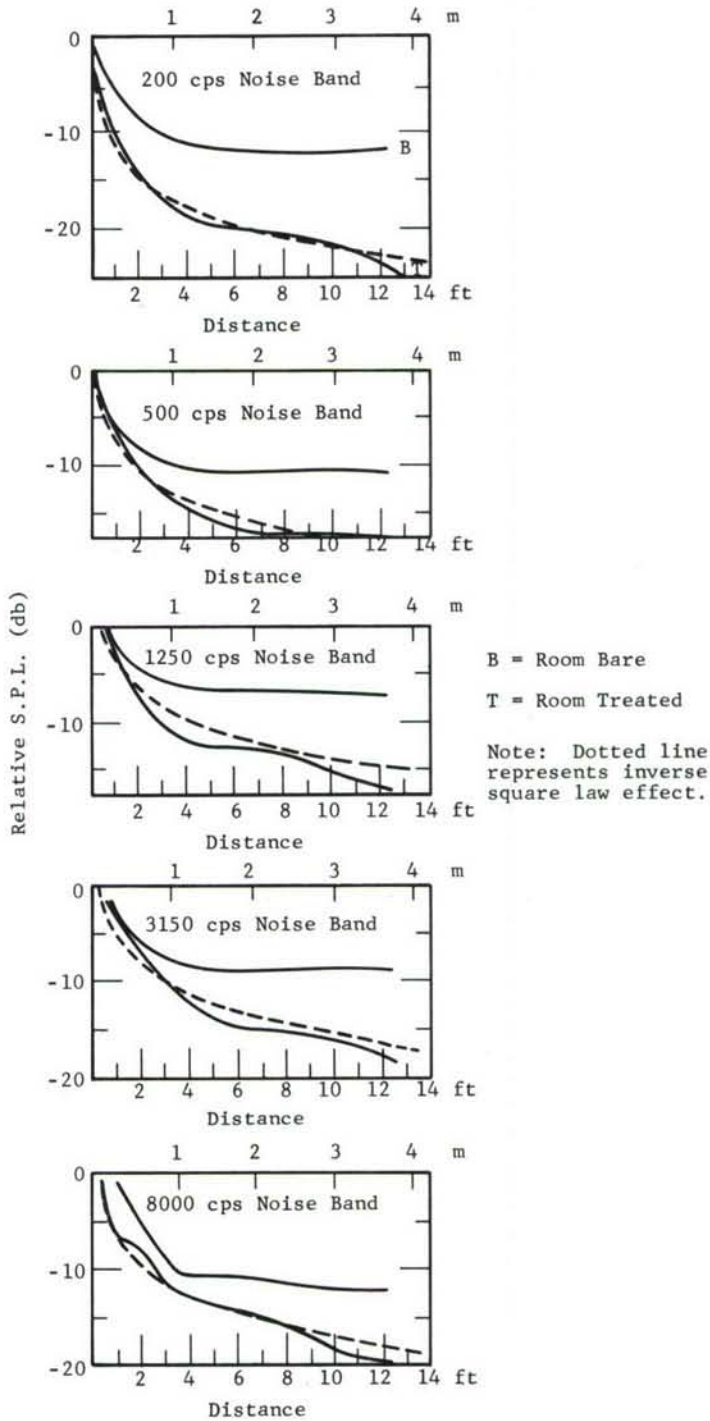

Figure 25. Spatial Sound Pressure Level Distribution Along Inclined Axis in Reverberation Room with Perimeter Treatment.

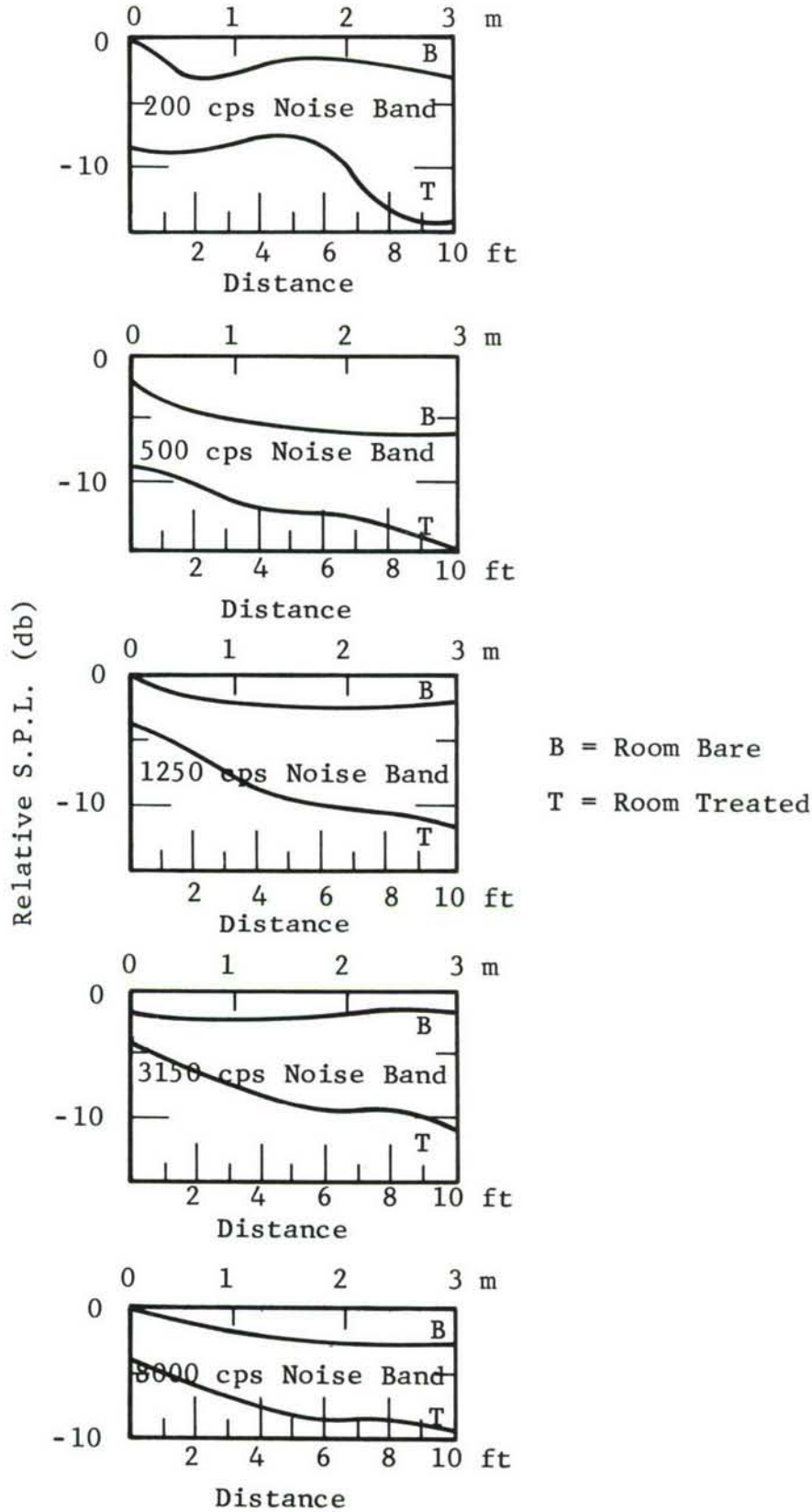

Figure 26. Spatial Sound Pressure Level Distribution Along Vertical Axis in Reverberation Room with Perimeter Treatment.

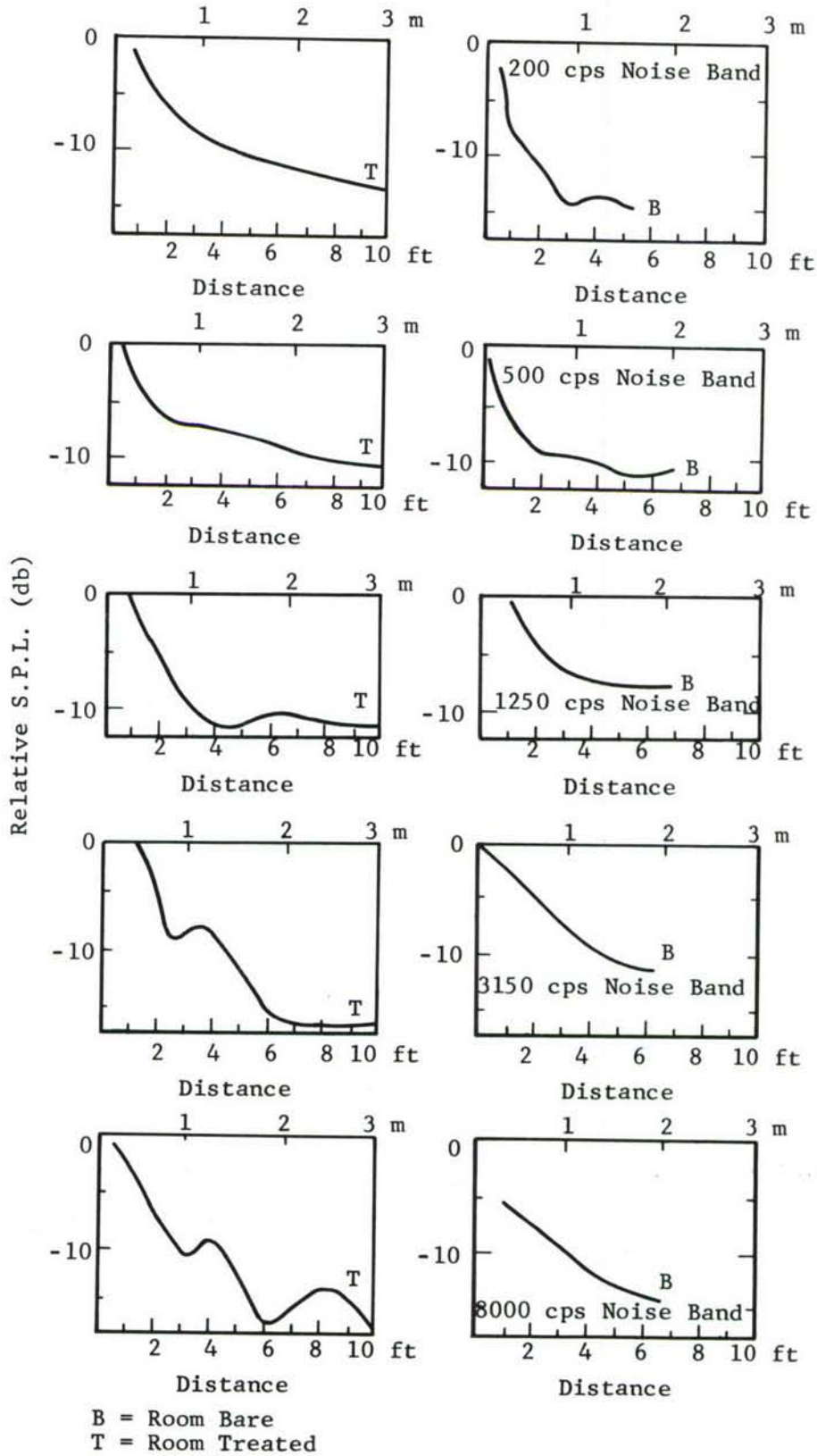

Figure 27. Spatial Sound Pressure Level Distribution Along Floor Diagonal in Reverberation Room with Ceiling Treatment.

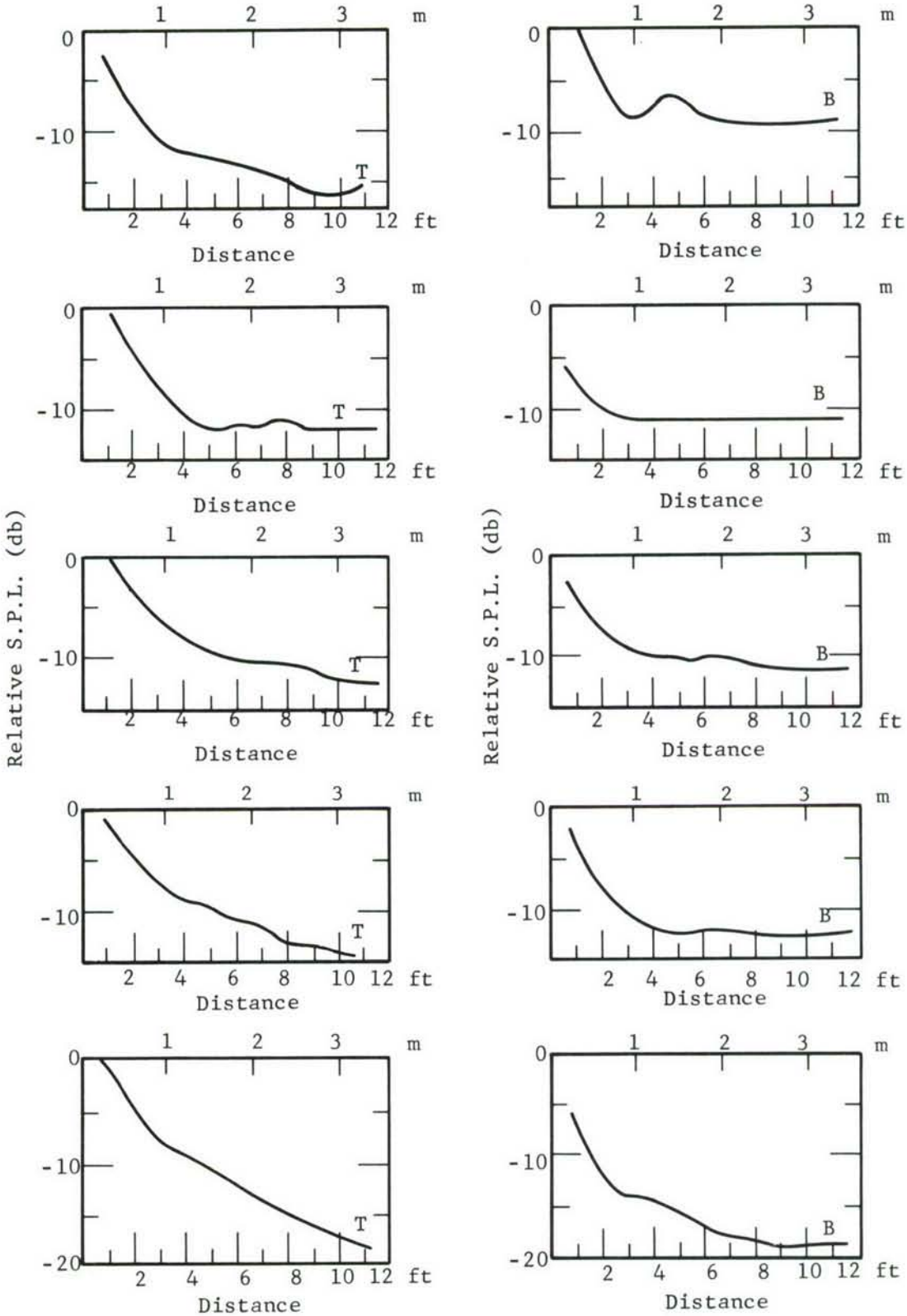

B = Room Bare
T = Room Treated

Figure 28. Spatial Sound Pressure Level Distribution Along Inclined Axis in Reverberation Room with Ceiling Treatment.

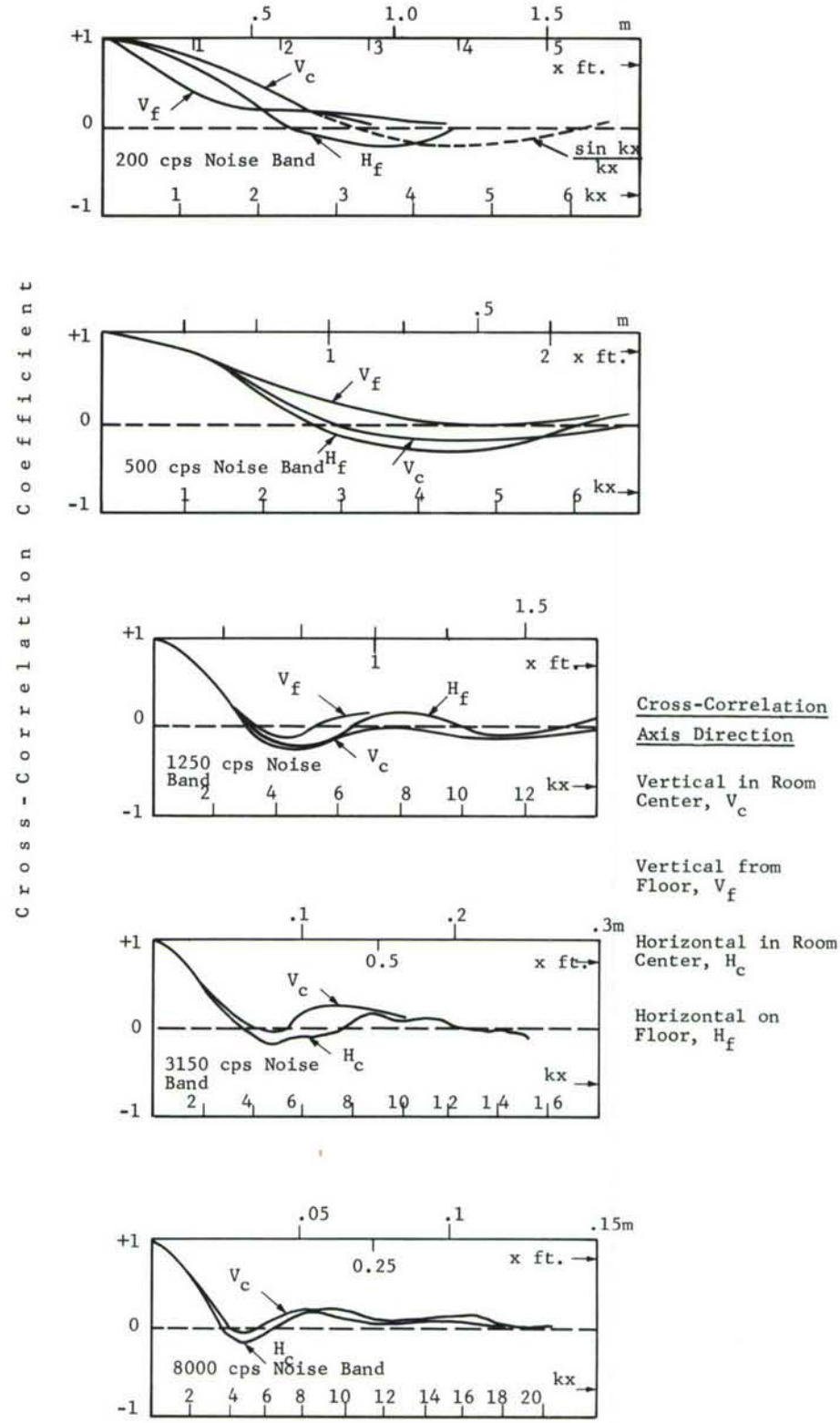

Figure 29. Cross-Correlation Coefficients in Reverberation Room Without Treatment.

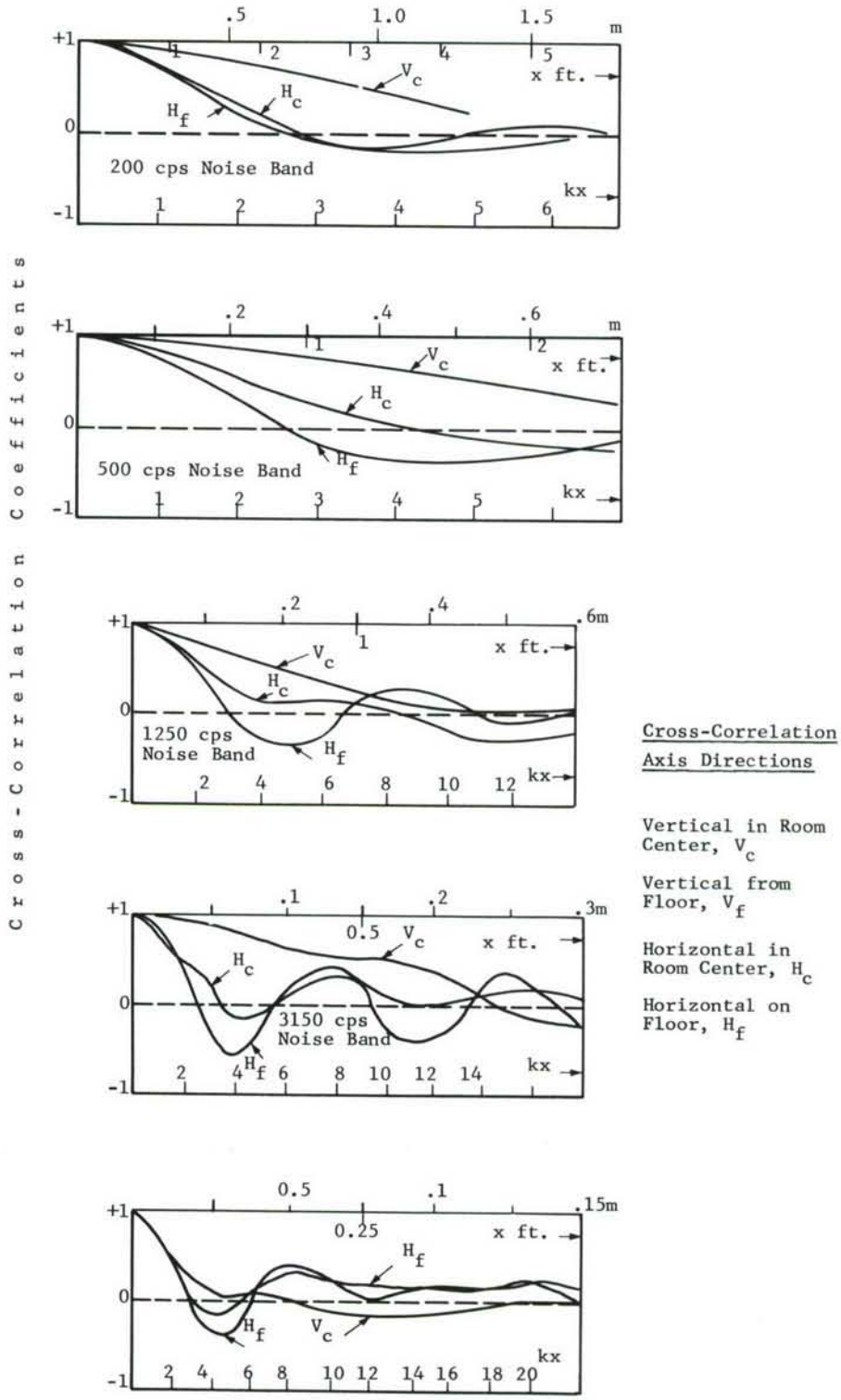

Figure 30. Cross-Correlation Coefficients in Reverberation Room With Ceiling Treatment.

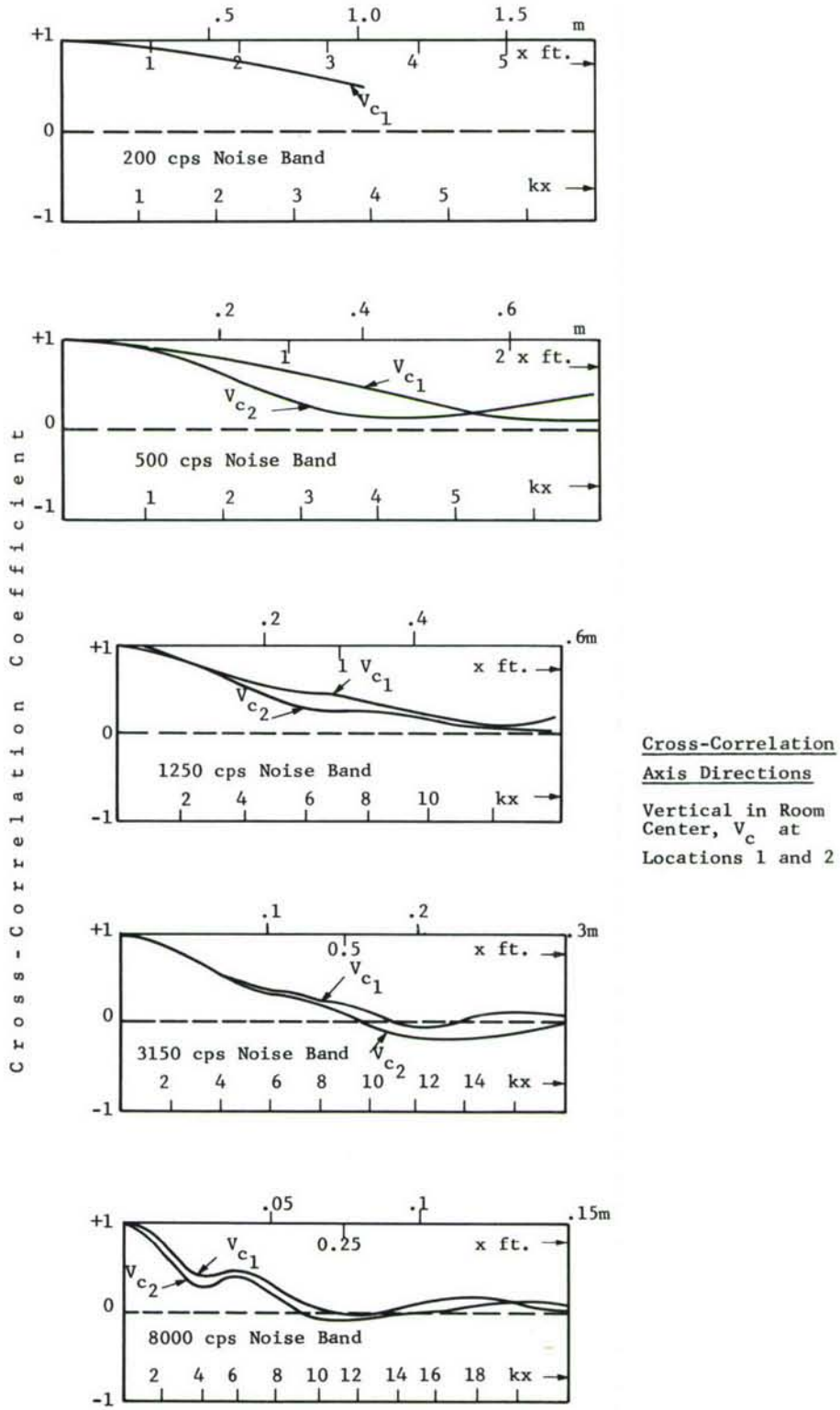

Figure 31. Cross-Correlation Coefficient in Reverberation Room with Perimeter Treatment.

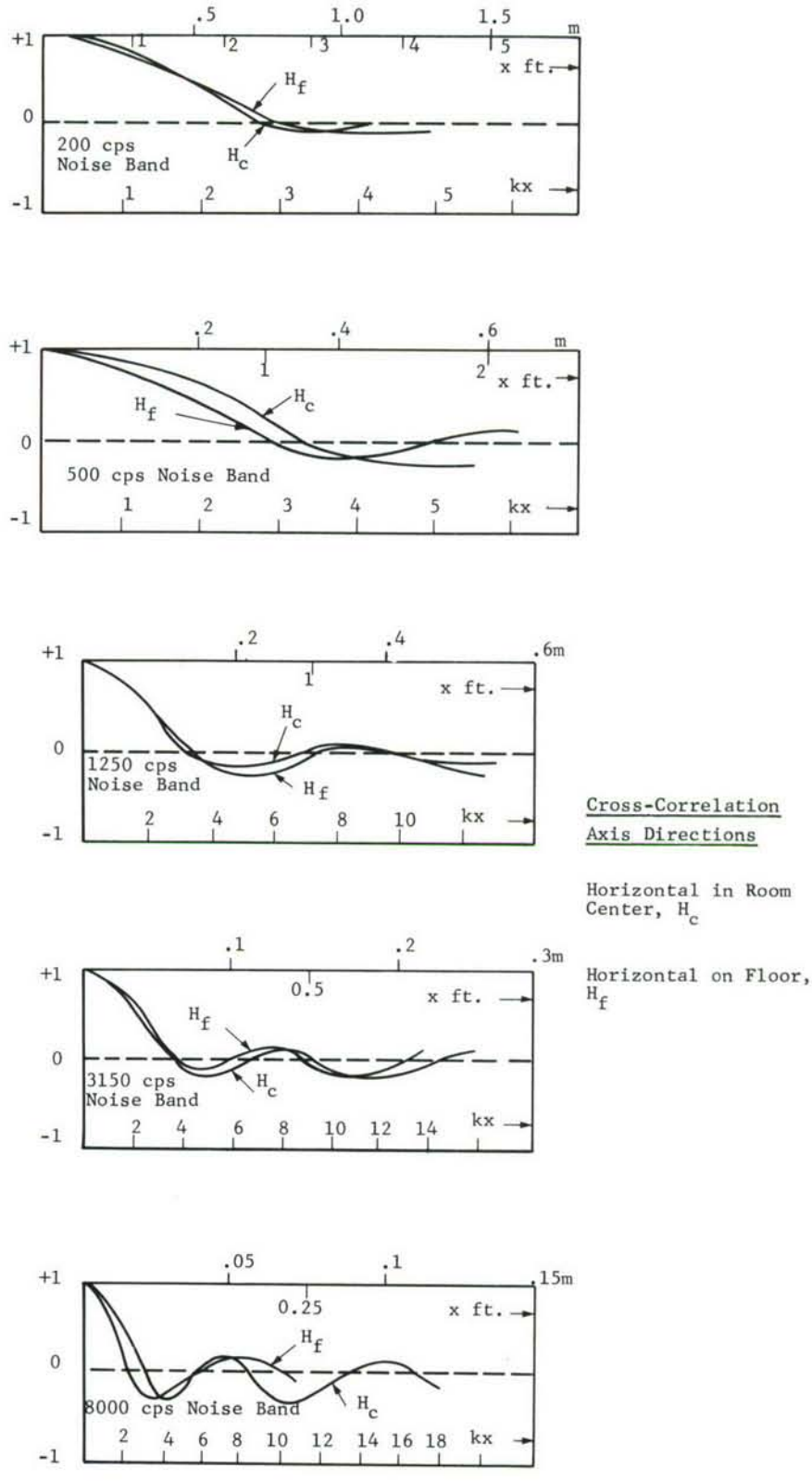

Cross-Correlation Axis Directions

Horizontal in Room Center, H_c

Horizontal on Floor, H_f

Figure 32. Cross-Correlation Coefficient in Reverberation Room with Perimeter Treatment.

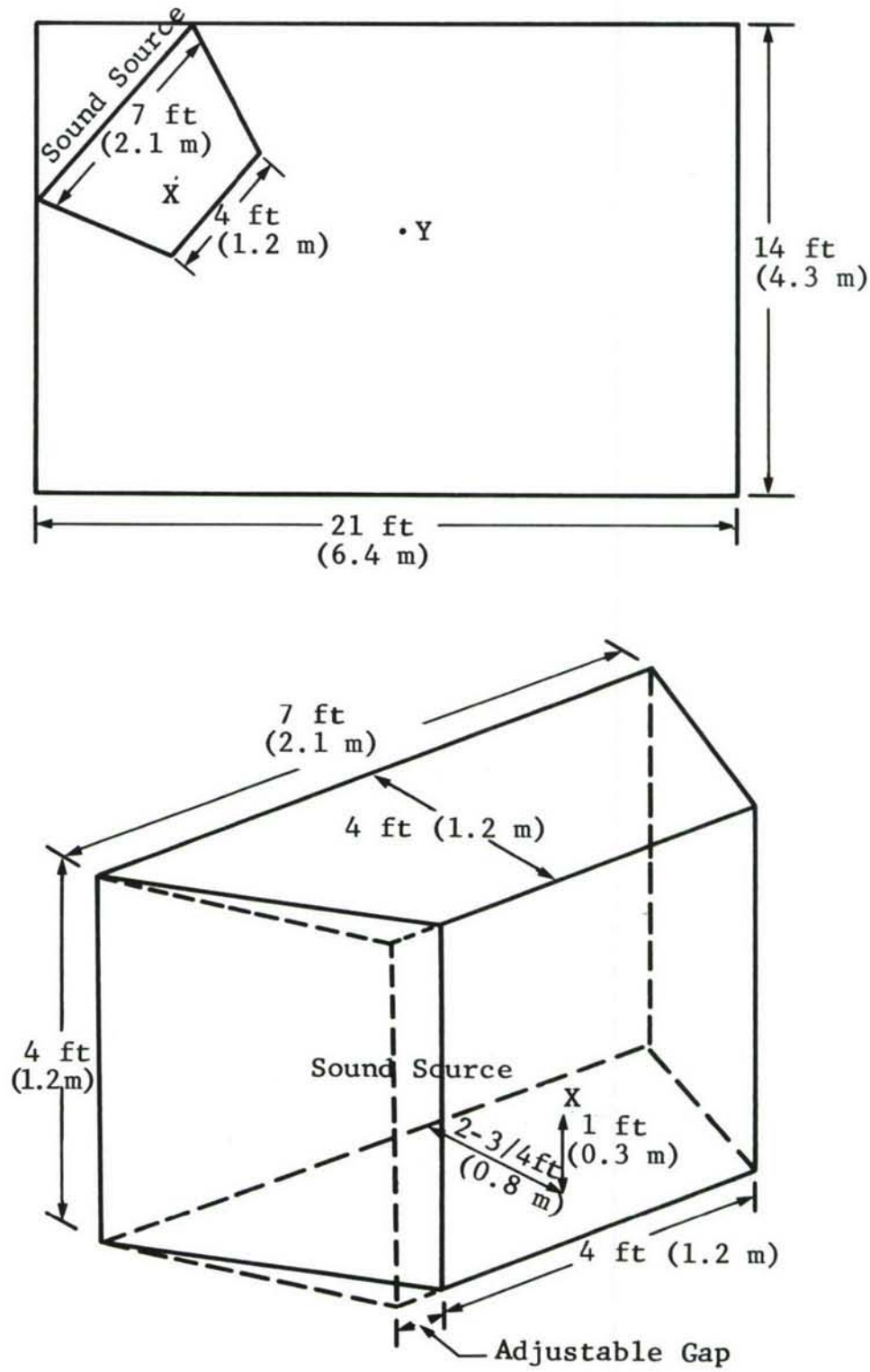

Figure 33. Plan of Enclosure Near Source System in Semi-Reverberant Room.

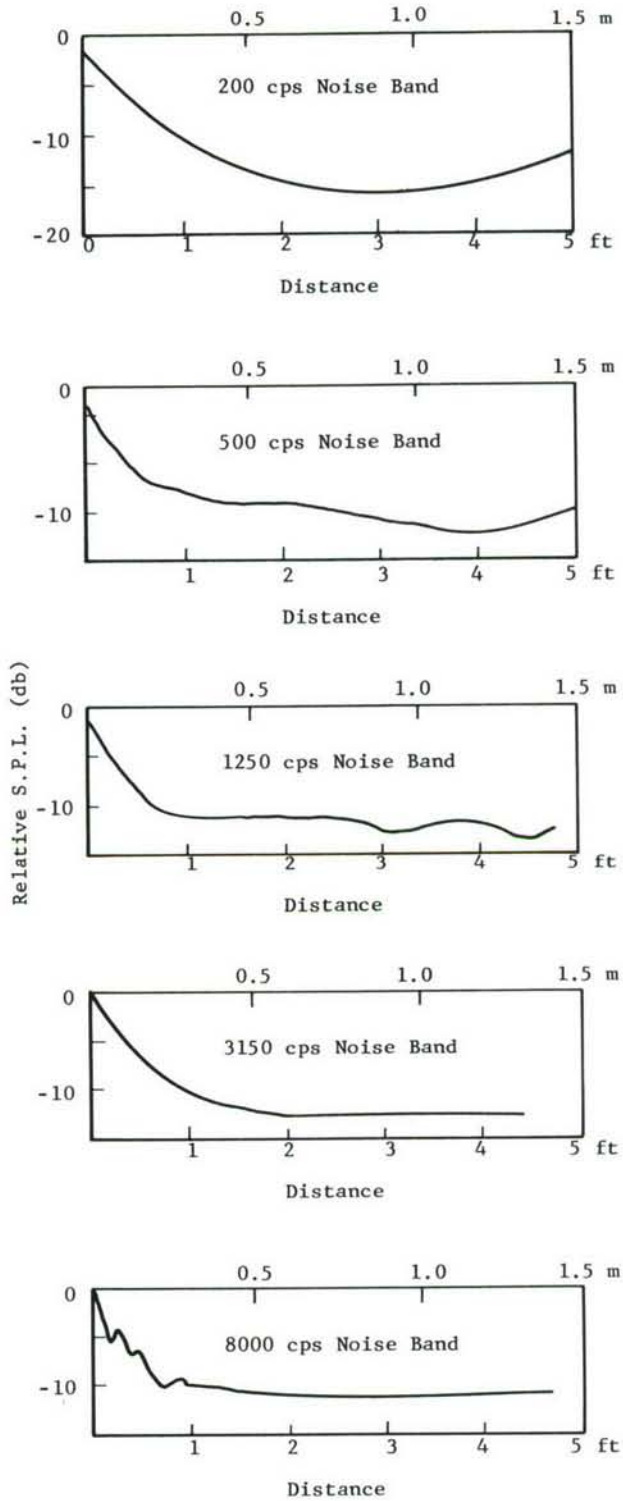

Figure 34. Spatial Sound Pressure Level Distribution in Small Enclosure in Reverberation Room.

In Incident Interference Minimum

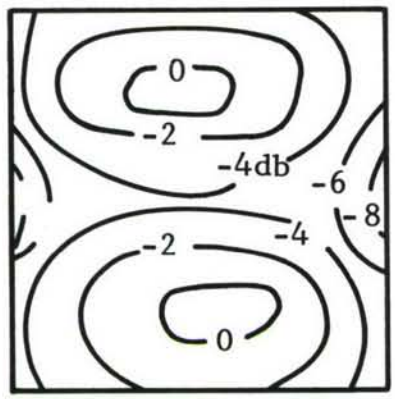

Side Toward Source

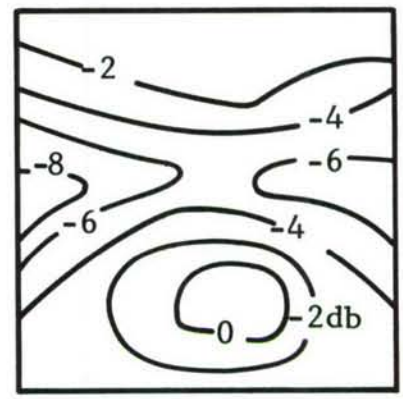

Side Away From Source

In Incident Interference Maximum

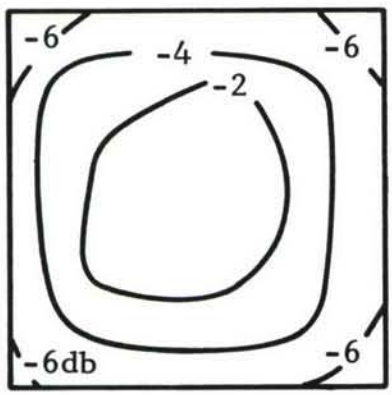

Side Toward Source

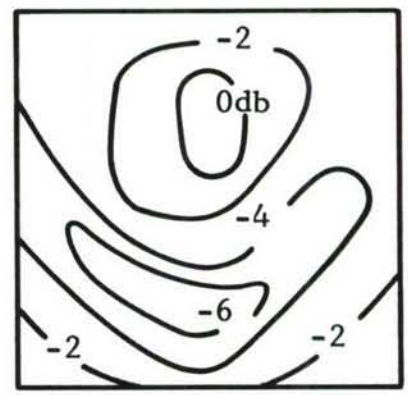

Side Away From Source

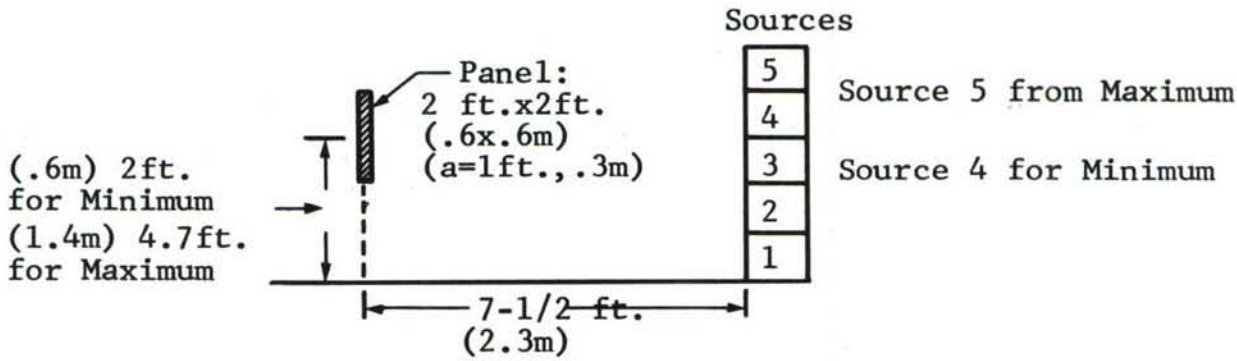

Figure 35. Sound Pressure Level Contours on a Vertical Panel in a Semi-Anechoic Environment, White Noise Excitation: 500 ± 100 cps.

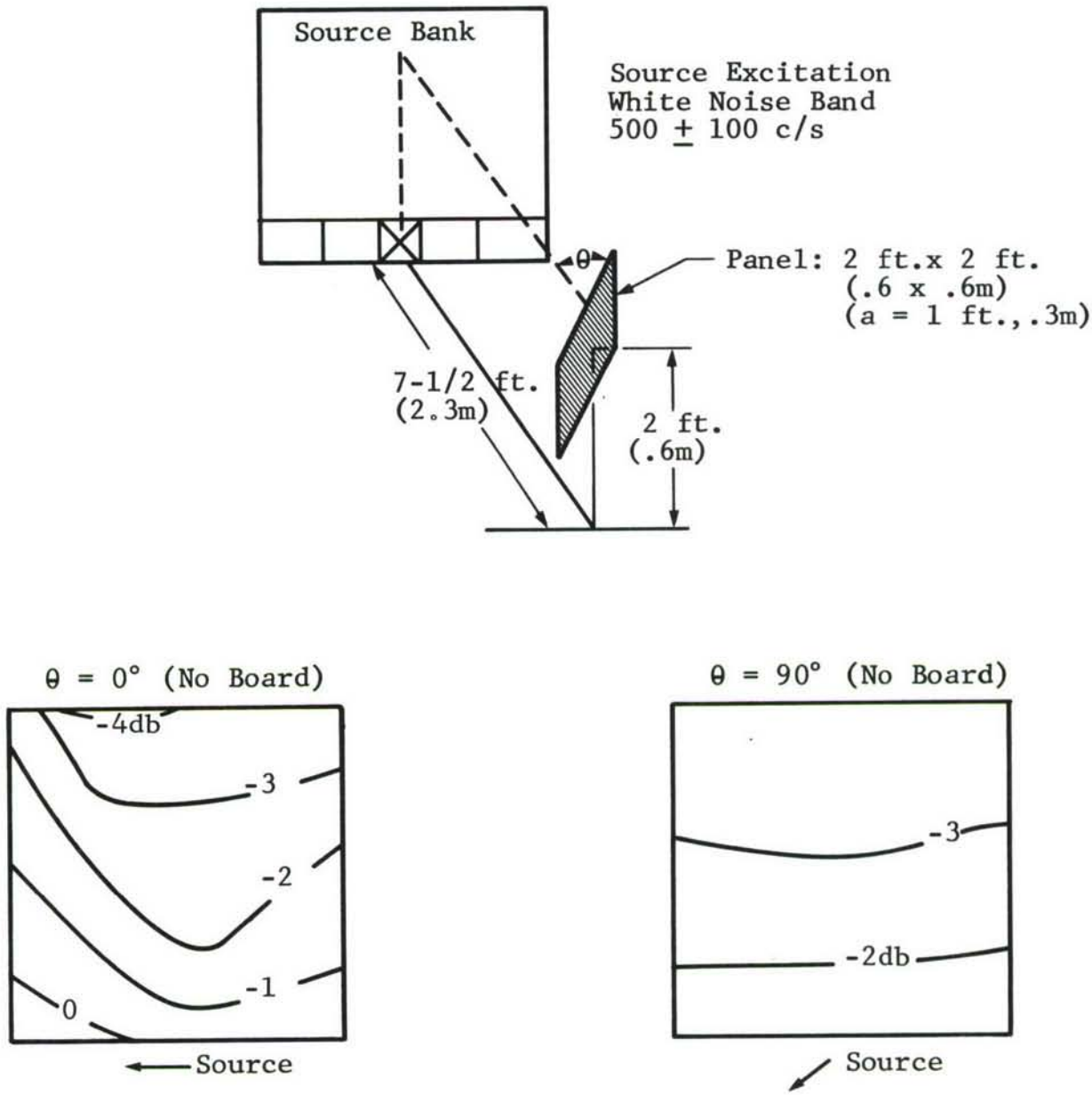

Figure 36. Sound Pressure Level Contours on a Vertical Panel in a Relative Minimum of the Incident Interference Field, Semi-Anechoic Case, Geometry of Experiment and Incident Field.

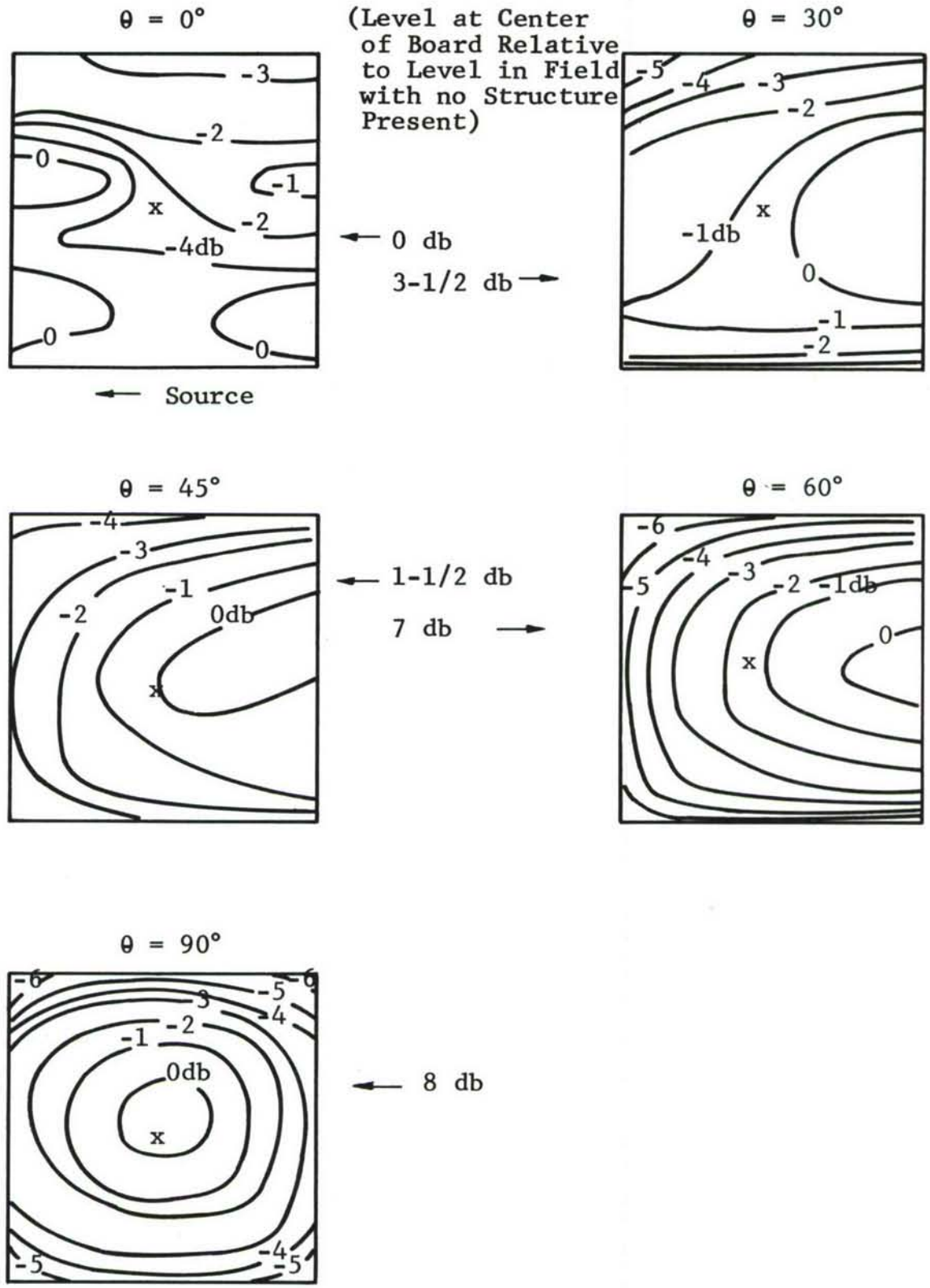

Figure 37. Sound Pressure Level Contours on a Vertical Panel in a Relative Minimum of the Incident Interference Field, Semi-Anechoic Case

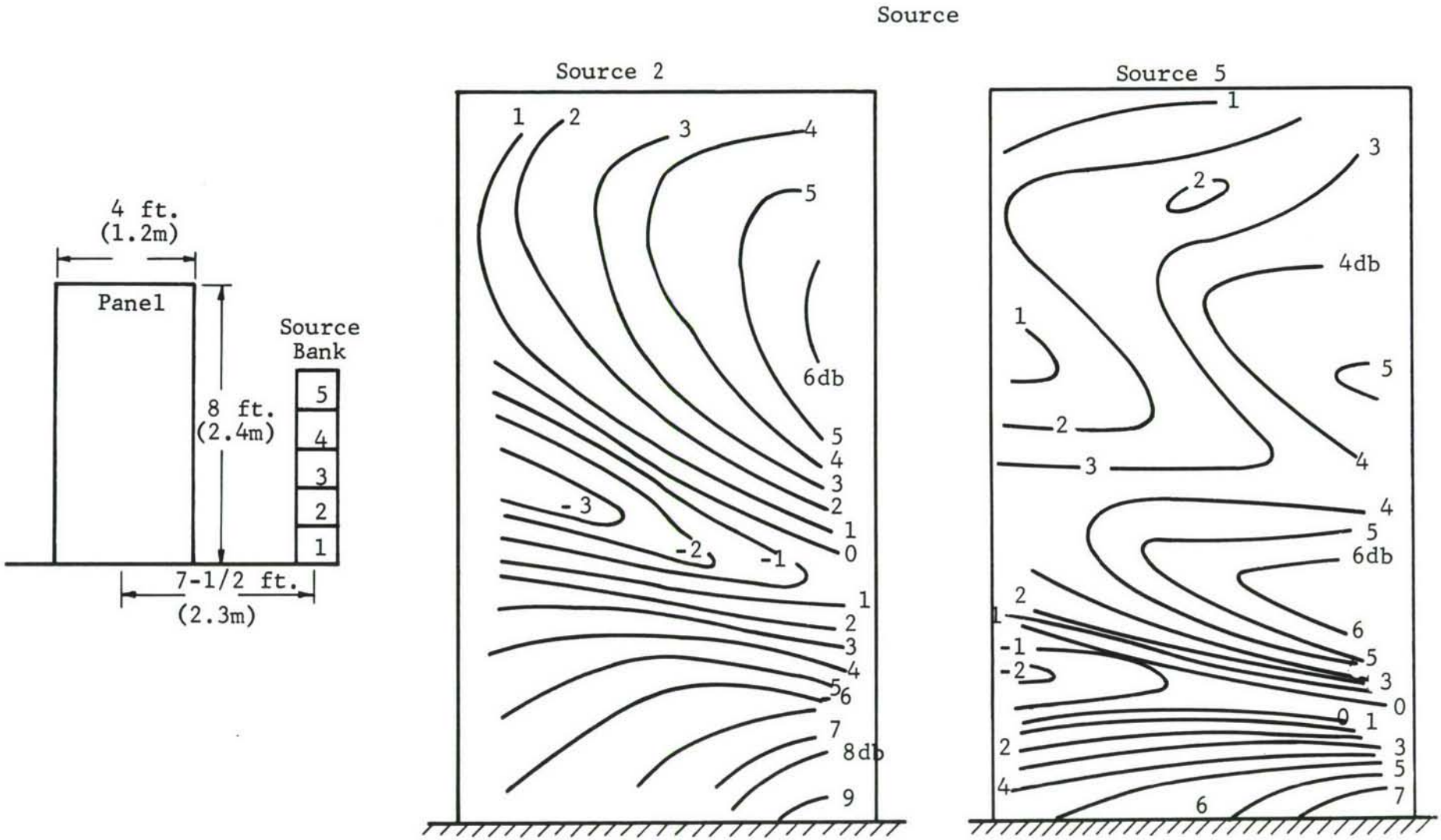

Figure 38. Sound Pressure Level Contours on a Vertical Panel (4 x 8 ft., 1.2 x 2.4m) Normal to the Source Plane, Semi-Anechoic Case, White Noise Band Excitation: 500 $\pm$ 100 cps.

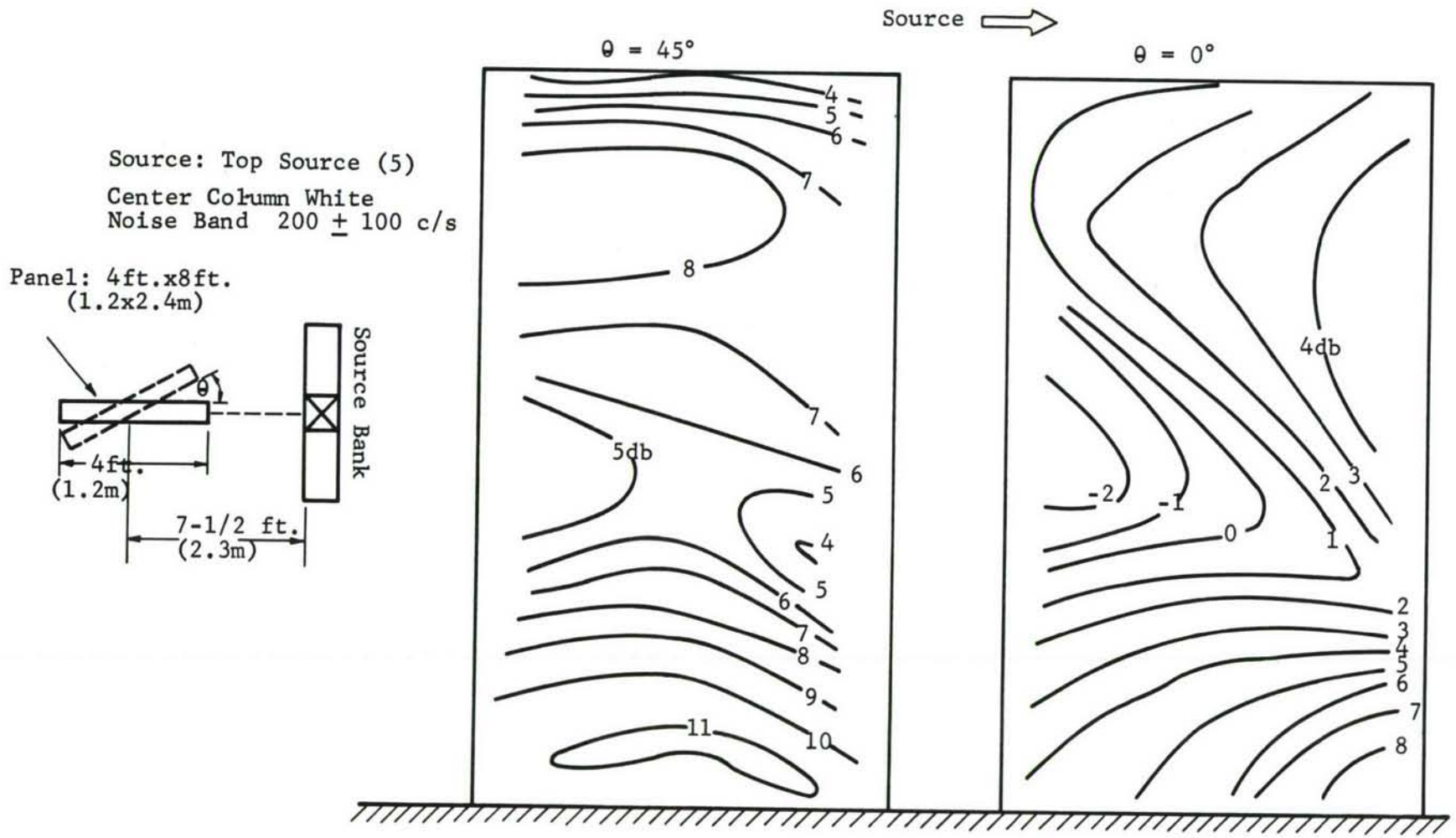

Figure 39. Sound Pressure Level Contours on a Vertical Panel (4 x 8 ft.,1.2 x 2.4m) as a Function of Inclination to the Source Semi-Anechoic Case.

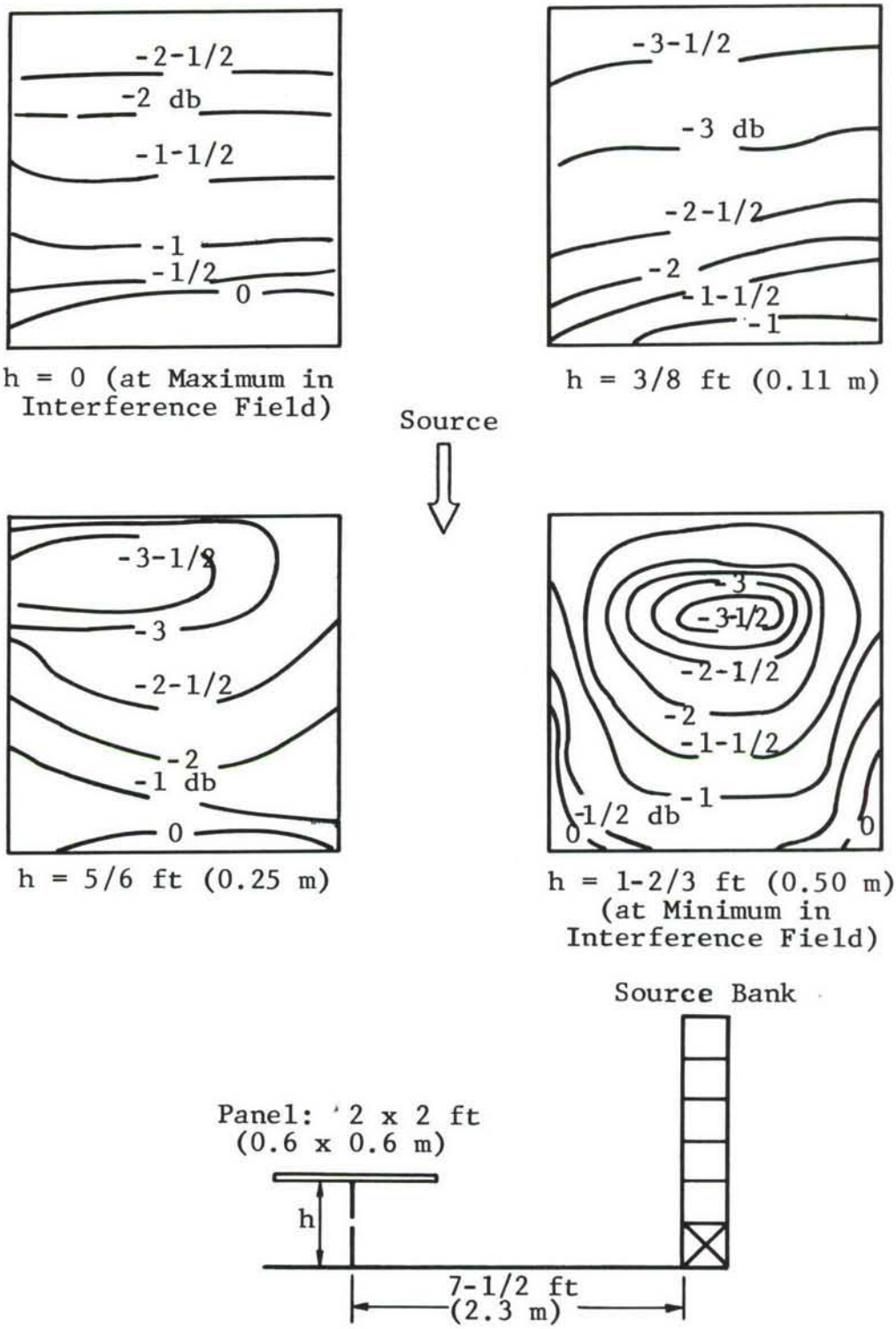

Figure 40. Sound Pressure Level Contours on a Horizontal Panel, Semi-anechoic Case, White Noise Band: 500 $\pm$ 100 cps.

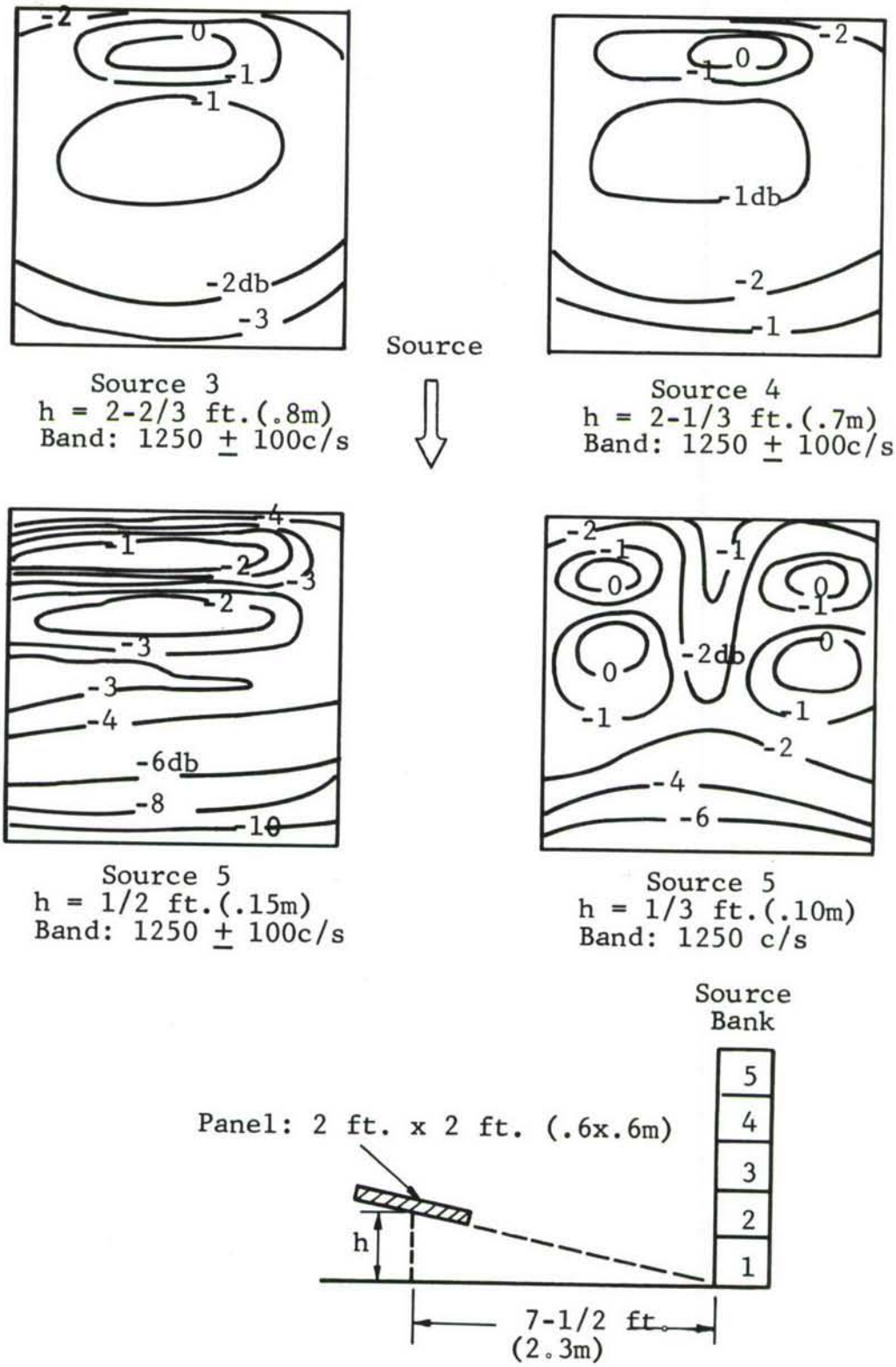

Figure 41. Sound Pressure Level Contours on an Inclined Panel in Relative Minima of Incident Interference Fields, Semi-Anechoic Case, White Noise Band Excitation.

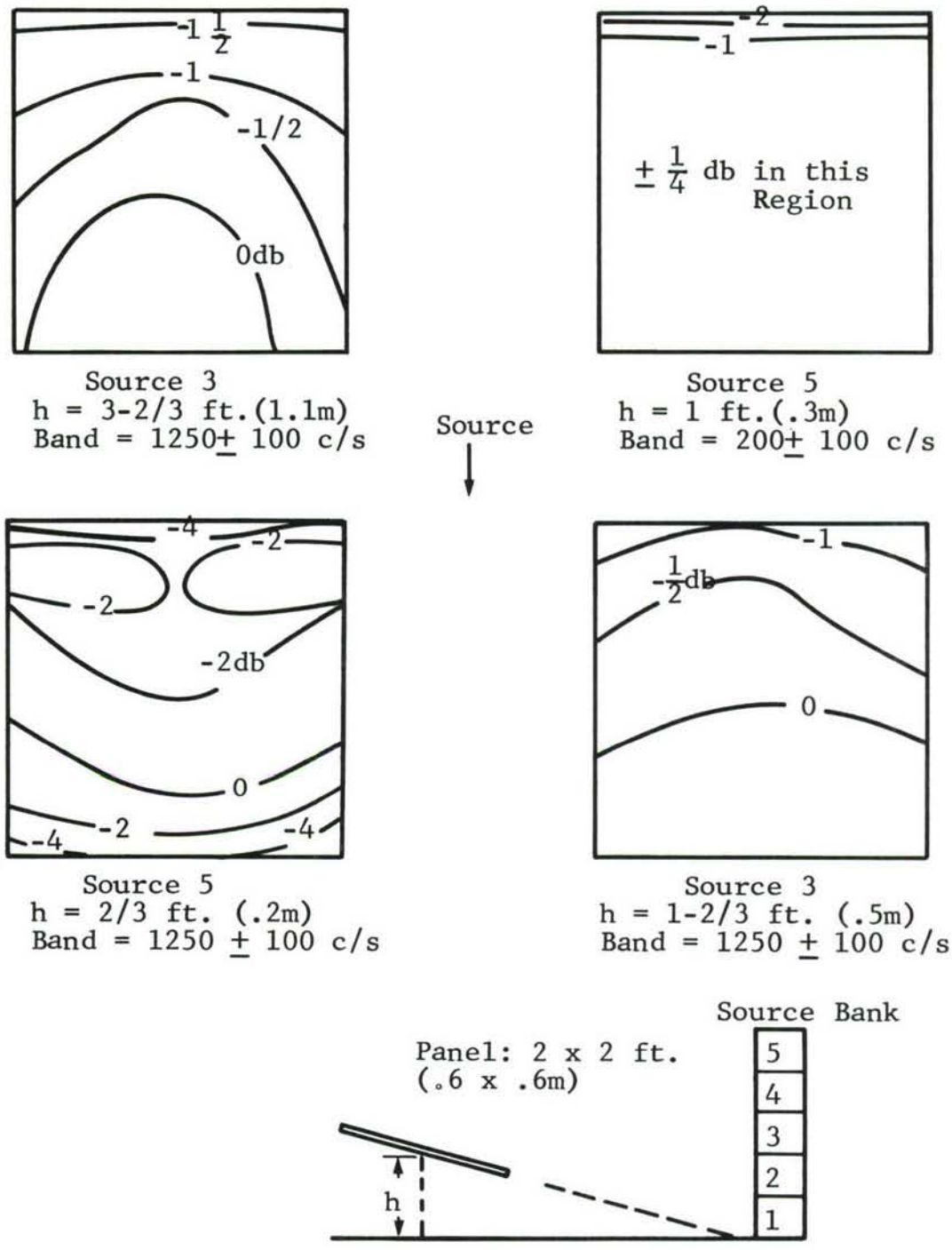

Figure 42. Sound Pressure Level Contours on an Inclined Panel in Relative Maxima of Incident Interference Fields, Semi-Anechoic Case, White Noise Band Excitation.

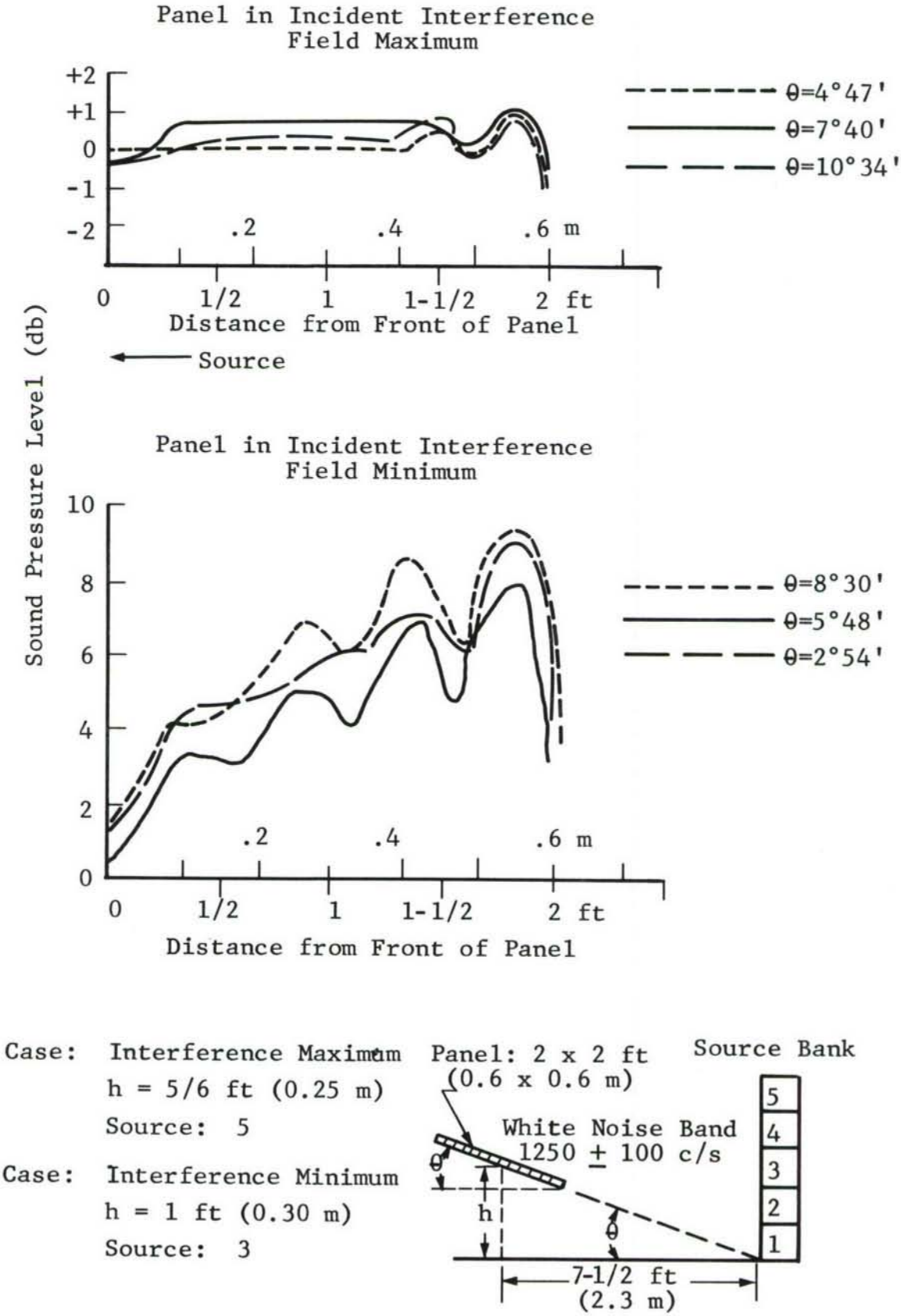

Figure 43. Importance of Alignment of an Inclined Panel in an Incident Interference Maximum and in a Minimum, Semi-anechoic Case.

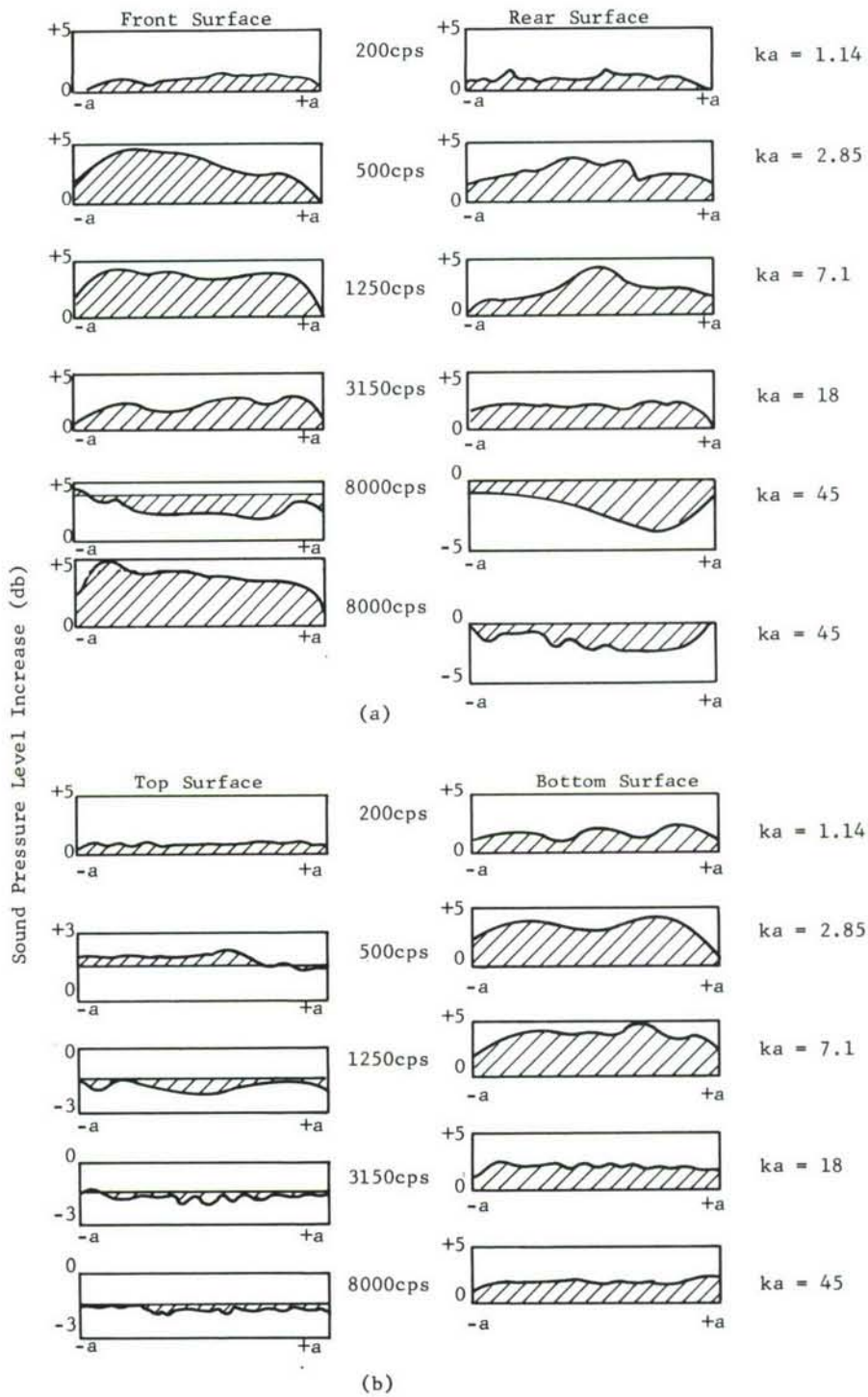

Figure 44. Sound Pressure Level Increase on (a) Vertical, and (b) Horizontal Panel of Dimensions 2a x 2a, Located in Reverberation Room with Ceiling Treatment.

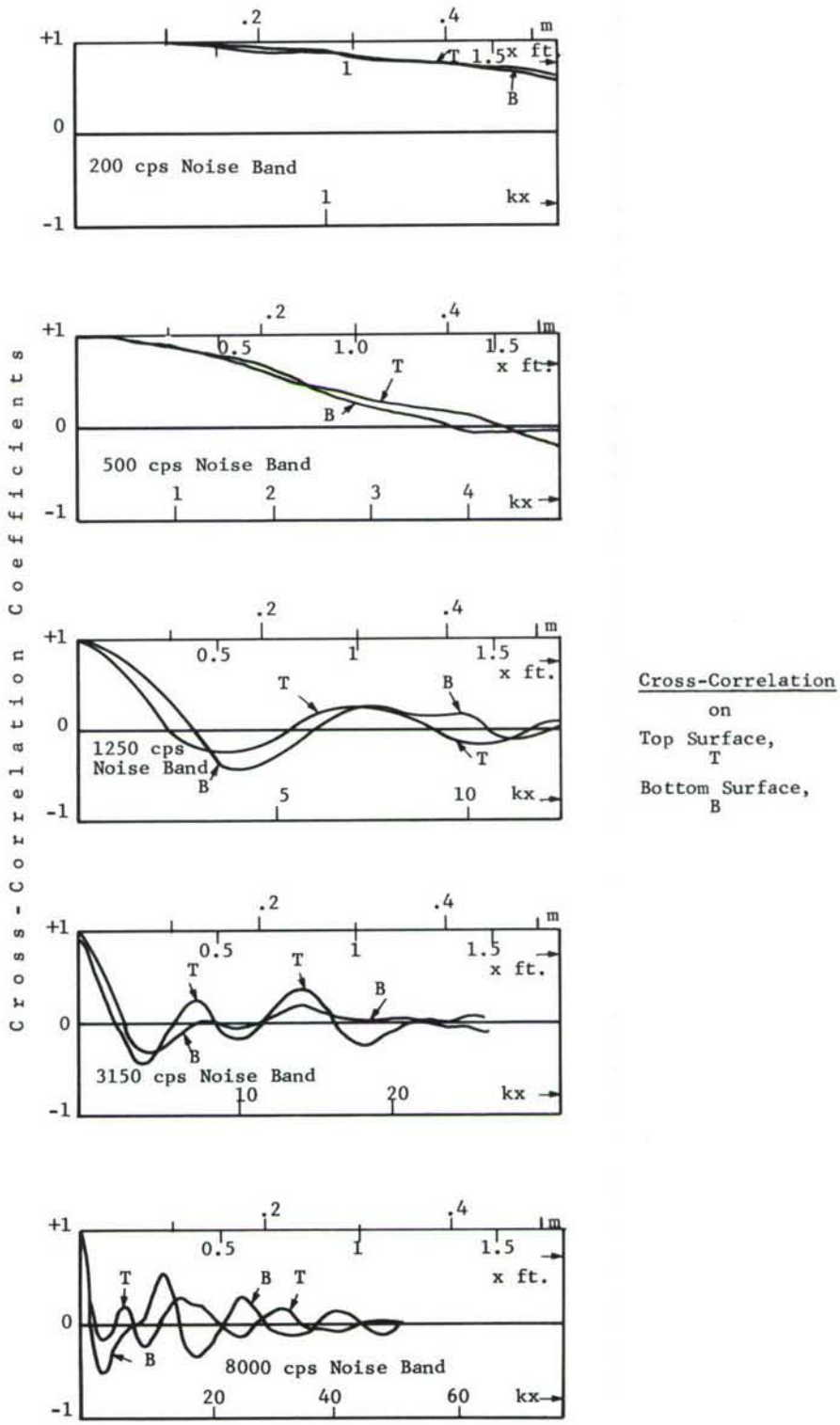

Figure 45. Cross-Correlation Coefficients over Surface of Horizontal Panel in Reverberation Room with Ceiling Treatment.

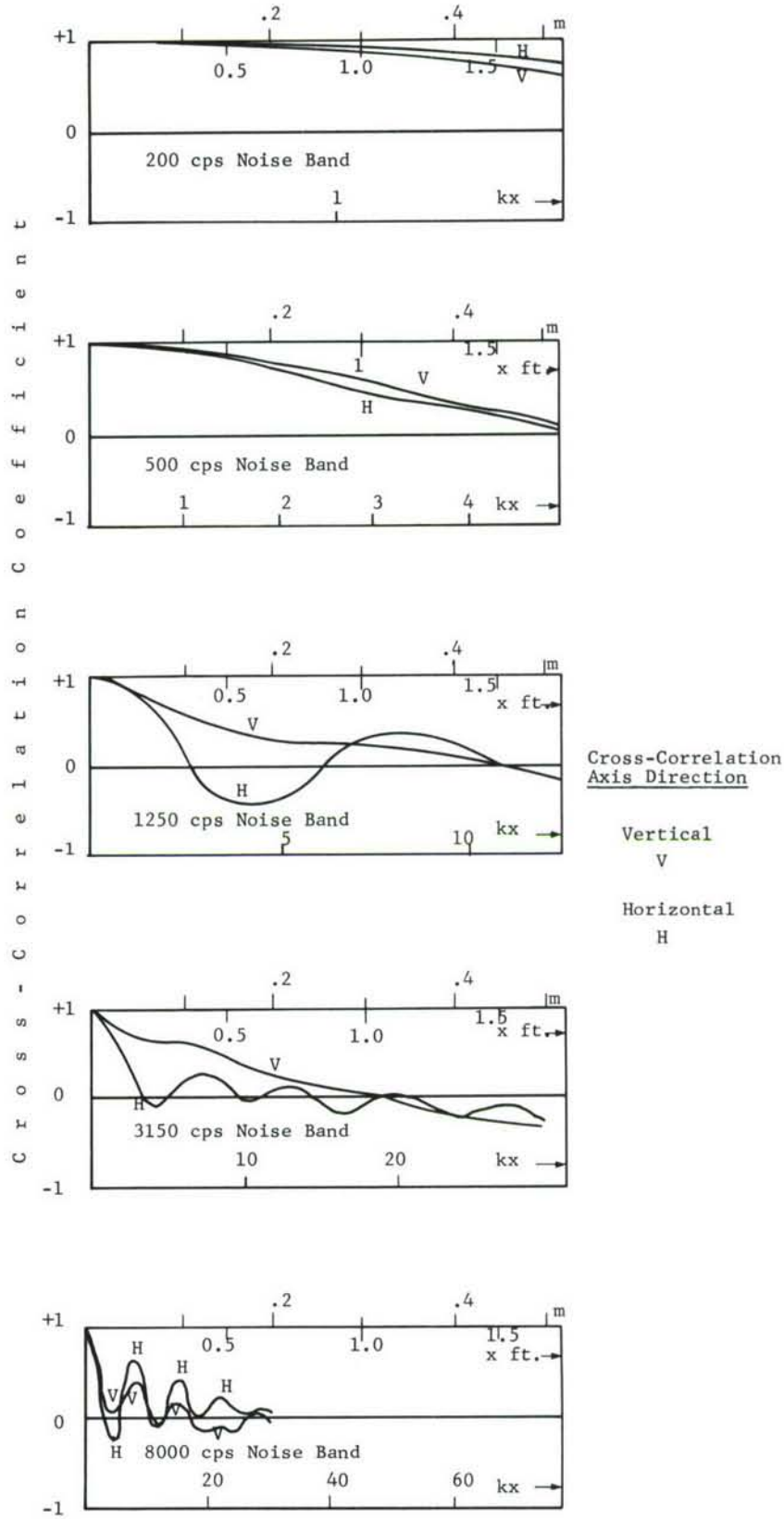

Figure 46. Cross-Correlation Coefficients over Surface of Vertical Panel in Reverberation Room with Ceiling Treatment.

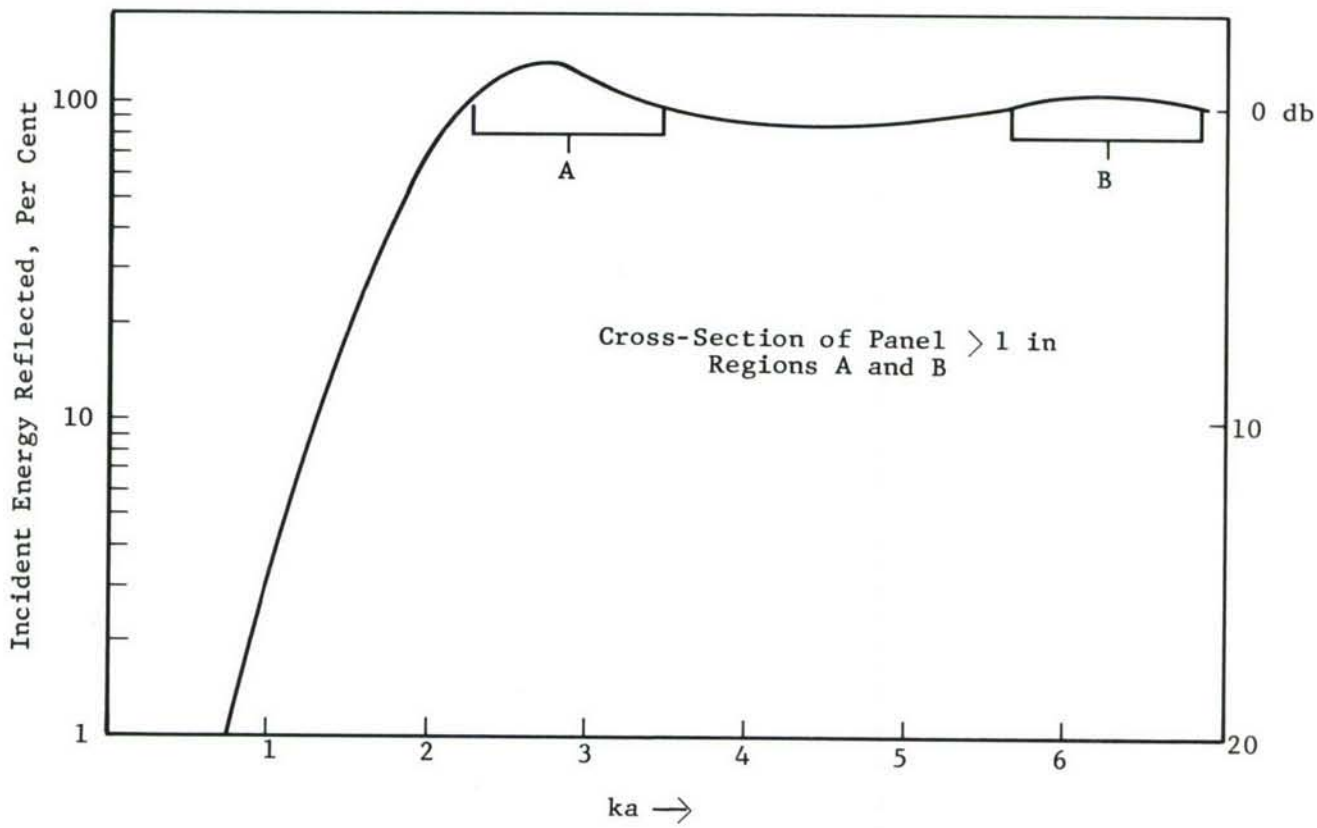

Figure 47. Energy Theoretically Reflected from Flat Disc of Diameter 2a Exposed to Normally Incident Sound of Wave Number k.

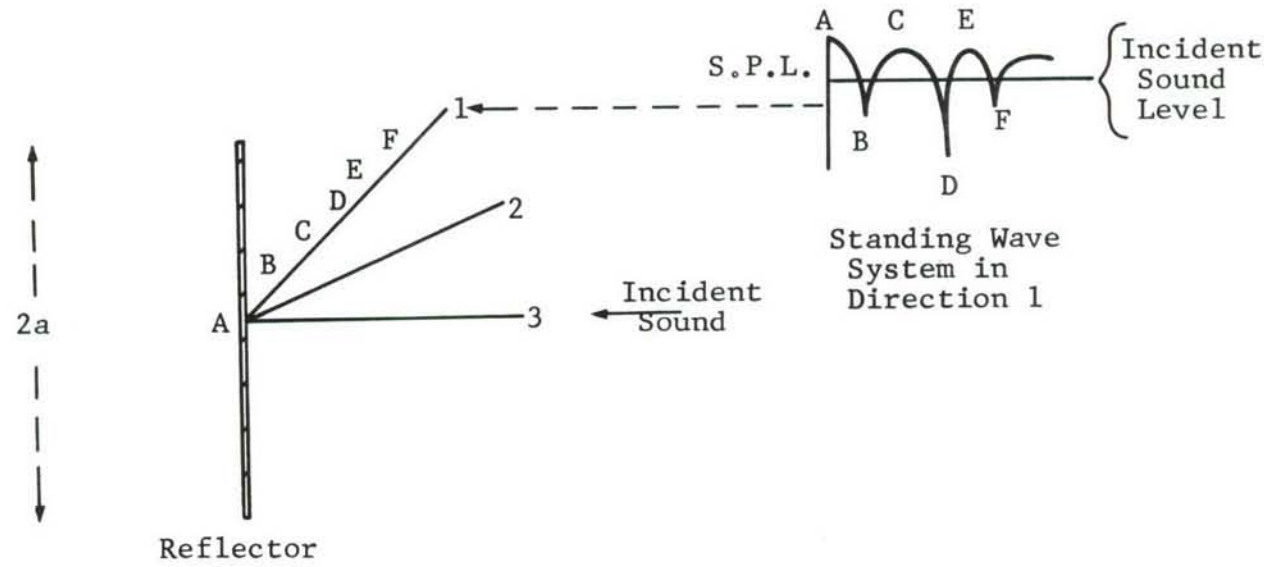

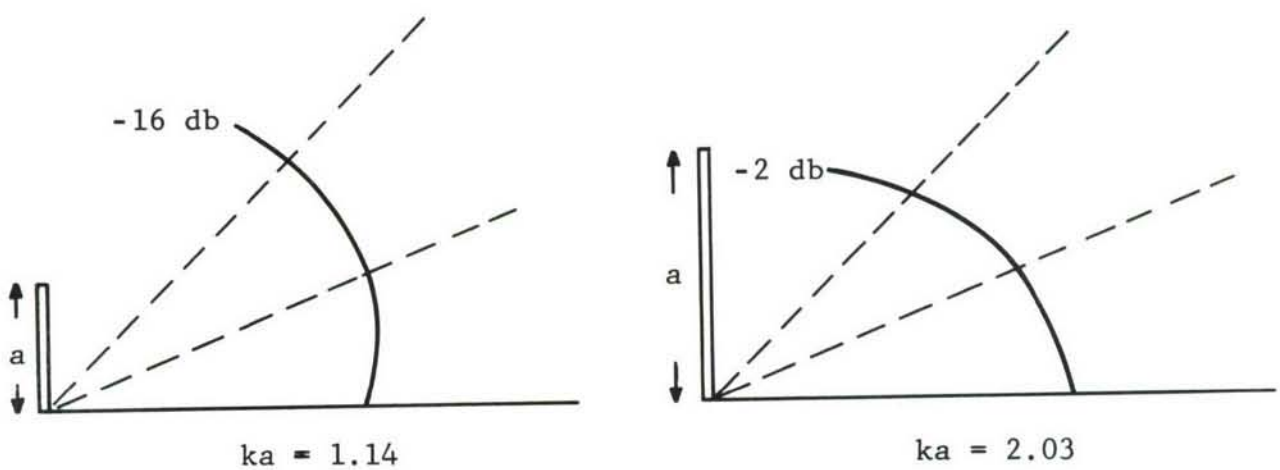

Figure 48. Near-Field of Reflectors (2a x 2a) Using Normally Incident Single Frequency Signals.

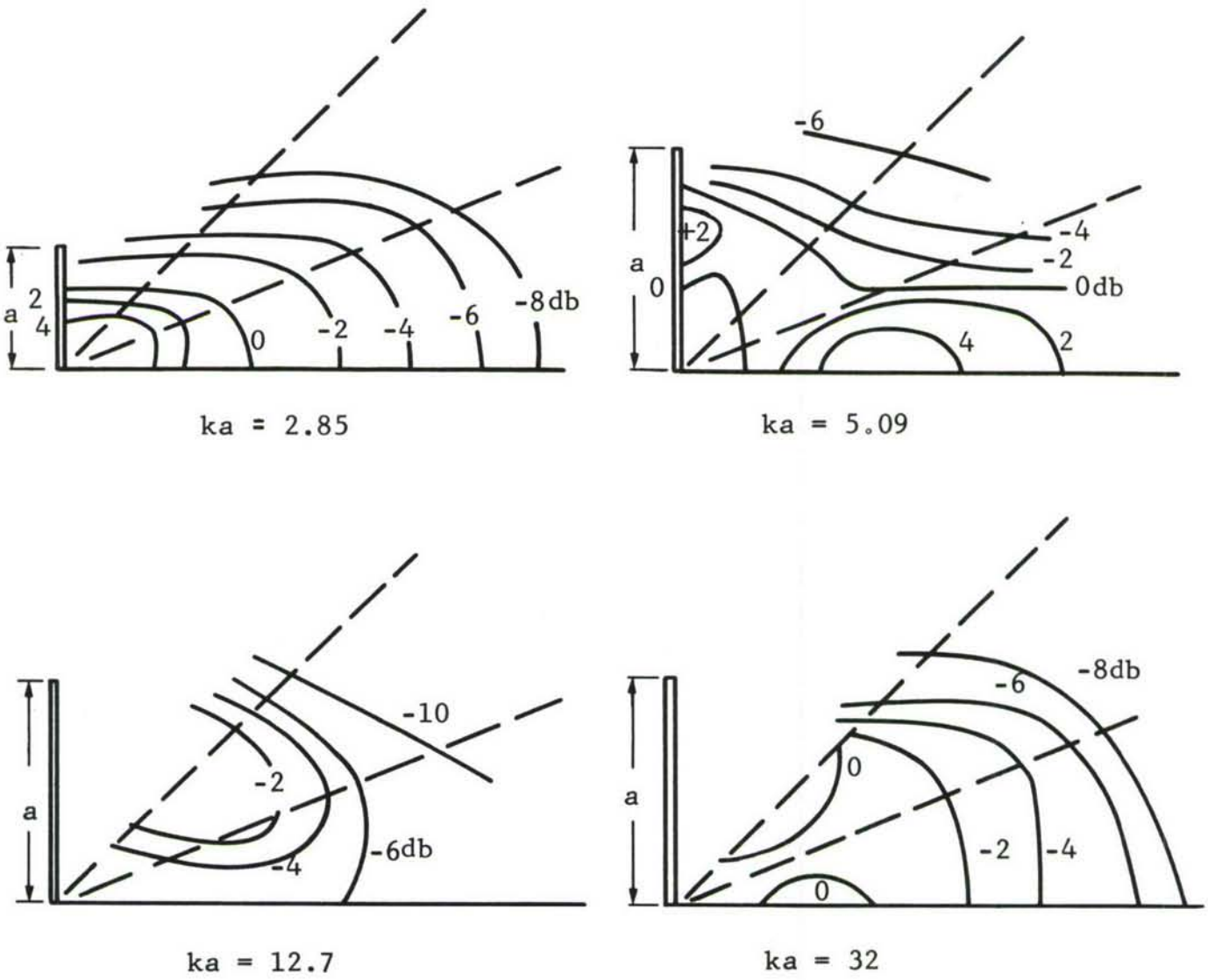

Figure 49. Near-Field of Reflectors (2a x 2a) Using Normally Incident Single Frequency Signals.

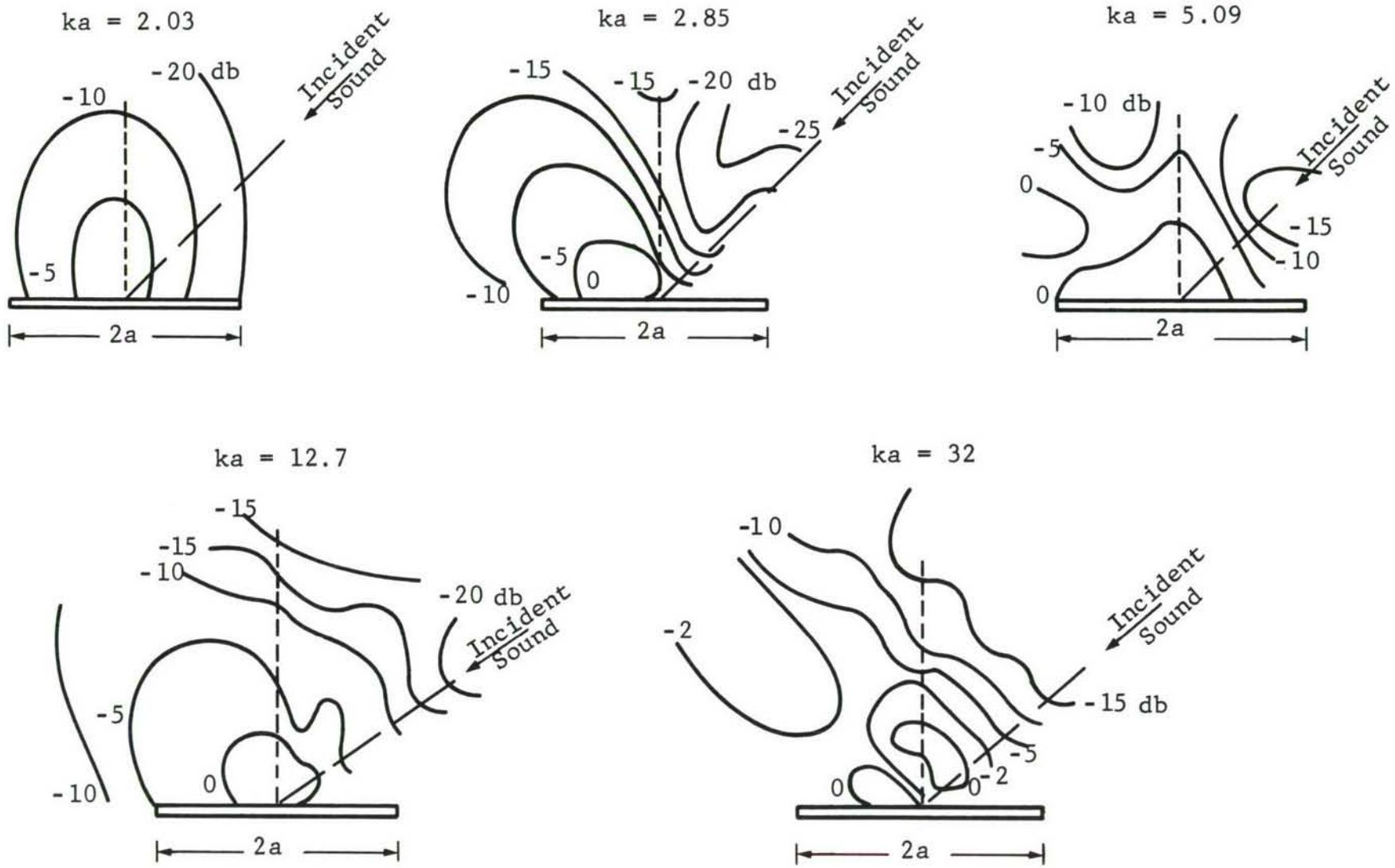

Figure 50. Near Field of Reflectors (2a x 2a) Using 45° Incident Single Frequency Signals.

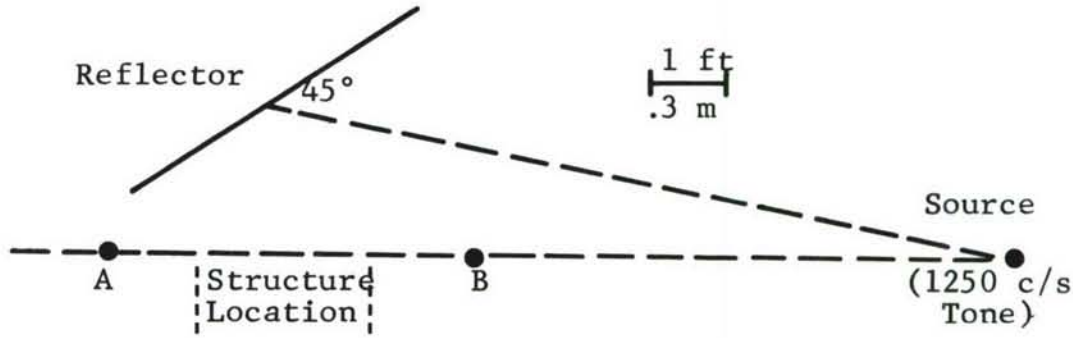

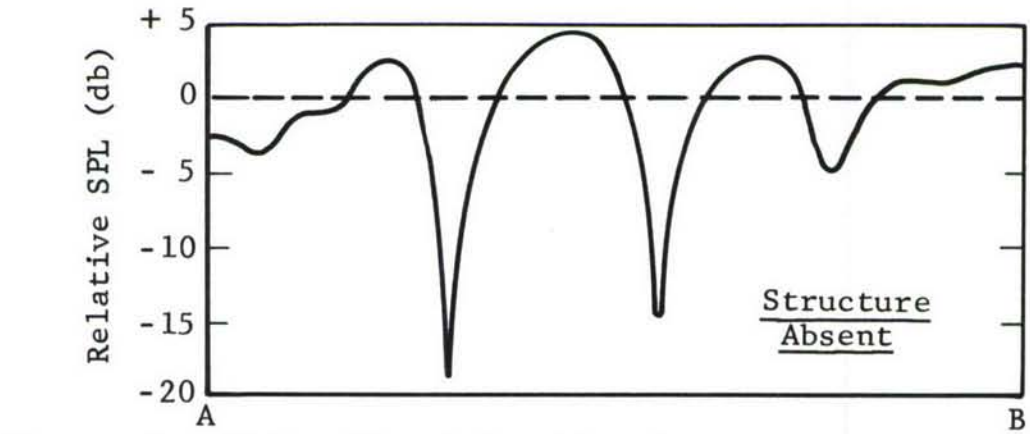

Measured	+2.5	-19	+4.3	-15	+3	-5	+1.5	db
Computed	+3.7	-14	+5.3	-15	+5.2	-4.2	+5	db

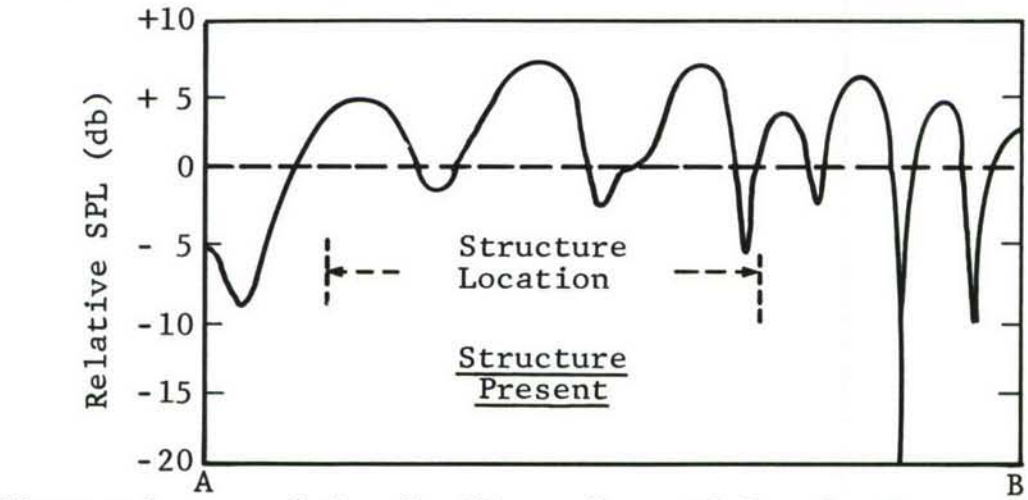

Measured		4.5	-2	+7	-3	+6.5	-6	db
Computed		6.5	-5	+8.5	-3.5	+8	-∞	db

Figure 51. Sound Field Modification Using Reflector in Anechoic Condition.

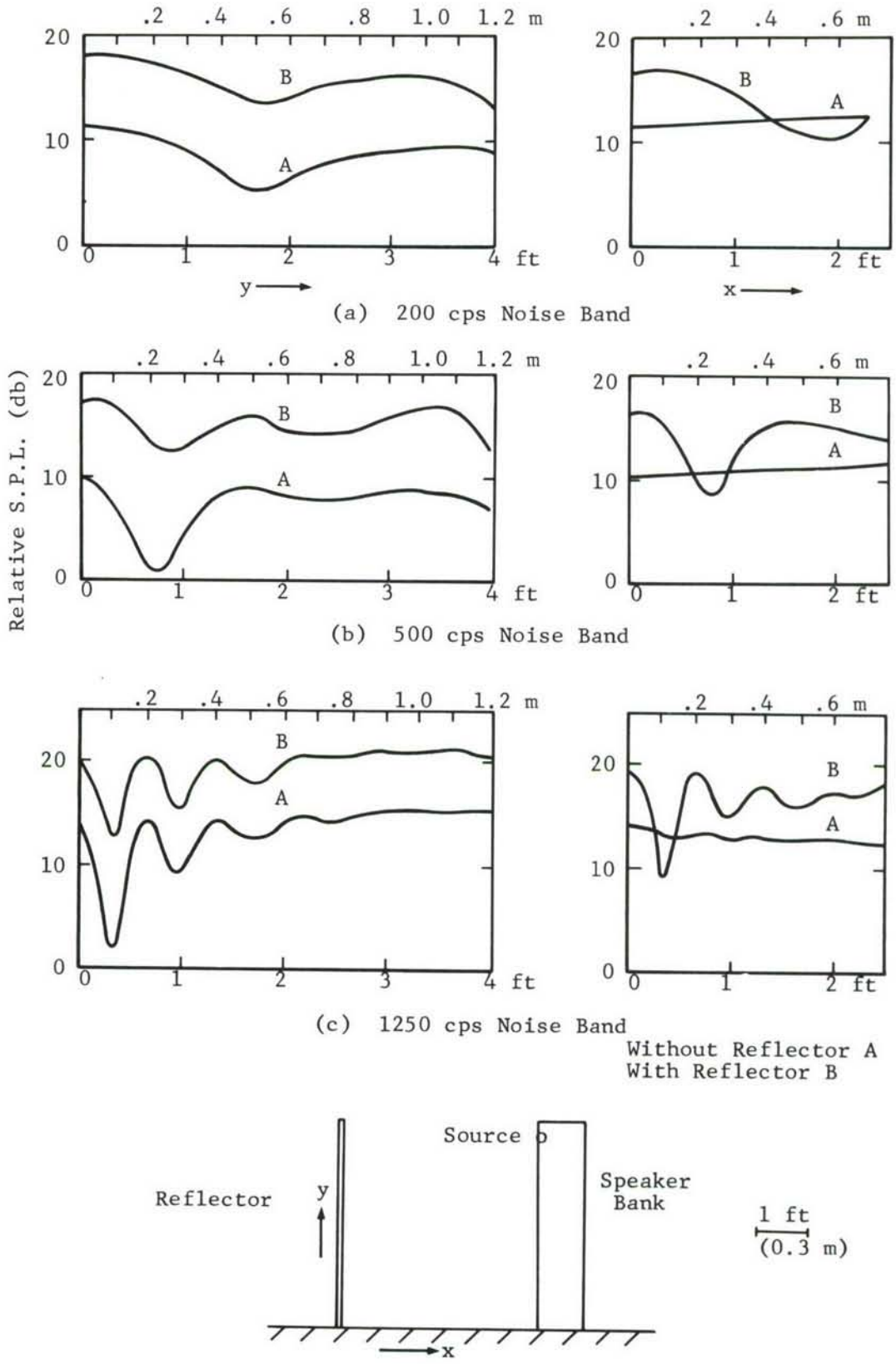

Figure 52. Sound Field Modification Along Floor, Using Reflector Device.

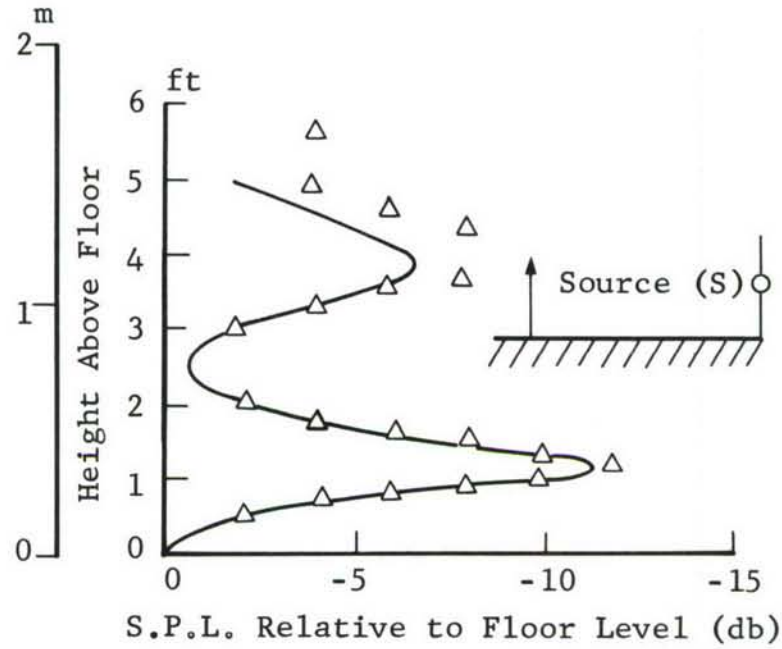

(a)

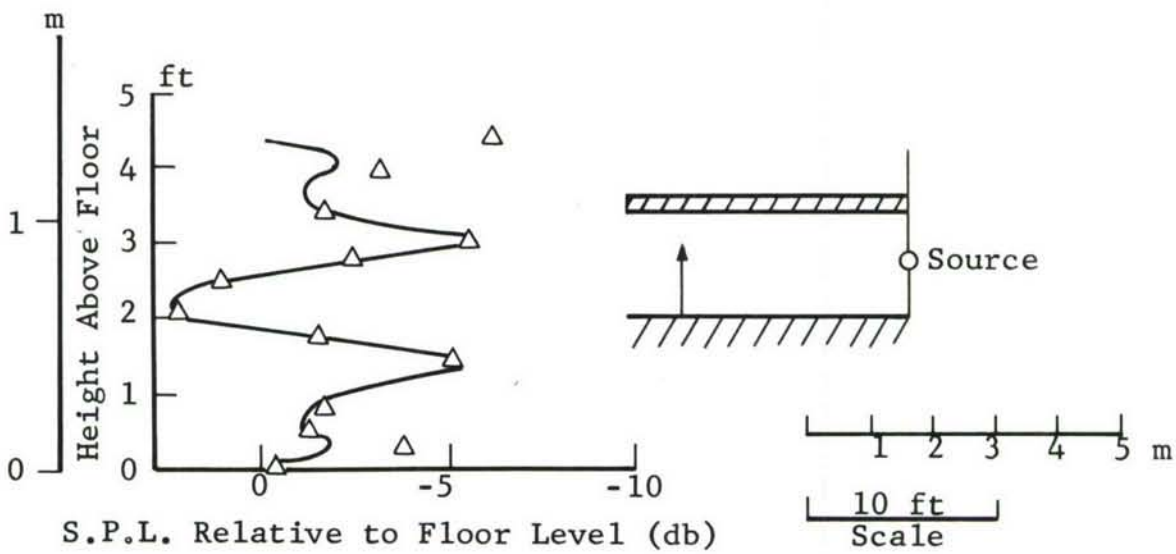

(b)

Figure 53. Sound Field Modification in Vertical Direction Above Floor, Using Reflector Device.

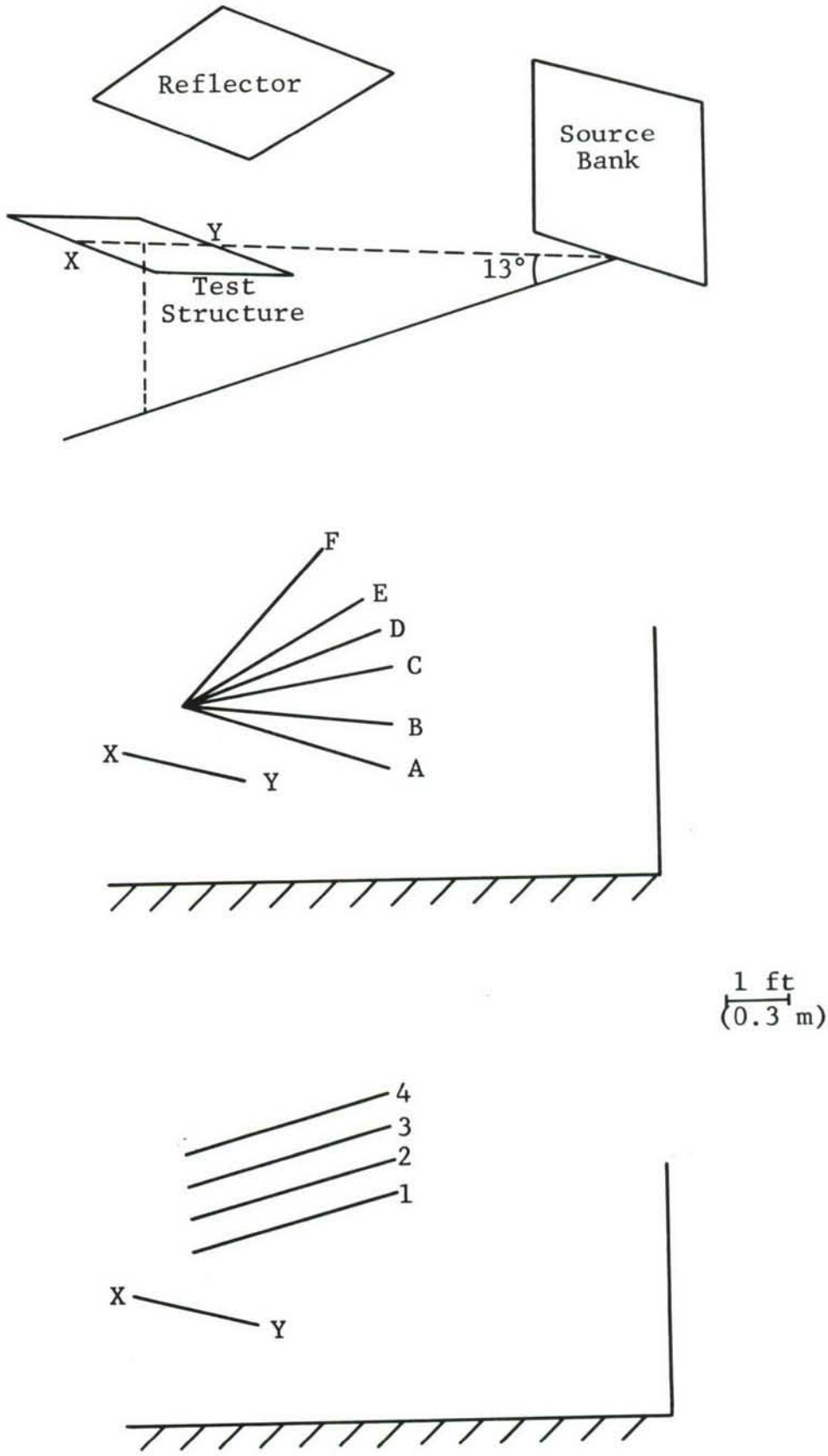

Figure 54. Location of Reflector and Test Structure in Semi-anechoic Environment.

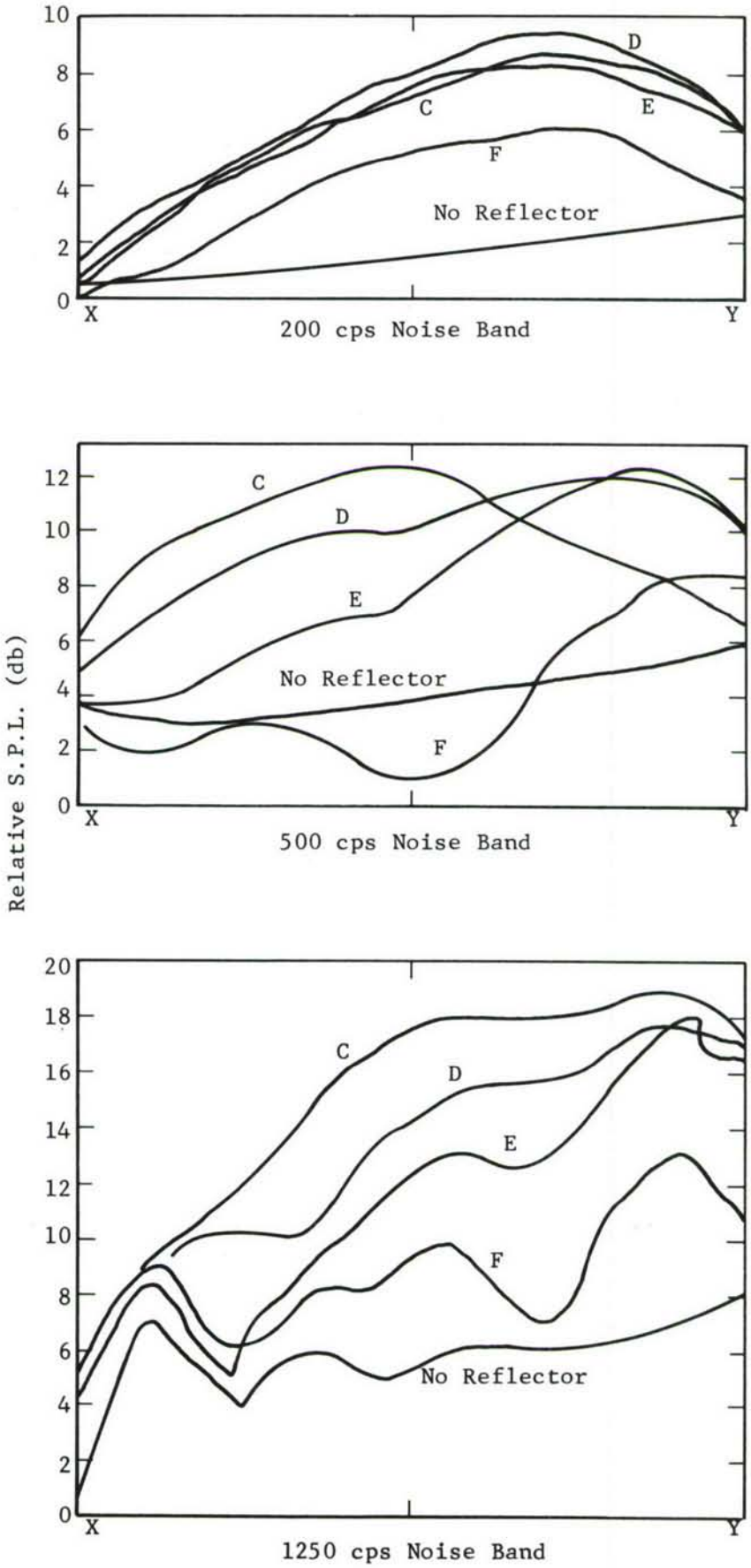

Figure 55. Sound Pressure Level Distribution on Test Structure Using Inclined Reflector.

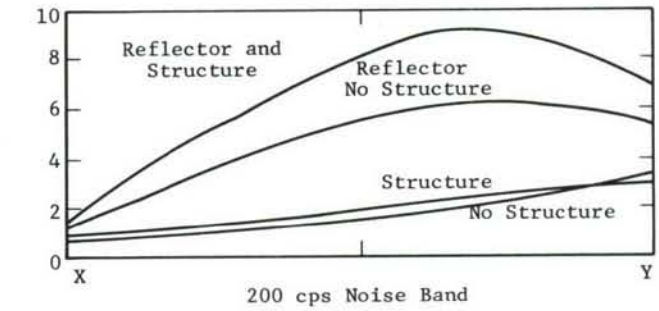

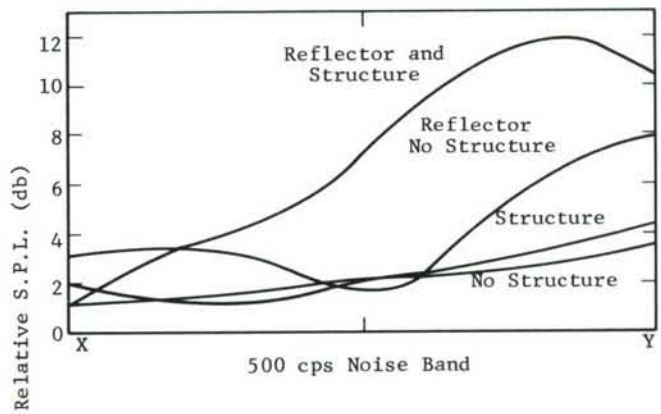

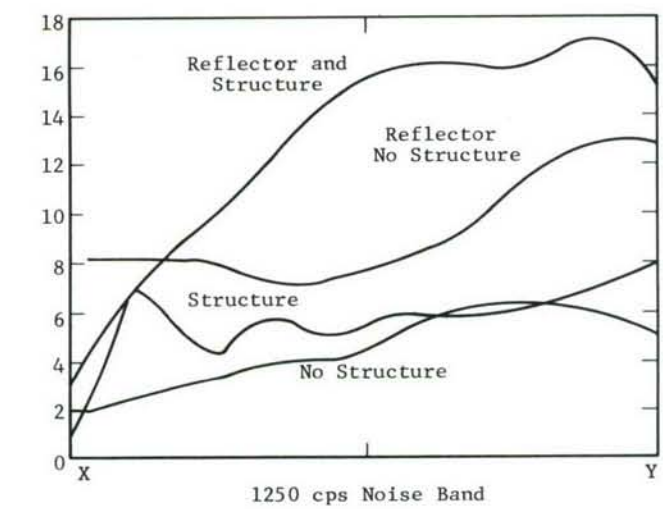

Figure 56. Sound Pressure Level Distribution in Region and on Test Structure Using Reflector Device.

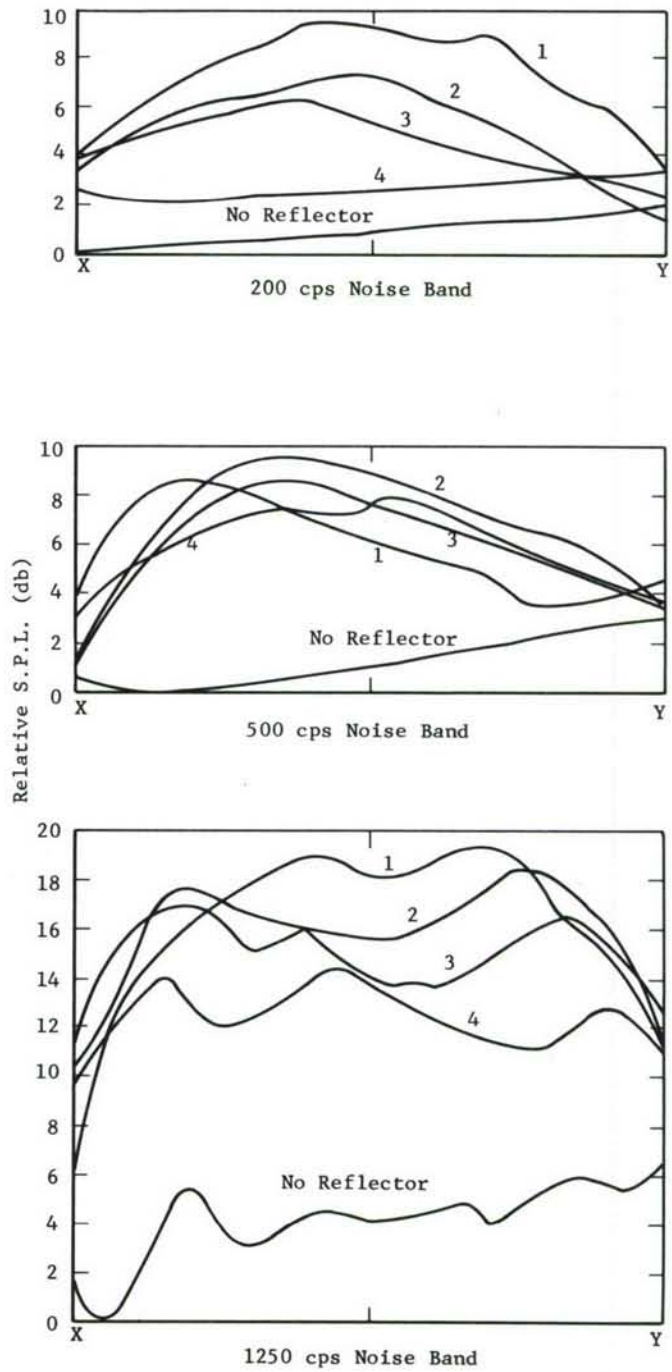

Figure 57. Sound Pressure Level Distribution on Test Structure Using Separated Reflector.

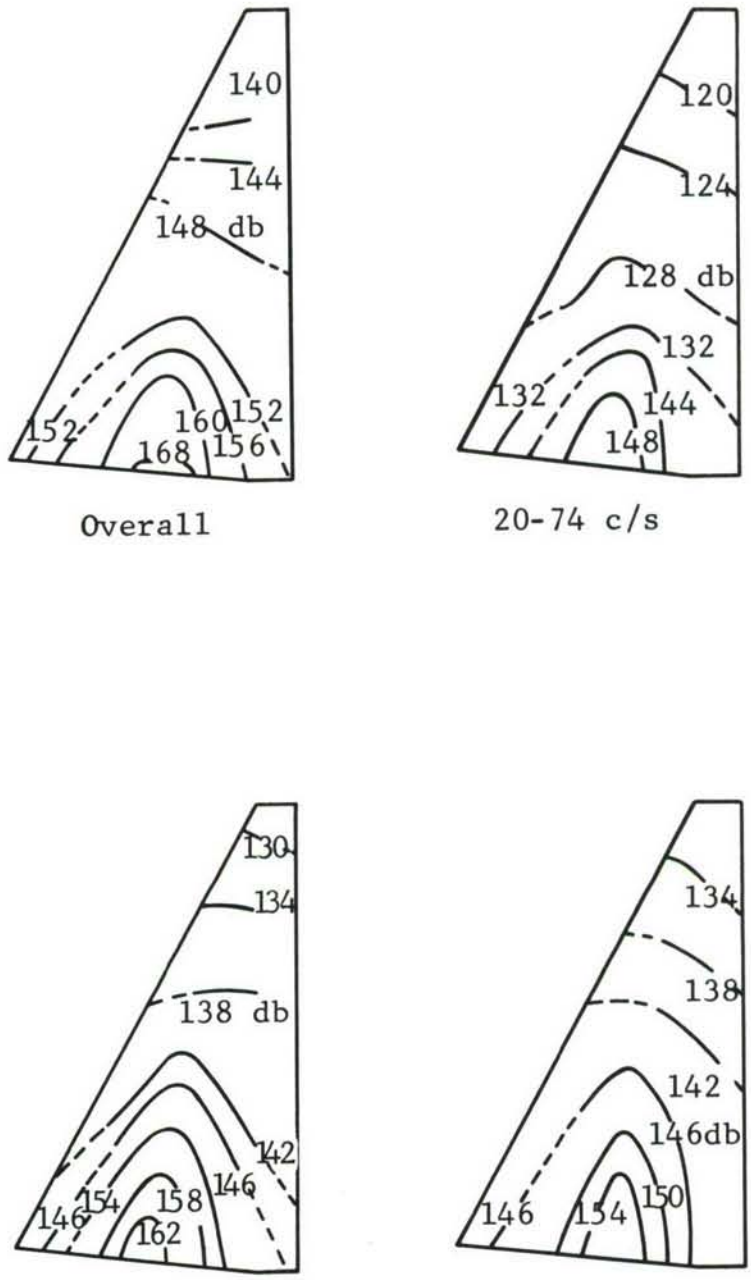

Figure 58. Experimental Sound Pressure Levels on B-58 Wing for Engines at Maximum Preheat.

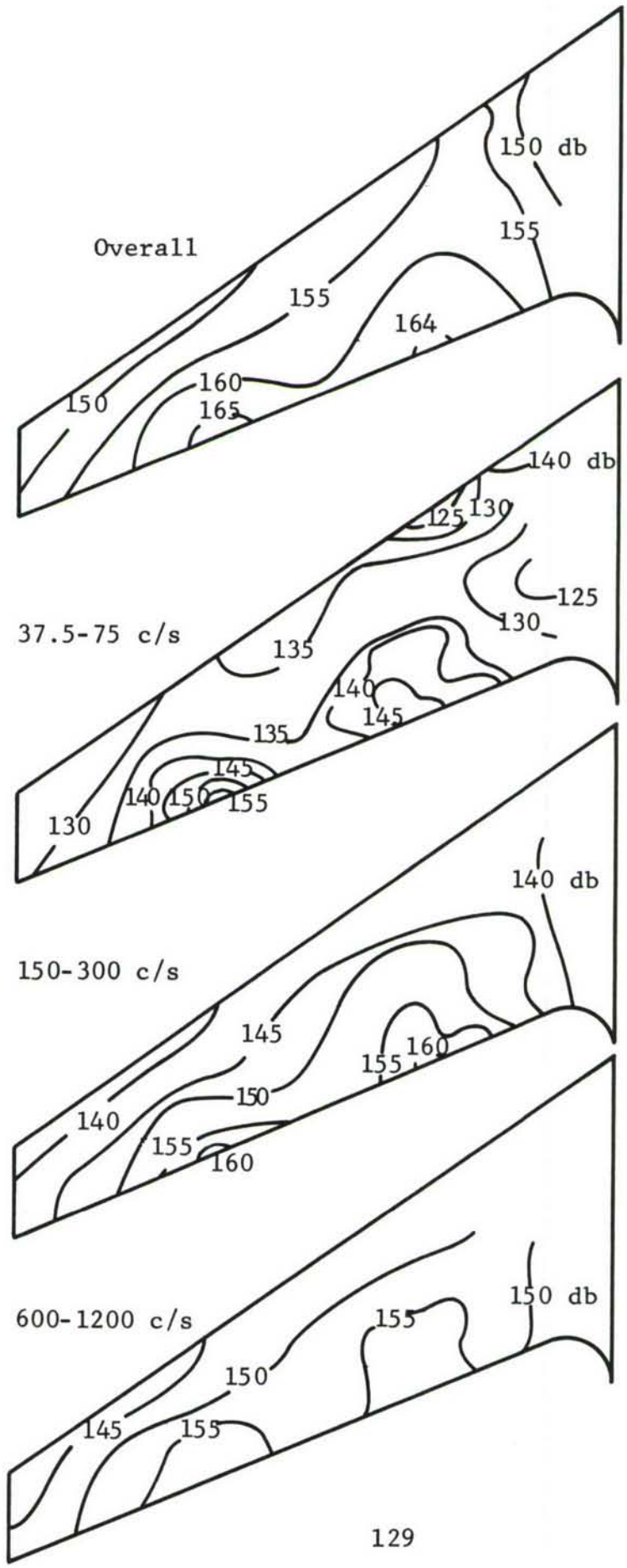

Figure 59. Experimentally Measured Sound Pressure Levels on KC-135 Wing for Engines Operating at Full Wet Power.

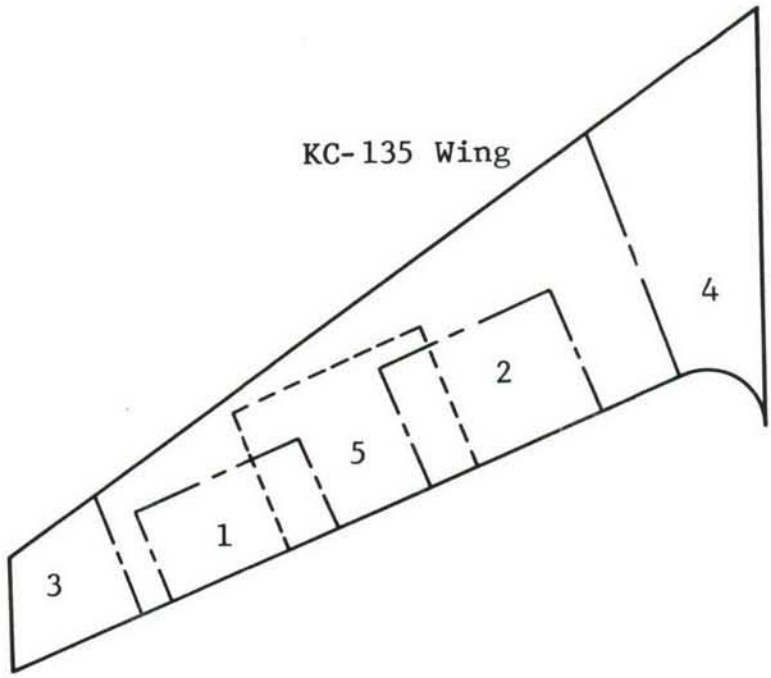

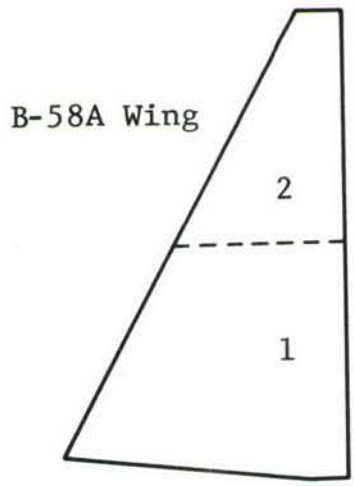

Figure 60. Subdivision of Two Wings into Areas with Simple Geometrical Shaped Sound Pressure Level Contours.

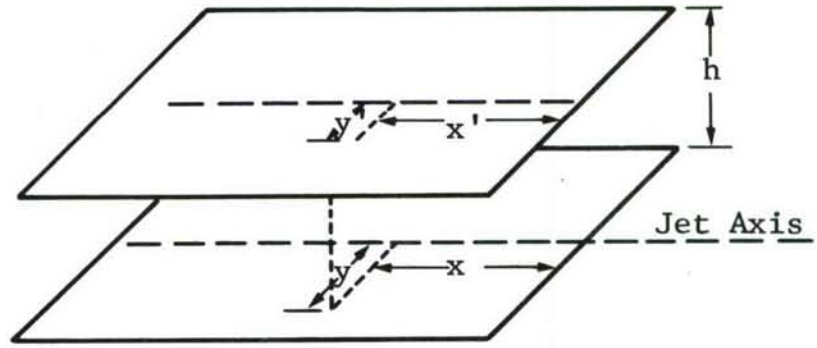

(a)

(b)

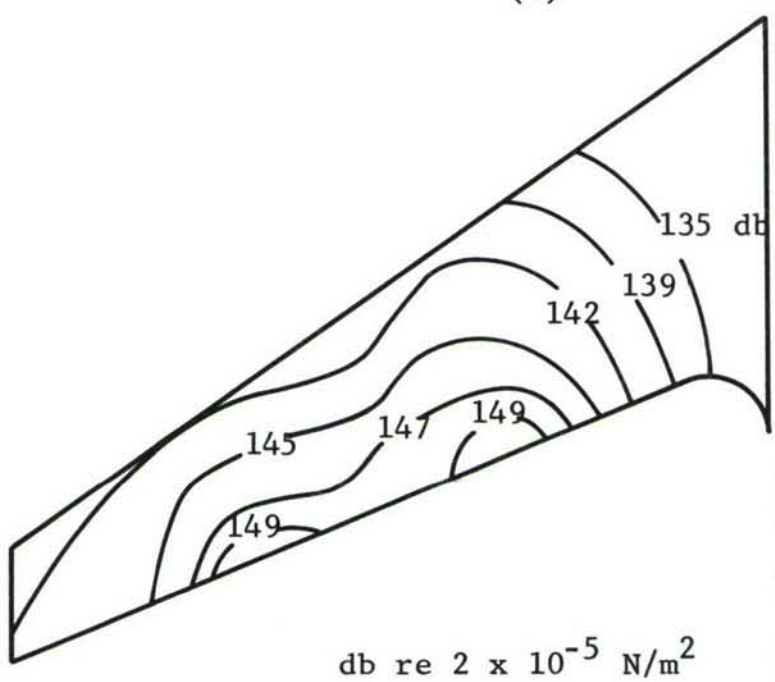

db re 2 x 10^{-5} N/m^2

Figure 61. (a) Geometrical Model Used to Calculate Sound Pressure Levels on a Wing from Engine Data.

(b) Calculated Overall Sound Pressure Levels on KC-135 Wing with Engines at Military Power.

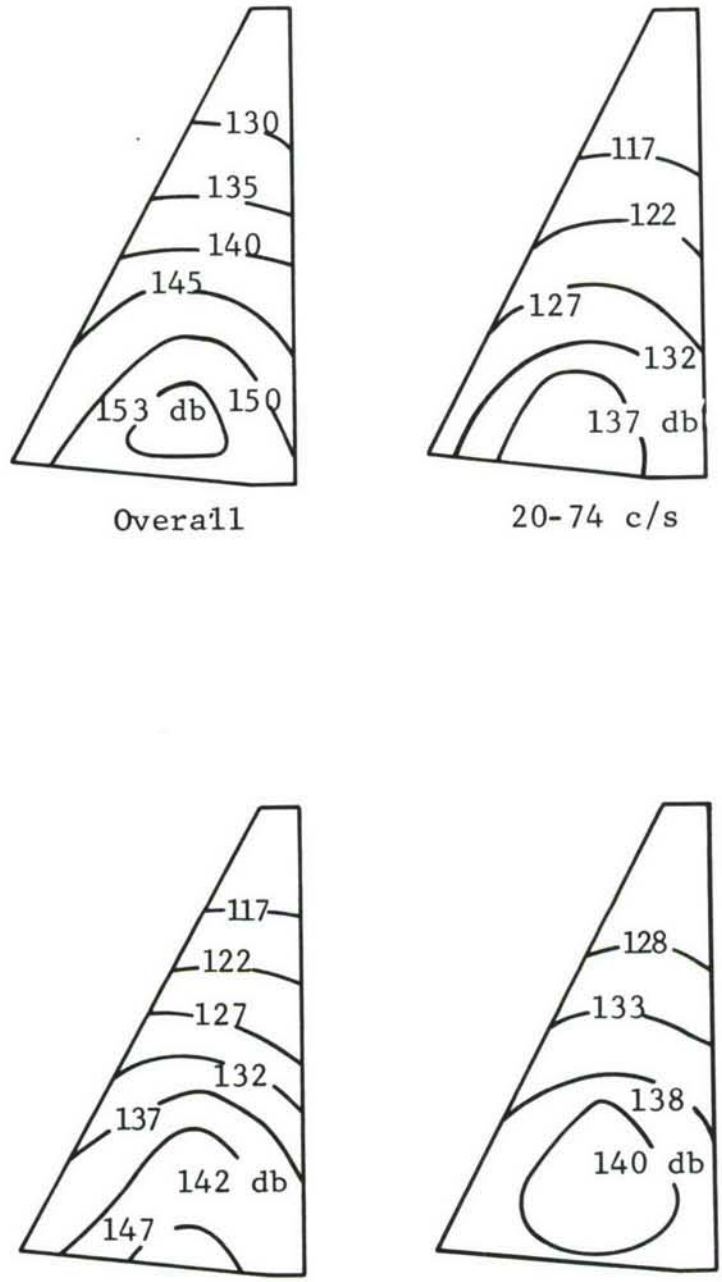

Figure 62. Calculated Octave Band Sound Pressure Levels on the B-58A Wing for Engines Operating under Full Afterburner Power.

APPENDIX A

EXAMPLE CALCULATION OF THE PRESSURE AND PHASE OF AN ACOUSTIC FIELD EXISTING IN A SEMI-ANECHOIC FACILITY

In Fig. 21 of the main text, the pressure and phase distribution along a vertical line above the reflecting floor of the model facility are shown. The following example illustrates how these data were obtained at a given single location. Figure A1 illustrates the chosen location A, located 4 ft above the floor. The source, S, radiates a noise band signal centered at a frequency of 1250 cps whose auto-correlation function, determined under anechoic conditions using an analog correlator, is shown in Fig. A2.

PRESSURE CALCULATION

The mean square pressure at A is [from Eq. (5)]

$$\overline{P_1^2} + \overline{P_2^2} + 2R(\tau)\sqrt{\overline{P_1^2} \cdot \overline{P_2^2}}$$

In this example the line ABX will be considered to be located in the far field so that $\overline{P1^2} \approx \overline{P2^2} \approx \overline{P3^2} \approx \overline{P4^2}$ $(= \overline{P^2}$, the mean square pressure level obtained under completely anechoic conditions at A, B, or X).

Thus the mean square pressure at A is

$$2\overline{P^2}\,[1 + R(\tau)]$$

where $\tau = |S'A - SA|/c = 1.36/1100 = 1.236$ msecs.

From Fig. A2, $R(\tau) = -0.56$, so the mean square pressure at A is $0.88\,\overline{P^2}$. Since the mean square pressure at X is equal to $2\overline{P^2}$, the level at A relative to that at X is equal to

$$10 \log_{10} \frac{0.88}{2.0} \qquad \text{i.e., } -6.4 \text{ db.}$$

This calculation was performed for several locations along this given vertical line, and the resulting calculated sound pressure level curve is shown in Fig. 21.

PHASE CALCULATION

In this example the line ABX is again considered to be located in the far field. Then the cross-correlation coefficient between A and B is shown in Eq. (8) to be

$$R_{A,B} = (R_{1,3} + R_{1,4} + R_{2,3} + R_{2,4})/4$$

where $R_{1,3}$ represents the cross-correlation coefficient between signal 1 at A and signal 3 at B, etc.

$R_{1,3}$ is determined in the following manner.

$$R_{1,3} = R(\tau)$$

where $\tau = |SA - SB|/c$.

If we choose B to be located at X and make this a phase reference location, then, because P_3 and P_4 will be identical,

$$R_{2,3} = R_{2,4}$$

and

$$R_{1,3} = R_{1,4}$$

So

$$R_{A,B(=X)} = (R_{1,3} + R_{2,3})/2.$$

Now

$$R_{1,3} = R(\tau)$$

where τ is now equal to $|SA - SX|/c = 0.08/1100 = 0.073$ msec. So from Fig. A2

$$R_{1,3} = + 0.78.$$

Similarly,

$$R_{2,3} = R(\tau)$$

where τ is now equal to $|S'A - SX|/c = 1.28/1100 = 1.164$ msec. So from Fig. A2

$$R_{2,3} = -0.55$$

Thus the value of

$$R_{A,B(=X)} = (+ 0.78 - 0.055)/2 = + 0.115$$

This calculated value of the cross-correlation function between the acoustic field at a point A located 4 ft above X and the field at X, together with calculations for additional locations is shown in Fig. 21.

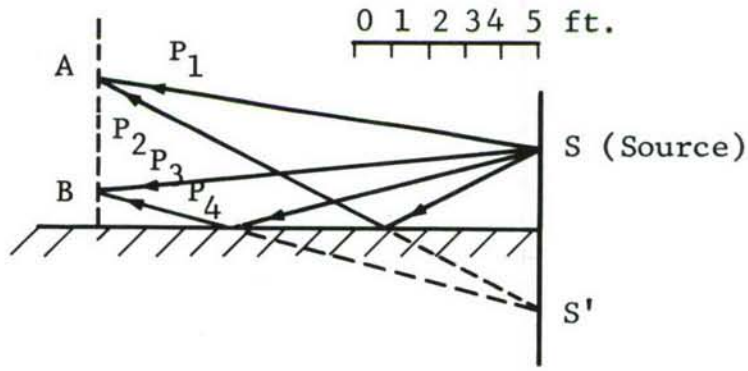

Figure A-1. Geometry of System Producing an Interference Field

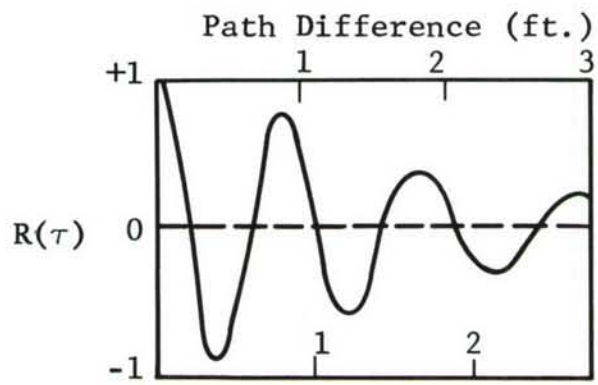

Figure A-2. Auto-Correlation Coefficient for Given Noise-Band Signal with Center Frequency 1250 cps.

APPENDIX B

CALCULATED PARAMETERS OF THE RTD AND IITRI REVERBERATION FACILITIES

The following values are based upon an assumption of rectangular facility shapes as shown in Fig. B1. Also, all surfaces are assumed to have negligible absorption coefficient except the acoustic treatment for which a value of 100 per cent is chosen.

(a) RTD Facility, fully reverberant

Surface area = 17,592 ft^2 (2 x 68 x 42, 2 x 68 x 54, 2 x 54 x 42)

Volume = 155,000 ft^3 (68 x 54 x 42)

(b) RTD Facility, collapsed wall treatment

Exposed area of treatment = 3,721 ft^2 (2 x 6-1/2 x 68, 2 x 6-1/2 x 41, 2 x 12 x 55, 2 x 12 x 41)

Untreated area = 13,247 ft^2 (68 x 54, 55 x 41, 2 x 30 x 68, 2 x 30 x 54)

Total area = 16,968 ft^2

Volume = 137,220 ft^3 (68 x 54 x 30, 55 x 41 x 12)

$\bar{\alpha}$ = 0.219, (3721/16,968) β = 4764 ft^2, [3721/(1 - 0.23)]

(c) RTD Facility, collapsed wall and ceiling treatment

Exposed area of treatment = 4,440 ft^2 (68 x 54, 2 x 4 x 55, 2 x 4 x 41)

Untreated area = 10,992 ft^2 (68 x 54, 2 x 30 x 68, 2 x 30 x 54)

Total area = 15,432 ft^2

Volume = 119,180 ft^3 (68 x 54 x 30, 55 x 41 x 4)

$\bar{\alpha}$ = 0.288, (4440/15,432) β = 6236 ft^2, (4440/1 - 0.288)

(d) IITRI Facility, fully reverberant

Surface area = 1428 ft^2 (2 x 21 x 14, 2 x 21 x 12
2 x 12 x 14)

Volume = 3528 ft^3 (21 x 14 x 12)

(e) IITRI Facility, perimeter treatment

Exposed area of treatment = 299 ft^2 (2 x 1-1/2 x 21,
2 x 1-1/2 x 11,
2 x 3-1/2 x 18,
2 x 3-1/2 x 11)

Untreated area = 1087 ft^2 (21 x 14, 18 x 11,
2 x 8-1/2 x 21,
2 x 8-1/2 x 14)

Total area = 1386 ft^2

Volume = 3192 ft^3 (21 x 14 x 8-1/2,
18 x 11 x 3-1/2)

$\bar{\alpha}$ = 0.216, (299/1386) β = 381 ft^2, (299/1 - 0.216)

(f) IITRI Facility, ceiling treatment

Exposed area of treatment = 222 ft^2 (actual size 18-1/2 x 12)

Untreated area = 1101 ft^2 (21 x 14, 2 x 10-1/2 x 21,
2 x 10-1/2 x 14, 2 x 21,
2-1/2 x 12)

Total area = 1323 ft^2

Volume = 3087 ft^3 (21 x 14 x 10-1/2)

$\bar{\alpha}$ = 0.168, (222/1323) β = 267 ft^2, (222/1 - 0.168)

(g) IITRI Facility, combined ceiling and perimeter treatment

Exposed area of treatment = 410 ft^2 (21 x 14, 2 x 2 x 18,
2 x 2 x 11)

Untreated area = 889 ft^2 (21 x 14, 2 x 8-1/2 x 21,
2 x 8-1/2 x 14)

Total area = $\overline{1299\ ft^2}$

Volume = $2895\ ft^3$ (21 x 14 x 8-1/2, 18 x 11 x 2)

$\overline{\alpha} = 0.316, (410/1299)$ $\beta = 599\ ft^2, (410/1 - 0.316)$

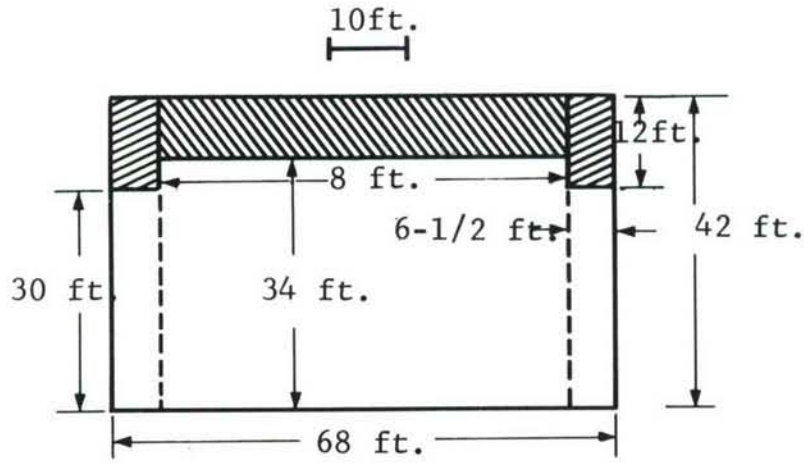

Approximate Dimensions of
RTD Facility 68 x 54 x 42 ft.

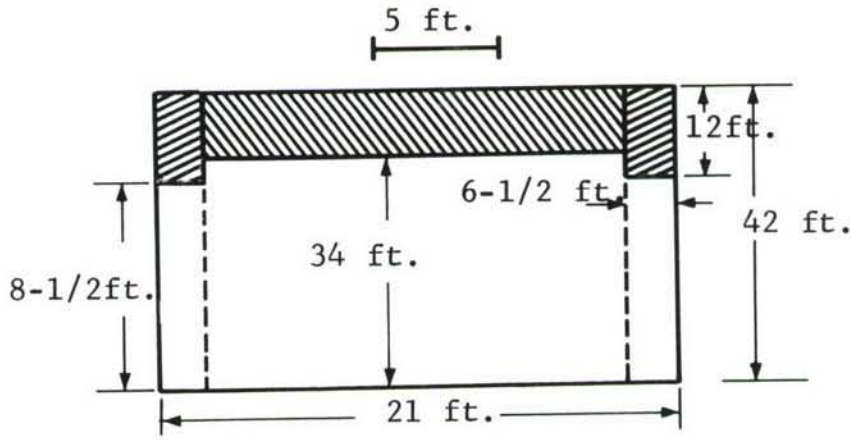

Approximate Dimensions of
IITRI Facility 21 x 14 x 12 ft.

Figure B-1. Rectangular Approximations for the Shapes of the RTD and the IITRI Reverberation Rooms.

Unclassified
Security Classification

DOCUMENT CONTROL DATA - R&D
(Security classification of title, body of abstract and indexing annotation must be entered when the overall report is classified)

1. ORIGINATING ACTIVITY *(Corporate author)*
IIT Research Institute
10 West 35th Street
Chicago, Illinois 60616

2a. REPORT SECURITY CLASSIFICATION
UNCLASSIFIED

2b. GROUP

3. REPORT TITLE
Theoretical and Experimental Model Investigations of Semi-Anechoic and Semi-Reverberant Environments and Their Application to the RTD Sonic Fatigue Facility

4. DESCRIPTIVE NOTES *(Type of report and inclusive dates)*
Final 15 November 1964 to 15 March 1966

5. AUTHOR(S) *(Last name, first name, initial)*
Pernet, David F.
Hruska, Gale R.

6. REPORT DATE	7a. TOTAL NO. OF PAGES	7b. NO. OF REFS
April 1966	138	29

8a. CONTRACT OR GRANT NO.
AF 33(615)-2174

b. PROJECT NO.
4437

c.
Task 443701

d.

9a. ORIGINATOR'S REPORT NUMBER(S)
AFFDL-TR-66-20

9b. OTHER REPORT NO(S) *(Any other numbers that may be assigned this report)*

10. AVAILABILITY/LIMITATION NOTICES
The distribution of this document is unlimited

11. SUPPLEMENTARY NOTES

12. SPONSORING MILITARY ACTIVITY
Air Force Flight Dynamics Lab.
Wright-Patterson AFB, Ohio 45433
RTD, AFSC

13. ABSTRACT

A study of the acoustic environments that could be produced in the RTD Sonic Fatigue Facility has been made using both theoretical methods and experimental modeling techniques. An analysis is presented which enables the semi-anechoic environment to be determined at any position in the facility. This analysis is verified experimentally. An experimental program has also enabled the semi-reverberant environment to be established and has revealed the part played by the absorbing treatment in determining this environment. Experimental programs have investigated the sound fields on structures located in the facility under both modes of operation. A study of reflector devices used to modify acoustic environments was made and has enabled limited prediction of their effects. An analysis of current service noise fields on aircraft structures has enabled determination of values of the major parameters of these fields for use in simulation studies.

DD FORM 1 JAN 64 1473

Unclassified
Security Classification

14. KEY WORDS	LINK A		LINK B		LINK C	
	ROLE	WT	ROLE	WT	ROLE	WT
Semi-Anechoic Environments Semi-Reverberant Environments RTD Sonic Fatigue Facility						

INSTRUCTIONS

1. ORIGINATING ACTIVITY: Enter the name and address of the contractor, subcontractor, grantee, Department of Defense activity or other organization *(corporate author)* issuing the report.

2a. REPORT SECURITY CLASSIFICATION: Enter the overall security classification of the report. Indicate whether "Restricted Data" is included. Marking is to be in accordance with appropriate security regulations.

2b. GROUP: Automatic downgrading is specified in DoD Directive 5200.10 and Armed Forces Industrial Manual. Enter the group number. Also, when applicable, show that optional markings have been used for Group 3 and Group 4 as authorized.

3. REPORT TITLE: Enter the complete report title in all capital letters. Titles in all cases should be unclassified. If a meaningful title cannot be selected without classification, show title classification in all capitals in parenthesis immediately following the title.

4. DESCRIPTIVE NOTES: If appropriate, enter the type of report, e.g., interim, progress, summary, annual, or final. Give the inclusive dates when a specific reporting period is covered.

5. AUTHOR(S): Enter the name(s) of author(s) as shown on or in the report. Enter last name, first name, middle initial. If military, show rank and branch of service. The name of the principal author is an absolute minimum requirement.

6. REPORT DATE: Enter the date of the report as day, month, year, or month, year. If more than one date appears on the report, use date of publication.

7a. TOTAL NUMBER OF PAGES: The total page count should follow normal pagination procedures, i.e., enter the number of pages containing information.

7b. NUMBER OF REFERENCES: Enter the total number of references cited in the report.

8a. CONTRACT OR GRANT NUMBER: If appropriate, enter the applicable number of the contract or grant under which the report was written.

8b, 8c, & 8d. PROJECT NUMBER: Enter the appropriate military department identification, such as project number, subproject number, system numbers, task number, etc.

9a. ORIGINATOR'S REPORT NUMBER(S): Enter the official report number by which the document will be identified and controlled by the originating activity. This number must be unique to this report.

9b. OTHER REPORT NUMBER(S): If the report has been assigned any other report numbers *(either by the originator or by the sponsor)*, also enter this number(s).

10. AVAILABILITY/LIMITATION NOTICES: Enter any limitations on further dissemination of the report, other than those imposed by security classification, using standard statements such as:

(1) "Qualified requesters may obtain copies of this report from DDC."

(2) "Foreign announcement and dissemination of this report by DDC is not authorized."

(3) "U. S. Government agencies may obtain copies of this report directly from DDC. Other qualified DDC users shall request through _____."

(4) "U. S. military agencies may obtain copies of this report directly from DDC. Other qualified users shall request through _____."

(5) "All distribution of this report is controlled. Qualified DDC users shall request through _____."

If the report has been furnished to the Office of Technical Services, Department of Commerce, for sale to the public, indicate this fact and enter the price, if known.

11. SUPPLEMENTARY NOTES: Use for additional explanatory notes.

12. SPONSORING MILITARY ACTIVITY: Enter the name of the departmental project office or laboratory sponsoring *(paying for)* the research and development. Include address.

13. ABSTRACT: Enter an abstract giving a brief and factual summary of the document indicative of the report, even though it may also appear elsewhere in the body of the technical report. If additional space is required, a continuation sheet shall be attached.

It is highly desirable that the abstract of classified reports be unclassified. Each paragraph of the abstract shall end with an indication of the military security classification of the information in the paragraph, represented as *(TS), (S), (C), or (U)*.

There is no limitation on the length of the abstract. However, the suggested length is from 150 to 225 words.

14. KEY WORDS: Key words are technically meaningful terms or short phrases that characterize a report and may be used as index entries for cataloging the report. Key words must be selected so that no security classification is required. Identifiers, such as equipment model designation, trade name, military project code name, geographic location, may be used as key words but will be followed by an indication of technical context. The assignment of links, roles, and weights is optional.

DD FORM 1 JAN 64 1473 (BACK)